

**W. W. SANDERS, JR.
H. A. ELLEBY
F. W. KLAIBER
M. D. REEVES
AUGUST 1975**

**Interim Report
ISU-ERI-Ames-76036**

ULTIMATE LOAD BEHAVIOR OF FULL-SCALE HIGHWAY TRUSS BRIDGES: PHASE II— SERVICE LOAD AND SUPPLEMENTARY TESTS

Highway Division—Iowa Department of Transportation

ERI Project 1118S

TA1
108p
1118S
Interim

**ENGINEERING RESEARCH INSTITUTE
IOWA STATE UNIVERSITY
AMES, IOWA 50010 USA**

The research summarized herein is supported by funds provided by the Highway Division—Iowa Department of Transportation, the United States Department of Transportation—Federal Highway Administration, and the Engineering Research Institute—Iowa State University. The bridges tested were made available through the cooperation of the United States Army Corps of Engineers and Boone County and Dallas County.

~~The contents of this report reflect the opinions of the~~

ac-
not
the
port
ula-

**IOWA DEPARTMENT OF
TRANSPORTATION LIBRARY**

TECHNICAL REPORT STANDARD TITLE PAGE

1. Report No.	2. Government Accession No.	3. Recipient's Catalog No.	
4. Title and Subtitle Ultimate Load Behavior of Full-Scale Highway Truss Bridges: Phase II - Service Load and Supplementary Tests		5. Report Date August 1975	
		6. Performing Organization Code	
7. Author(s) W. W. Sanders, Jr., H. A. Elleby, F. W. Klaiber, and M. D. Reeves		8. Performing Organization Report No. ERI - 76036	
9. Performing Organization Name and Address Engineering Research Institute Iowa State University Ames, Iowa 50010		10. Work Unit No.	
		11. Contract or Grant No. HR-169	
12. Sponsoring Agency Name and Address Highway Division Iowa Department of Transportation Ames, Iowa 50010		13. Type of Report and Period Covered Interim Report Jan. 1-Aug. 31, 1975	
		14. Sponsoring Agency Code	
15. Supplementary Notes			
<p>16. Abstract</p> <p>As a result of the construction of the Saylorville Dam and Reservoir on the Des Moines River, six highway bridges crossing the river were scheduled for removal. Two of these were incorporated into a comprehensive test program to study the behavior of old pin-connected high-truss single-lane bridges. The test program consisted of ultimate load tests, service load tests and a supplementary test program.</p> <p>The results reported in this report cover the service load tests on the two bridges as well as the supplementary tests, both static and fatigue, of eyebar members removed from the two bridges. The field test results of the service loading are compared with theoretical results of the truss analysis.</p>			
17. Key Words bridges, fatigue, field tests, steel, timber, trusses, wrought iron		18. Distribution Statement No Restrictions	
19. Security Classif. (of this report) Unclassified	20. Security Classif. (of this page) Unclassified	21. No. of Pages 101	22. Price

**ENGINEERING
RESEARCH**

**ENGINEERING
RESEARCH**

**ENGINEERING
RESEARCH**

**ENGINEERING
RESEARCH**

**ENGINEERING
RESEARCH**

INTERIM REPORT

**ULTIMATE LOAD BEHAVIOR
OF FULL-SCALE HIGHWAY TRUSS
BRIDGES: PHASE II—
SERVICE LOAD AND
SUPPLEMENTARY TESTS**

**W. W. Sanders, Jr.
H. A. Elleby
F. W. Klalber
M. D. Reeves
August 1975**

**Sponsored by the
Highway Division—
Iowa Department of Transportation
In Cooperation with the
U. S. Department of Transportation
FEDERAL HIGHWAY ADMINISTRATION**

**ISU-ERI-Ames-76036
ERI Project 1118S**

**ENGINEERING RESEARCH INSTITUTE
IOWA STATE UNIVERSITY AMES**

TABLE OF CONTENTS

	<u>page</u>
LIST OF FIGURES	i
LIST OF TABLES	iv
CHAPTER 1. INTRODUCTION	1
Objectives	2
General Test Program	4
CHAPTER 2. THE TEST BRIDGES	5
Truss Descriptions	5
A. Hubby Bridge	5
B. Chestnut Ford Bridge	6
Physical Properties	8
CHAPTER 3. FIELD TESTS AND TEST PROCEDURES	11
Hubby Bridge - Span 1	12
Hubby Bridge - Span 2	13
Chestnut Ford Bridge	13
CHAPTER 4. LABORATORY TESTS AND TEST PROCEDURE	15
Fatigue Tests	15
Static Tests	17
CHAPTER 5. RESULTS AND ANALYSIS	18
Service Load Tests	18
Service Load Test - Trusses	18
Service Load Test - Floorbeams	21
Service Load Test - Timber Deck	22
Fatigue Tests	24
Fatigue Tests - Undamaged Eyebars	24
Fatigue Tests - Damaged and Repaired Eyebars	27
Static Tests	30
Static Tests - Undamaged Bars	30
Static Tests - Damaged and Repaired Eyebars	33
CHAPTER 6. SUMMARY AND CONCLUSIONS	36
Summary	36
Conclusions	39
REFERENCES	41
ACKNOWLEDGEMENTS	42
FIGURES	44

LIST OF FIGURES

	<u>page</u>
Fig. 1. Photographs of the Hubby Bridge.	45
Fig. 2. Details of the Hubby Bridge.	46
Fig. 3. Photographs of the Chestnut Ford Bridge.	47
Fig. 4. Details of the Chestnut Ford Bridge.	48
Fig. 5. Timber deck layout - Hubby Bridge.	49
Fig. 6. Timber deck layout - Chestnut Ford Bridge.	50
Fig. 7. Description of truck for Hubby Bridge testing (wheel locations).	51
Fig. 8. Description of truck for Chestnut Ford Bridge testing (wheel locations).	51
Fig. 9. Location of deflection dials for Span 1 - Hubby Bridge.	52
Fig. 10. Location of strain gages on Span 1 - Hubby Bridge.	53
Fig. 11. Location of strain gages on floorbeams in Span 1 - Hubby Bridge.	54
Fig. 12. Photograph of truck being weighed.	55
Fig. 13. Photograph of truck on the centerline of the bridge.	55
Fig. 14. Photograph of truck on the edge of the bridge.	56
Fig. 15. Location of strain gages on floorbeams in Span 2 - Hubby Bridge.	57
Fig. 16. Location of strain gages on Span 2 - Hubby Bridge.	58
Fig. 17. Location of deflection dials for Span 2 - Hubby Bridge.	59
Fig. 18. Location of strain gages on Chestnut Ford Bridge.	60
Fig. 19. Photograph of fatigue apparatus.	61
Fig. 20. Photograph of pin in fatigue test apparatus.	62
Fig. 21. Photograph showing the repair for a fracture in the forging at a turnbuckle.	62

	<u>page</u>
Fig. 22. Photograph showing the repair for a fracture in the forging at the neck of an eye.	63
Fig. 23. Photograph showing the repair for a fracture in the eye of an eyebar.	63
Fig. 24. Photograph showing typical static test specimen with strain gages.	64
Fig. 25. Photograph showing static test apparatus.	64
Fig. 26. Influence lines for Span 1 - Hubby Bridge.	65
Fig. 27. Influence lines for Span 2 - Hubby Bridge.	67
Fig. 28. Influence lines - Chestnut Ford Bridge: truck on centerline.	72
Fig. 29. Influence lines - Chestnut Ford Bridge: truck 2' from left edge.	76
Fig. 30. Influence lines for truss deflection: Span 2 - Hubby Bridge.	80
Fig. 31. Moment for floorbeams at L_3 , L_4 , L_5 , L_6 .	81
Fig. 32. Deck deflection at mid-span between L_2 and L_3 , Span 2 - Hubby Bridge, truck on centerline of deck.	84
Fig. 33. Deck deflection at mid-span between L_2 and L_3 , Span 2 - Hubby Bridge, truck 2' from left edge of deck.	84
Fig. 34. Deck deflection at mid-span between L_2 and L_3 , Span 2 - Hubby Bridge, truck 2' from right edge of deck.	85
Fig. 35. Deck deflection at mid-span of panel, Chestnut Ford Bridge: truck on centerline of deck.	86
Fig. 36. Deck deflection at mid-span of panel, Chestnut Ford Bridge: truck 2' from left edge.	86
Fig. 37. Deck deflection at mid-span of panel, Chestnut Ford Bridge: truck 2' from right edge.	87
Fig. 38. Photograph showing fatigue fracture in forging near a turnbuckle.	88
Fig. 39. Photograph showing extent of an initial crack in a forging.	88
Fig. 40. Photograph showing two typical locations of fracture in an eye.	89

	<u>page</u>
Fig. 41. Photograph showing a fracture on both sides of an eye.	89
Fig. 42. S-N curve for undamaged eyebars.	90
Fig. 43. Photograph showing repair and fracture of an eyebar that was repaired in the field.	91
Fig. 44. Photograph showing the fatigue fracture in the forging near an eye.	91
Fig. 45. Load vs strain distribution around an eye made from a square bar.	92
Fig. 46. Load vs strain distribution in tip of eye.	93
Fig. 47. Load vs strain distribution in side of eye.	95

LIST OF TABLES

	<u>page</u>
Table 1. Physical properties.	9
Table 2. Wheel loadings of trucks.	11
Table 3. Load distribution factors.	23
Table 4. Results of fatigue tests on undamaged eyebars.	25
Table 5. Results of fatigue tests on damaged and repaired eyebars.	29
Table 6. Results of static tests on undamaged eyebars.	32
Table 7. Summary - static test results.	33
Table 8. Results of static tests on damaged and repaired eyebars.	35

CHAPTER 1. INTRODUCTION

The construction of the Saylorville Dam and Reservoir on the Des Moines River created an ideal opportunity to study bridge behavior. Due to the dam and reservoir construction, six highway bridges crossing the river were scheduled for removal. Five of these are old pin-connected, high-truss, single-lane bridges and are typical of many built around the turn of the century throughout Iowa and the country. Only limited information on their design and construction is available because these bridges were built circa 1900. Since there is an increasing need to determine the strength and behavior characteristics of all bridges, the removal of these five was invaluable by allowing the study of bridge behavior through the testing of actual prototype bridges rather than physical or mathematical models. The purpose of this testing program was to relate design and rating procedures presently used in bridge design to the observed field behavior of this type of truss bridge.

A study to determine the feasibility of performing these load tests was conducted several years ago by Iowa State University.¹ Included in the study findings was a recommendation that a broad range of programs be conducted on several of the truss bridges involved in the removal program. The first truss bridge to be replaced, the Hubby Bridge, was available for testing in June 1974. A research program was developed and undertaken by Iowa State University to conduct a number of the recommended tests. A previous report² details the research and findings of the first phase of the program - the ultimate load behavior of the high truss bridge. This report details the second phase of the program -

the service load testing of the Hubby and Chestnut Ford Bridges. The tests on the Chestnut Ford Bridge were performed while the bridge was still open to traffic. Also included in this report are the results of several supplemental programs, including the fatigue and static testing of eyebars obtained from both of the above mentioned bridges. A final summary report on the entire project will be prepared that will include an outline of the results of the program and recommendations for implementation of the findings.

Since the major portion of this report summarizes the results of a study on the same bridge used for the research reported in the first interim report², the reader is referred to that report for details of the main test bridge and instrumentation common to the two test programs. Only a summary of this information is presented herein.

Objectives

Specifications and manuals adopted by the American Association of State Highway and Transportation Officials (AASHTO)^{3,4} contain criteria used in the design and rating of highway bridges in the United States. These criteria are based on rational structural analysis, actual experimental investigations, and engineering judgment. These criteria also attempt to take into account actual bridge behavior to assure safe and serviceable structures. However, as a result of the catastrophic collapse of several old bridges in the last 10 years, considerable interest has been generated in determining the actual load-carrying capacity of bridges. The load capacity of newer bridges can generally be obtained from existing plans and specifications that can be supplemented by field examinations and, if necessary, actual field tests.

However, for the old pin-connected, high-truss bridges, there are generally no technical data available, and there is also a complete lack of field load test data at service load levels, or at ultimate load capacity. The general objective of this phase of the program was to provide data on the behavior of this bridge type in the service load range and data on the remaining fatigue life of the tension members in the truss.

As engineers undertake the analysis and rating of these bridges, many questions arise. These include the condition of the joints, the strength of the eyes (including forgings) in the tension bars, and the behavior of the floorbeams and deck. The results reported here are limited to the two bridges tested, but the results should nevertheless provide an indication of possible answers to the questions posed above.

The specific objectives of this load test program were:

1. Relate appropriate AASHTO criteria to the actual bridge behavior as determined from tests on the available truss bridges.
2. Determine an estimate of the remaining fatigue life of the bridge components.
3. Determine the effect of repairs on the remaining fatigue life of the bridge components.

The results of the research will provide a better understanding of the actual strength of the hundreds of old high-truss bridges existing throughout Iowa as well as the country as a whole.

General Test Program

This phase of the test program consisted of the field service load testing of the west two spans of the Hubby Bridge in Boone County and of the west span of the Chestnut Ford Bridge in Dallas County. The tests were conducted using loaded county gravel trucks to simulate a standard H-truck loading. The trucks were driven along the centerline and along the edges of the roadway of each bridge.

The laboratory tests that were conducted consisted of fatigue testing 23 eyebars in their original condition and nine eyebars after they had been damaged and then subsequently repaired. Static tests were conducted on 19 eyebars in their original condition and on three eyebars that had been damaged and then subsequently repaired. Three different types of damage and repair were used which simulated the possible types of damage in the forgings and in the eyes of the eyebars.

CHAPTER 2. THE TEST BRIDGES

The highway bridges selected for testing were located on the Des Moines River northwest of Des Moines, Iowa, in an area which will be included in the Saylorville Reservoir. One of the high-truss bridges selected was the Hubby Bridge built in 1909 (Figs. 1 and 2), and located in southern Boone County about 25 miles northwest of Des Moines. It was composed of four modified Parker type high-truss simple spans, each 165 ft. long.

The other bridge selected was the Chestnut Ford Bridge (Figs. 3 and 4), located in northern Dallas County about 20 miles northwest of Des Moines and five miles south of the Hubby Bridge. This bridge was built circa 1900 and was composed of four high-truss simple spans. The first, third and fourth spans, from east to west, were modified Pratt-type trusses each 150 ft. long, and the second span was a Pratt truss 180 ft. long. Testing was conducted in the fourth, or west, span.

Truss Descriptions

A. Hubby Bridge

The trusses consisted of tension eyebars of both square and rectangular cross sections, built-up laced channels for the end posts and upper chord compression members, and laced channels for the other compression members. The square tension eyebars ranged in size from $3/4$ in. to $1\ 1/8$ in. and were used for truss hangers and diagonals. The rectangular tension eyebars ranged in size from $5/8$ in. x 3 in. to $13/16$ in. x 4 in. and were used for diagonals and the truss lower chord.

The eyes for these two types of eyebars were formed by bending a bar around to form a tear-drop shaped eye. This tear-shaped eye was then forged to a bar to form one end of the eyebar. The channels ranged in size from four in. to nine in. deep and were used for truss compression members.

The deck was built of timber stringers, timber crossbeams, and timber floor planks. The stringers in the west two spans (which were load tested) were creosote treated, while the stringers in the east two spans were not. The stringers stood on edge and were supported by rolled I-shaped floorbeams. Stringers were positioned with their longest dimension parallel to the length of the bridge. Crossbeams, spaced approximately one foot apart, were placed flat on top of the stringers and were positioned with their longest dimension perpendicular to the length of the bridge. The floor planks were placed flat on top of the crossbeams and were positioned with their longest dimension parallel to the length of the bridge. All of the timber members were 3 in. x 12 in. and approximately 17 ft. long. A typical deck panel consisted of 15 stringers, 8 crossbeams, and 16 floor planks as shown in Fig. 5.

The floorbeams were standard I-sections 12 in. deep and weighing 30.6 pounds per foot of length. The floorbeams were connected to the truss with clip angles and 1/2 in. bolts.

B. Chestnut Ford Bridge

The test truss consisted of tension eyebars of circular, square, or rectangular cross sections for tension members, of built-up laced channels for end posts and upper chord compression members and of laced channels for the remaining compression members. One in. square tension

eyebars were used for the truss hangers. Rectangular tension eye-bars ranged in size from 9/16 in. x 2 in. to 7/8 in. x 4 in. and were used for the truss lower chords and for some of the diagonals. Three-fourth in., 7/8 in. and one in. diameter round eyebars were also used for truss diagonals. The eyes for the square, round, and the smaller rectangular eyebars were formed by bending a bar around to form a tear-shaped eye and then forging this eye to the main bar. The eyes for the larger tension eyebars were machined from a plate to form a round-shaped eye and then forged to the bar. The channels ranged in size from six in. deep to eight in. deep and were used for the truss compression members.

The deck was built of timber stringers and timber floor planks. The stringers were 3 in. x 16 in. and approximately 22 ft. long. The stringers stood on edge with their longest dimension parallel to the length of the bridge and were supported by rolled I-shaped floorbeams. The cross planks were 3 in. x 4 in. x 16 ft. and were placed on edge on top of the stringers with their longest dimension perpendicular to the length of the bridge. The cross planks were laminated together with bolts and were spiked to the stringers every two ft. A typical panel consisted of 13 stringers with the continuous floor planking as shown in Fig. 6.

The floorbeams were standard I-sections, 15 in. deep and weighing approximately 35 pounds per foot. The floorbeams were connected to the truss by means of clip angles and 1/2 in. bolts.

Physical Properties

Chemical analysis and physical property tests were made of sections from the Hubby Bridge. The tension eyebars were determined to be made of wrought iron and the other members of steel. The results of the chemical analysis are shown in Table 1. Tensile tests were conducted on coupons from typical members of both wrought iron and steel to obtain material properties. Six tests were conducted on coupons from wrought iron specimens. Three coupons were from a square eybar (typical of truss hangers and some diagonals) and measured approximately 1/2 in. x 3/4 in. The other three were from a rectangular eybar (typical of truss lower chords and some diagonals) and measured approximately 1 1/4 in. x 1/2 in. Three tests were conducted on coupons from two steel channels (typical of truss compression members) and measured approximately 1 1/8 in. x 1/8 in. All of the coupons had a gage length of eight in. The results are shown in Table 1. The results shown in Table 1 indicate that the steel satisfies the requirements for ASTM A36 steel even though the steel was manufactured around the turn of the century. The wrought iron conforms to ASTM specifications (A207-71).

Chemical analysis and physical property tests were also made of sections from the Chestnut Ford Bridge. Tensile tests were conducted on three specimens made from one in. square tension eyebars to obtain material properties. The results from the physical properties tests and the chemical analysis are shown in Table 1. The results show that the wrought iron conforms to ASTM specification (A85-49) for common iron.

The timber members were made from Douglas Fir which had been sized and pressure-treated with creosote in accordance with Iowa State Highway

Table 1. Physical properties.

a. Chemical Properties			
	Hubby Bridge		Chestnut Ford Bridge
Element	Percentage in Wrought Iron	Percentage in Steel	Percentage in Wrought Iron
Carbon	<0.03	0.19	<0.3
Manganese	<0.05	0.40	0.25
Phosphorus	0.29	0.012	0.130
Sulfur	0.042	0.029	0.036
Nickel	<0.05	<0.05	<0.05
Chromium	<0.05	<0.05	<0.05
Molybdenum	<0.03	<0.03	<0.03
Copper	<0.03	0.03	0.08
Aluminum	0.03	----	----
Vanadium	<0.01	----	----
Silicon	0.22	<0.05	0.12
Cobalt	0.02	----	----

b. Material Properties				
Bridge	Material	σ_y (ksi)	σ_{ult} (ksi)	E(ksi)
Hubby	Wrought Iron	35.5	49.1	28,000
	Steel	42.0	58.7	30,900
	Timber	----	4.02	1,150
Chestnut Ford	Wrought Iron	34.9	48.6	25,300
	Steel	----	----	----

Commission Standards. Flexure tests, using two equal loads placed equidistant from mid-span to develop a pure moment region, were conducted on typical timbers in both the flat and on-edge positions to determine material properties. The modulus of elasticity for the timber was determined from the load-deflection curves of the specimens tested. The results are shown in Table 1.

Typical stress strain curves for the wrought iron and steel and the load deflection curve for the timber beams can be found in the Phase I report².

CHAPTER 3. FIELD TESTS AND TEST PROCEDURES

This section outlines the details of the specific service load tests that were performed in the field during the summer of 1974. Service load tests were performed on the two west spans of the Hubby Bridge in Boone County and on the west span of the Chestnut Ford Bridge in Dallas County. The tests were accomplished using loaded gravel trucks supplied by Boone County and Dallas County. The trucks were weighed using portable scales before each test by a State Weight Officer (Fig. 12). Descriptions of the trucks are shown in Figs. 7 and 8 and the weights of the trucks for each test are given in Table 2.

Table 2. Wheel loadings of trucks.

<u>Test</u>	<u>Front (lbs)</u>		<u>Rear (lbs)</u>		<u>Total (lbs)</u>
	<u>Left</u>	<u>Right</u>	<u>Left</u>	<u>Right</u>	
Hubby Bridge - Span 1	3790	3780	10290	11010	28870
Hubby Bridge - Span 2	4120	3820	12500	11250	31690
Chestnut Ford	3850	3690	10260	11520	29320

The procedures used for each of the tests were the same, but the instrumentation varied. The testing procedure for each test was:

1. Take an initial reading on all instrumentation with the truck completely off the bridge,
2. Move the truck to the first desired position on the bridge,
3. Stop the truck there while readings are taken on the instrumentation,
4. Move the truck to the next desired position,
5. Repeat steps 3-4 until all desired readings have been taken, and then

6. Move the truck completely off the bridge and take a final reading of the instrumentation.

Hubby Bridge - Span 1

The instrumentation for this test consisted of 108 strain gages and five deflection dials. The deflection dials were located at the centerline, quarter points, and near the ends of the floorbeam at L_5 (Fig. 9). Of the 108 strain gages, 76 were mounted on selected truss members (Fig. 10) and 32 were mounted floorbeams 3, 4, 5, and 6 (Fig. 11).

The strain gages on the floorbeams were mounted on the compression and tension flanges of the floorbeams and they were located at the centerlines, third points, and also near the ends of floorbeams 4 and 5 and at the centerline and near the ends of floorbeams 3 and 6 (Fig. 11).

The tension members of the truss, each of which was composed of two eyebars, had one gage mounted on each eyebar. The compression members, which were composed of two laced channels, had four strain gages, one strain gage on each flange of each channel. This allowed the measurement of the moment about each axis as well as the measurement of the resultant axial force. All of the strain gages used in the tests were encapsulated and self-temperature compensating for steel. A three wire load hook-up was used to reduce the temperature effects of the long lead wires.

The truck was driven down the centerline of the bridge first (Fig. 13), stopping with its rear wheels in line with the panel points. The truck was then driven down each side, with the center

of the wheels approximately two feet from the edge of the roadway (Fig. 14), stopping only at L_3 , L_4 , L_5 , and L_6 .

Hubby Bridge - Span 2

The instrumentation for this test span consisted of 116 strain gages and six deflection dials. Eight gages were mounted on the compression and tension flanges at the centerline of the floorbeams at L_2 , L_3 , L_8 , and L_9 (Fig. 15) and the remaining 108 were mounted on the truss members (Fig. 16). The deflection dials were set on the ground beneath the sides of the bridge at L_3 , L_5 , and L_7 (Fig. 17), to measure the truss deflection. Deflection readings were also taken on the stringers at the midpoint between L_2 and L_3 .

The truck was driven down the centerline of the bridge first, stopping with its rear wheels in line with the panel points. The truck was then driven down each side stopping only at L_5 and halfway between L_2 and L_3 .

Chestnut Ford Bridge

The instrumentation for this test bridge consisted of 15 strain gages mounted on the north truss of the west span (Fig. 18). The strain gages were mounted on tension members only.

The truck was driven down the centerline of the bridge and then down one side of the bridge stopping at each panel point.

After this part of the test was completed the truck was located on the bridge with its rear wheels halfway between panel points.

Deflection measurements of the deck were taken while the truck was at the center of the bridge roadway and at eccentric positions on the left and right sides of the bridge roadway.

CHAPTER 4. LABORATORY TESTS AND TEST PROCEDURE

The service load field tests were completed in September 1974 and the bridges were removed in January 1975. The contract for the salvage of the bridges stated that the east span of the Hubby Bridge and the west span of the Chestnut Ford Bridge were to be removed as if they were to be reconstructed. Over 100 eyebars from these spans were shipped to the laboratory.

This section outlines the details of the specific tests that were performed in the laboratory.

Fatigue Tests

The main thrust of the laboratory testing program was the fatigue testing of 30 eyebars. The fatigue tests were accomplished using a special apparatus (Fig. 19) designed so that the loads could be applied to the eyebars through pins placed in the eyes (Fig. 20). The pins used were actual pins taken from the test bridges. The pin used in the eye of an eyebar was not necessarily the one that was originally in that particular eye, but it was nevertheless a pin of the same size.

The eyebars were inspected for dimensions, flaws, and peculiarities before they were tested. It had been planned to include the use of an ultrasonic crack detector but the surface of the eyebars was too rough and there were too many inclusions in the wrought iron. A dye penetrant was used for inspection on the first ten specimens but it did not reveal any cracks that were not already visible, so this method was discontinued. Therefore, the remainder of the eyebars were inspected by eye in their natural "as is" condition.

The cyclic stresses that were imposed on the eyebars varied from a minimum of two ksi to a maximum of 16-24 ksi. All of the fatigue tests were run with a cyclic frequency of three to four hertz.

Some of the tests were performed on undamaged eyebars and some of the tests were performed on eyebars that had been purposefully damaged in the laboratory and then repaired. Three types of damage and repair were investigated:

1. The first type of damage simulated a fracture in the forging area near a turnbuckle. Two eyebars were cut at a forging near a turnbuckle (Fig. 21) and were then welded back together. Two pieces of cold-rolled bar stock of the same dimensions as the eyebar were spliced onto the eyebar over the fracture (Fig. 21). The splices extended for at least one foot in each direction from the fracture. All of the welds were made in the flat position using E7024 welding rod at 200 amps.

2. The second type of damage simulated a fracture in the neck of an eye. Four eyebars were cut in the neck of an eye and were then welded back together (Fig. 22). Pieces of cold-rolled bar stock were spliced over the fracture. The splices extended as far into the eye as possible and at least two ft. along the bar past the fracture (Fig. 22).

3. The third type of damage simulated a fracture in the eye (Fig. 23). In this case the eye was cut off completely and a new eye was formed out of cold-rolled bar stock. The eye was formed by heating the bar stock cherry red and bending it into a tear-shape. This new eye was then welded onto the original eyebar (Fig. 23).

Static Tests

The second part of the laboratory testing program consisted of the static testing of 22 specimens taken from various eyebars. The specimens were cut from the ends of the eyebars and consisted of the eye plus two to four ft. of the bar (Fig. 24). The specimens were loaded using a standard universal testing machine. The bar end of a specimen was locked into the mechanical grips at one head of the machine and a pin was placed through the eye at the other end of the bar. The pin end was then brought to bear against the other head of the machine (Fig. 25). Nineteen specimens were tested as undamaged members while three were tested as damaged and repaired members. The three latter specimens were damaged and repaired in the same three ways that were employed for the fatigue test specimens.

In addition, two of the undamaged specimens had strain gages mounted on them (Fig. 24) to determine a rough approximation of the stress distribution around and through the eye.

CHAPTER 5. RESULTS AND ANALYSIS

Service Load Tests

Service load tests were performed in the field on the Hubby Bridge and the Chestnut Ford Bridge. Loads were applied to the bridges using loaded county gravel trucks. The exact procedure for conducting the service load tests of the two bridges was discussed in Chapter 3. The results presented here are divided into three groups representing the three basic components of the bridges, namely, the trusses, the floorbeams, and the timber deck. In each case the experimental results are compared with theoretical results found by a computer analysis of an ideal determinate bridge assuming pinned connections and assuming that the eyebars could not withstand compression forces.

Service Load - Trusses

Figures 26 and 27 illustrate some of the experimental and theoretical influence lines obtained from the results of the service load tests for selected truss members of the Hubby Bridge. Figures 28 and 29 illustrate all of the experimental and theoretical influence lines obtained from the results of the service load tests for selected truss members of the Chestnut Ford Bridge.

The experimental influence lines were found by calculating the forces in the members using the strain measurements that were recorded for each position of the truck. The theoretical influence lines were determined by placing a theoretical truck of the same configuration as the

experimental truck (Figs. 7 and 8), at each panel point and calculating the resultant bar force using determinate analysis. Each of the graphs shows the theoretical influence line for the member as a solid line. In the testing of the two spans of the Hubby Bridge both the north and the south truss were instrumented. The experimental influence lines for both trusses are shown as broken lines. Only the influence lines for a truck on the centerline of the bridge are shown. For the truck on other transverse positions on the bridge, the influence lines would have the same shape and be proportional to those shown.

In the testing of the one span of the Chestnut Ford Bridge only the north truss was instrumented. The experimental influence lines are shown as broken lines. For the Chestnut Ford Bridge influence lines are shown for a truck on the centerline of the bridge (Fig. 28) and for a truck two ft. from the left edge of the deck (Fig. 29).

It can be seen in Figs. 26 through 29 that in most cases for the Hubby Bridge and in all cases for the Chestnut Ford Bridge, the experimental results agree closely with the theoretical values. Figure 27h is typical of this relationship. The general shape of the experimental influence line is the same as the shape of the theoretical influence line, although the magnitude of the experimental values is less than the magnitude of the theoretical values. This difference is due in part to the partial continuity of the deck which was not taken into account in the theoretical analysis, the condition of the joints, as well as problems in the instrumentation.

In the service load tests of both spans of the Hubby Bridge, the 100 channel data acquisition system was not available due to technical problems and, thus, the strain measurements were taken using older

equipment. This resulted in a longer period of time being required to take all of the strain measurements. It took three to four times as long to take all of the strain measurements by hand with the older equipment as it would have taken with the automatic data acquisition system. This longer time period meant that variances in the power line voltage to the strain indicators, indicator drift, and the changing temperature in the bridge members occurred. These changes had an indeterminable effect on the strain measurements and resulted in unusual behavior in several members. This effect can be seen in Fig. 27i where the experimental results oscillate around the theoretical values making it impossible to make any correlation in these cases. Thus, only a limited number of influence lines are given.

However, in the service load test on the Chestnut Ford Bridge only fifteen gages were used. Battery operated strain indicators were used to take these readings, and the readings could be taken very quickly helping to eliminate errors in readings caused by time effects. Thus the results are more dependable.

In addition to the recording of member strains during the service load testing of the Hubby Bridge, truss deflections were also recorded. Figure 30 compares the experimental deflection of the truss at L_3 , L_5 and L_7 in Span 2 of the Hubby Bridge with the theoretical deflections of the truss. Again the results are shown in the form of an influence line. The experimental deflections were measured during the test with the truck at each panel point. The theoretical deflections were determined from an analysis of the truss treated as an ideal pin-connected truss. It can be seen from Fig. 30 that the experimental deflections are much lower than the theoretical deflections. This is due to

the partial continuity of the deck, which was not taken into account in the theoretical analysis, and the frozen conditions of many of the pin-connections.

Thus, it appears that the analysis of a pin-connected truss, even though the condition of the pins is unknown, as a simple determinate truss, will provide a conservative indication of the bar forces and truss deflections. Similar results were found during the static ultimate load tests conducted on the Hubby Bridge and reported in the first interim report².

Service Load Test - Floorbeams

Figure 31 shows the experimental moment diagram for the floorbeams at L_3 , L_4 , L_5 , and L_6 compared with the theoretical moment diagrams with the truck placed on the centerline and edges of the bridge. The experimental moments were determined from strain gages mounted on the floorbeams. The experimental moments fall between the theoretical values for fixed ends and pinned ends. The experimental moment diagrams for the floorbeams at L_3 and L_5 tend to agree more closely with the theoretical pinned end moments, while the experimental moment diagrams for the floorbeams at L_4 and L_6 tend to agree more closely with the theoretical fixed end moments. This shows the difference in stiffness between the two types of joints. These results agree with the results reported in the first interim report². The results here also show the excellent distribution properties of the deck.

Service Load Test - Timber Deck

Figures 32 through 37 show the experimental deflections of the timber stringers compared with the theoretical deflections. The deflections were measured at the middle of the panel halfway between L_2 and L_3 in Span 2 of the Hubby Bridge and at the middle of a panel in Span 4 of the Chestnut Ford Bridge.

Figure 32 shows the deflections of the Hubby Bridge deck with the truck on the centerline and Figs. 33 and 34 show the deflections with the truck on the left and right sides respectively. Figure 35 shows the deflections of the Chestnut Ford Bridge deck with the truck on the centerline and Figs. 36 and 37 show the deflections with the truck on the left and right sides of the bridge. The solid lines show the theoretical deflections of the deck assuming the stringers to be fixed or pinned at the far ends. The theoretical deflections were calculated by the method presented by Hetenyi⁵.

In all of the cases the experimental deflections are close to the theoretical values for stringers with pinned ends, however, when the gross deflections are large, as in the case with the truck on the edge, the experimental values move away from the values for the theoretical pinned-end condition and toward the theoretical values for the fixed end assumption. This shows that when the deflections of the deck become large, the load distribution characteristics improve due to the improved effects of the layered deck.

The load distribution characteristics of the bridge deck can be found approximately by using the deflection readings taken during the service load testing. The AASHTO specifications for load distribution state that the load to be taken by each stringer is found using the

equation S/D where S is the stringer spacing for the deck in feet and D is given as 4 for the Hubby Bridge deck and 4.5 for the Chestnut Ford Bridge deck. The value of D can be found from the recorded deck deflections using the following equation:

$$D = W \cdot \sum \Delta_i / (N_r \cdot \Delta_{\max})$$

where Δ_i is the deflection of a stringer, Δ_{\max} is the maximum deflection of a stringer, N_r is the number of deflection readings taken on the deck, and W is the width of the deck. Table 3 lists the experimental values of D found for the deck tests on the Hubby and Chestnut Ford Bridges. Table 3 also lists the percentage of the total load carried by the most heavily loaded stringer. From this table it can be seen that the AASHTO specifications are conservative for the timber deck system used on the Hubby Bridge. For the Chestnut Ford Bridge, the Specifications appear to be nonconservative for the eccentric position, however, it should be noted that the maximum deflections were essentially the same in both cases.

Table 3. Load distribution factors.

Test	Equivalent Distribution Factor	Percentage of the load Distributed to the most Heavily loaded stringer
Hubby Bridge		
Truck in Center	5.83	9.6%
Truck on Left	5.71	9.8%
Truck on Right	5.77	9.7%
Chestnut Ford Bridge		
Truck in Center	4.52*	13.6%
Truck on Left	3.24*	19.0%

*Maximum deflection of critical stringer the same in both cases.

Fatigue Tests

Fatigue tests were performed on 26 tension eyebars taken from the Hubby Bridge and four tension eyebars taken from the Chestnut Ford Bridge. Some of the eyebars received at the laboratory had kinks and bends in them that were formed during the dismantling of the bridges. However, these bars were straightened on a rebar bender before testing. The residual stresses induced in the eyebars due to the straightening had no apparent effect on the fatigue life of the eyebars. This is a reasonable assumption since no failures occurred at the points of bending.

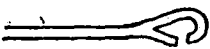
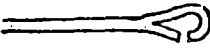
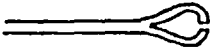
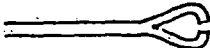
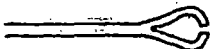
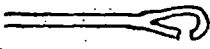
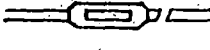

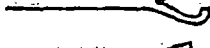




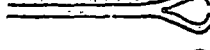
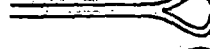
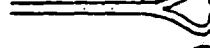
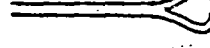


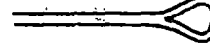
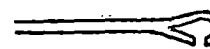
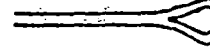
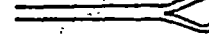
The eyebars tested were all of square cross-section and varied from 3/4 in. to 1 1/8 in. in dimension.

Fatigue Tests on Undamaged Eyebars

Twenty-three of the eyebars were tested in their undamaged (except for straightening) condition. The maximum stress for the tests varied from 16 to 24 ksi with a uniform minimum stress of two ksi. All of the eyebars were tested at a cyclic rate of three to four hertz. The results of the fatigue tests on undamaged eyebars can be found in Table 4. This table lists the identification number of the eyobar, its location on the truss, the dimensions of the eyobar, the stress range that the eyobar was subjected to, the number of cycles required to fail the eyobar, and a diagram illustrating the location of the failure.

Two of the 23 undamaged eyebars fractured in one of the forgings joining the turnbuckle to the eyobar, as illustrated in Fig. 38. These two eyebars initially had large cracks at the point of fracture prior

Table 4. Results of fatigue tests on undamaged eyebars.

Identification Number*	Member	Dimensions	Stress Range (ksi)	Number of Cycles	Location of Fracture
H3	L4M3	1 1/8" x 1 1/8"	14	1,415,200	
H6	L4M3	1 1/8" x 1 1/8"	16	446,180	
H5	L4M3	1 1/8" x 1 1/8"	18	121,610	
H16 ₁ **	U4M5	1" x 1"	14	2,033,250+	
H9	U4M5	1" x 1"	16	787,410	
H10	U4M5	1" x 1"	16	371,950	
C32	----	1" x 1"	16	500,450	
H16 ₂ **	U4M5	1" x 1"	18	63,040	
H8	U4M5	1" x 1"	18	70,570	
C31	----	1" x 1"	18	154,960	
H1	U4M3	1" x 1"	20	102,210	
H18	U4M5	1" x 1"	20	127,320	
C30	----	1" x 1"	20	173,330	
C29	----	1" x 1"	22	63,220	
H12	L4M5	7/8" x 7/8"	14	99,200	
H20	L4M5	7/8" x 7/8"	15.5	112,750	
H13	L4M5	7/8" x 7/8"	16	106,100	
H15	L4M5	7/8" x 7/8"	16	165,280	
H14	L4M5	7/8" x 7/8"	20	74,790	
H19	L4M5	7/8" x 7/8"	20	94,440	
H23	L1U1	3/4" x 3/4"	16	314,950	
H24 ₁ **	L5M5	3/4" x 3/4"	16	329,990	
H25 ₁ **	L3M3	3/4" x 3/4"	16	314,310	
H28	L3M3	3/4" x 3/4"	16	510,200	

* Prefix C indicates that the eyebar came from the Chestnut Ford Bridge.
H indicates Hubby Bridge.

** Subscript indicates the order of the tests on a single eyebar.

to the beginning of the fatigue tests. The extent of one of these cracks can be seen in Fig. 39. This photograph was taken after the completion of the fatigue test and indicates that only 75 percent of the metal cross-section was effective.

The remaining 21 eyebars each fractured in one of the eyes of the eyobar. The fractures in the eyes occurred in two different places: 1) at the tip, and 2) at the side of the eye. These two types of fractures are illustrated in Fig. 40. As the load is applied to the eyobar, the eye distorts slightly to conform to the shape of the pin. This is due to the fact that the pin is usually slightly smaller than the hole in the eye. Thus, the sides of the eye are pulled inwardly toward the pin. This induces a stress concentration on the inside of the eye and is therefore a place where fatigue cracks will most likely form. These cracks will then propagate outwardly leading to a fracture at this point. Nine out of the 21 fractures that occurred in the eye were located on the side of the eye. Figure 41 shows a fracture that occurred when cracks formed in both sides of the eye.

If the pin is significantly smaller than the hole in the eye, the eye will also be bent at the tip. Thus, the point of maximum stress concentration will now occur at the tip of the eye. Fatigue cracks will now form on the outside of the eye and propagate inward until fracture occurs. The remaining 12 of the 21 failures occurred as described above.

A careful study of Table 4 will show that different eyobar sizes generally behaved in the same way except for the $7/8$ in. eyebars which all failed at significantly lower numbers of stress cycles. This table also shows that the two fractures near the turnbuckles occurred at much lower numbers of stress cycles than did the fractures in the eyes.

Figure 42 shows the range over which the undamaged eyebars failed in fatigue. The vertical scale gives the stress range and the horizontal scale gives the number of cycles. A regression analysis was performed to find the best fit line through the points. This line approximates the S-N curve (stress range vs. number of cycles to failure) for the eyebars. From this figure it is possible to see the wide variance in fatigue strength of the eyebars taken from the bridges. This variation could be expected due to the non-homogeneity of wrought iron and the various degrees of deterioration of the eyebars.

It is assumed in the inspection and rating of bridges that the critical section of the eyebar is the section at a forging, where many small cracks exist. Since it is impossible to determine the extent of these cracks by inspection, consultants in Iowa usually assume for rating purposes that there is a reduction in strength of the eyebar of 60 percent. In other words, the forging is assumed to have a capacity of only 40 percent of the strength of the eyebar.

In the fatigue tests it was found that the forgings are usually not the critical points for fracture. Twenty-one of the 23 eyebars tested fractured in the eyes and not in the forgings. This indicates that the repeated flexing occurring in the eyes is the critical factor determining the remaining fatigue strength of the eyebar.

Fatigue Tests on Damaged and Repaired Eyebars

Fatigue tests were performed on nine eyebars taken from the Hubby Bridge in order to determine the effect, if any, of repairs on their fatigue life. Two of these were eyebars that had already been tested as undamaged eyebars. The minimum stress and maximum stress for all of

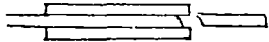
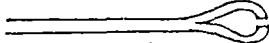
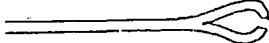
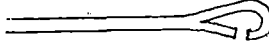
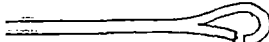
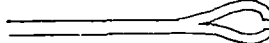
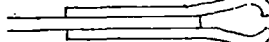
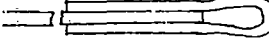
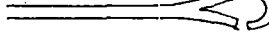
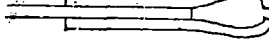
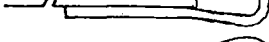

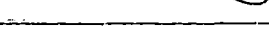
the tests were 2 ksi and 18 ksi, respectively (stress range of 16 ksi). All of the tests were run at a cyclic rate of three to four hertz. The results of the fatigue tests on these damaged and repaired eyebars are shown in Table 5.

One of the nine damaged and repaired eyebars tested was an eyebar that was damaged and repaired at the bridge site an estimated 40 years ago (Table 5; H4). The eyebar had fractured at the forging connecting the eye to the bar and the repair consisted of welding the pieces back together with two additional splice bars (one on each side). The design of the repair was inadequate since the splice did not extend very far onto the eye. In addition, the weld was of very poor quality with very little penetration into the base metal. The fatigue failure occurred at the point of repair. Figure 43 shows the repair and the fracture after the completion of the fatigue test.

Six of the eyebars were damaged and repaired in the laboratory. Four of these simulated fractures near an eye and two simulated fractures near a turnbuckle. The methods of repair for these fractures were given in Chapter 4. These repairs proved to be at least as strong as the bars since no failures occurred near the repairs. Upon testing, five of the eyebars fractured in the eyes as shown in Fig. 40, and one of the eyebars fractured in the forging near the eye at the end opposite from the repaired end (Fig. 44).

Two eyebars (Table 5; H24, H25) that were used for simulated damage and repair were eyebars that had already been tested as undamaged eyebars and had fractured in the eyes. The fractured eye was cut off each eyebar and a new eye was formed from cold-rolled bar-stock and welded on (Fig. 23). Upon reloading, each of the eyebars fractured in

Table 5. Results of fatigue tests on damaged and repaired eyebars.

Identification Number	Type of Repair **	Member	Dimensions	Stress Range (ksi)	Number of Cycles	Location of Fracture	
H4	2	L ₄ M ₃	1-1/8" x 1-1/8"	16	109,370	††	
H2	2	U ₄ M ₃	1" x 1"	16	295,860	†	
H7	2	U ₄ M ₅	1" x 1"	16	319,550	†	
H11	1	U ₄ M ₅	1" x 1"	16	450,840	†	
H17	1	L ₄ M ₅	7/8" x 7/8"	16	130,870	†	
H24 ₂ *	3	L ₅ M ₅	3/4" x 3/4"	16	626,130	†	
H24 ₃ *	3	L ₅ M ₅	3/4" x 3/4"	16	398,660		
H24 ₄ *	3	L ₅ M ₅	3/4" x 3/4"	16	1,152,560		
H25 ₂ *	3	L ₃ M ₃	3/4" x 3/4"	16	537,850	†	
H25 ₃ *	3	L ₃ M ₃	3/4" x 3/4"	16	99,880		
H25 ₄ *	3	L ₃ M ₃	3/4" x 3/4"	16	1,791,840		
H26	2	L ₃ M ₃	3/4" x 3/4"	16	243,960	†	
H27	2	L ₃ M ₃	3/4" x 3/4"	16	242,200	†	

* Subscript indicates the order of tests on an eyebar.

**
 1 indicates damage and repair to a forging near a turnbuckle.
 2 indicates damage and repair to a forging at an eye.
 3 indicates damage and repair to an eye.

† The fracture did not occur near the repair.

†† This member was damaged and repaired in the field.

in the eye at the end opposite to the repaired eye. Subsequently, these fractured eyes were cut off and new eyes were welded on. Each of the eyebars now consisted of the original bar with a new eye welded on at each end. The eyebars were again fatigue tested to determine the strength of the new eyes. Both of the eyebars broke in the eyes due mainly to the improper fit of the pins. The new eyes that had fractured were then cut off and the bar was gripped mechanically and fatigue tested again. The eyebars broke in the other repaired eyes. The life of the new eyes varied greatly. This can be attributed to the fit of the pin in the new eyes and the shape of the new eyes.

Table 5 shows the results of the tests of damaged and repaired eyebars. It can be seen from this table that only two eyebars repaired in the laboratory fractured due to the presence of a weld. These fractures occurred at well over 1,000,000 cycles (many more than could be expected in a normal remaining bridge life) in eyebars that had been repaired three times. Thus, any of these repair methods appears to be appropriate for field use. Care, however, should be taken to provide good quality welding.

Static Tests

Undamaged Bars

Static tests were performed on 17 specimens from eyebars taken from the Hubby Bridge and the Chestnut Ford Bridge. The specimens consisted of an eye plus two to four ft. of bar. The eyebars were square round, and rectangular cross sections with seven, four, and six bars of each size tested, respectively. In addition to these specimens,

two static tests were conducted on specimens consisting of round bars with turnbuckles. The results of the static tests are shown in Table 6.

As can be seen in Table 6, all of the round eyebars, including the two turnbuckle specimens, fractured in the bars and not in the eyes on forgings. Of the seven square eyebars tested, four fractured in the bar and three fractured in the forgings. All of the rectangular eyebars fractured in the forgings.

Table 7 shows the average yield and ultimate stresses for the different shapes of eyebars and the different locations for the fractures.

It can be seen from Table 7 that the average yield stress was approximately the same for all of the eyebars. The average ultimate stress, however, varied for the different types of eyebars. The average ultimate stress for the square eyebars that fractured in the forgings was almost five ksi less than the average ultimate stress for the square eyebars that fractured in the bar away from any forgings. Thus, the forgings that fractured in the square eyebars were 93 percent effective on the average with a lower bound of 90 percent. The forgings in the rectangular eyebars were 87 percent effective on the average with a lower bound of 59 percent.

Two of the undamaged specimens had strain gages mounted on them in order to determine an approximation of the stress concentration factors in and around the eye. One eyebar, a square eyebar, had five strain gages mounted on it, and the second eyebar, a rectangular eyebar, had 11 strain gages mounted on it. The results from these strain gages are shown in Figs. 45, 46, and 47.

Table 6. Results of static tests on undamaged eyebars.


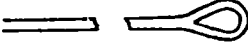
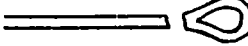
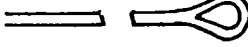
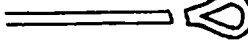
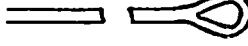
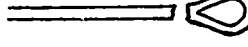
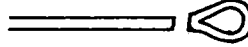
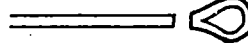
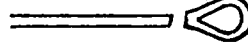
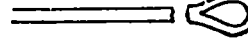
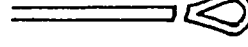
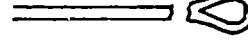
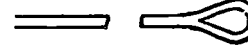
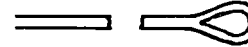
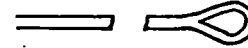
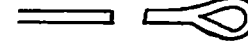


Identification Number	Dimensions	Yield Stress (ksi)	Ultimate Stress (ksi)	Location of Fracture
H21	7/8" x 7/8"	32.7	58.4	
A	3/4" x 3/4"	29.7	44.7	
H	3/4" x 3/4"	31.9	43.9	
B	1" x 1"	35.0	48.0	
D	1" x 1"	36.4	46.1	
E	1" x 1"	33.3	50.2	
F	1" x 1"	36.5	47.0	
I	2.1" x .8"	36.1	49.4	
J	2.1" x .8"	34.6	45.1	
K	2.1" x .8"	35.1	46.8	
L	2.1" x .8"	---	28.9	
M	2.1" x .8"	37.6	38.7	
T	2.1" x .8"	33.9	47.1	
N	7/8" Dia	35.9	50.4	
P	7/8" Dia	35.1	50.3	
Q	7/8" Dia	37.7	48.4	
S	7/8" Dia	33.4	50.0	
O	7/8" Dia	35.3	50.9	
R	7/8" Dia	35.5	44.6	

Table 7. Summary - static test results.

Type of Eyebars	Location of Fracture	Average Yield Stress	Range in Ultimate Stress	Average Ultimate Stress
Round	bar	35.5 ksi	44.6-50.0	49.1 ksi
Rectangular	forging	35.5 ksi	28.9-49.4	42.7 ksi
Square	bar	32.7 ksi	44.7-58.4	50.3 ksi
Square	forging	34.5 ksi	43.9-47.0	45.7 ksi

These graphs show that as the load increased the outside edge of the tip of the eye went into tension and the outside edge of the side of the eye went into compression. This was caused by the distorting of the eye as it conformed to the shape of the pin.

The stress concentration factor for the outside edge at the tip of the eye was approximately 1.8. The stress concentration factor for the inside edge of the side of the eye was found by extrapolation of the data from Fig. 46b to be approximately 2.2. This agrees with the results from the fatigue tests, where it was found that when the pin had a good fit in the eye, the maximum stress occurred on the inside edge of the side of the eye.

Damaged and Repaired Eyebars

Static tests were also performed on three damaged and repaired specimens of square cross-section. Each of the specimens was damaged and repaired by one of the methods described in Chapter 4. One of the specimens simulated a fracture and repair at the forging near a turnbuckle (Fig. 21). Upon loading, this specimen fractured in the bar away from the repair. The ultimate stress was 48.5 ksi based on

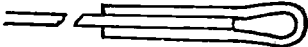
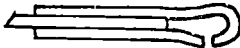

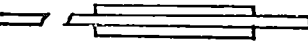
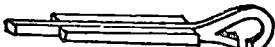
the original cross section of the bar. The second specimen simulated a fracture and repair at the forging near an eye (Fig. 22). Upon loading, this specimen fractured in the bar next to the repair. The ultimate stress was 48 ksi. The eyebar was reloaded, this time gripping the bar in the repair. The failure occurred in the eye this time at a load that would have been the equivalent of 83 ksi in a bar which had the same cross section as the original bar. This shows that the eye is much stronger than the bar. This would be expected since a cross section through the eye has an equivalent area of two bars. This would be 41.5 ksi in the cross section of the eye.

The third specimen simulated a fracture in the eye and a repair by welding on a new eye (Fig. 23). Upon loading, the specimen fractured in the bar away from the repair. The ultimate stress was 47.3 ksi. The specimen was reloaded by gripping in the repair. This time the specimen fractured in the new eye at a load that would have been an equivalent 115.4 ksi in the bar. This would be approximately 57 ksi in the eye assuming double the area in the cross section of the eye.

The ultimate strength of the eyebars is slightly less than that listed in Table 1 because the stress in the eyebars was calculated using the gross cross section of the bar. This shows that after several years of rusting and corroding, the eyebars are still a nominal 94 percent effective.

The results of the static tests on damaged and repaired eyebars are shown in Table 8. It can be seen from this table that if repairs to damaged eyebars are made similarly to those used in these tests, then the ultimate strength of the eyebar will be unaffected by the repair.

Table 8. Results of static tests on damaged and repaired eyebars.

Identification Number	Type of Repair*	Dimensions	Yield Stress (ksi)	Ultimate Stress (ksi)	Ultimate Force (kips)	Location of Fracture
U ₁	3	3/4"x3/4"	32.1	47.3	26.5	
U ₂	3	3/4"x3/4"	--	--	64.6	
V	1	1"x1"	33.8	48.5	48.5	
W ₁	2	1"x1"	36.8	48.0	48.0	
W ₂	2	1"x1"	--	--	83.0	

- *
 1 indicates damage and repair to a forging near a turnbuckle (Fig. 21)
 2 indicates damage and repair to a forging at an eye (Fig. 22)
 3 indicates damage and repair to an eye (Fig. 23)

CHAPTER 6. SUMMARY AND CONCLUSIONS

Summary

As a result of the construction of the Saylorville Dam and Reservoir on the Des Moines River, six highway bridges were scheduled for removal. Two of these, old high-truss single-lane bridges, were selected for a testing program which included service load tests in the field and fatigue and static tests on tension eyebars in the laboratory.

The purpose of the service load tests was to relate design and rating procedures presently used to the field behavior of this type of truss bridge. Another objective of this phase of the program was to provide data on the behavior of this bridge type in the service load range and also, data on the remaining fatigue life of the tension members in the truss.

The information available on service-load behavior of actual bridges is limited mainly to beam-and-slab type bridges. This test program was intended to provide information on the behavior of high-truss bridges.

The test program consisted of service load testing two spans of the Hubby Bridge plus one span of the Chestnut Ford Bridge, and fatigue and static testing eyebars received from the above mentioned bridges. The service load tests were performed using loaded county gravel trucks (approximately H15) to apply the loads to the bridges.

Strain readings were taken to determine the forces in members of the trusses. Also, deflection readings were taken of the trusses in one span and of the deck and strain readings in the floorbeams to determine the moments.

The experimental forces in the members of the truss agreed with the forces found theoretically using a determinate analysis. There were some discrepancies but these were mainly due to problems in the instrumentation. The experimental deflections of the trusses in one span were found to be much smaller than the theoretical deflections. This was due to the partial continuity of the deck which was not taken into account in the theoretical analysis, and also due to the partial rigidity of the joints.

Deck deflections were measured at the middle of the panels with the truck on the centerline of the bridge and on the edges of the bridge. The experimental deflections were between the theoretical values for stringers assuming fixed ends and assuming pinned ends. The behavior of the deck compared quite well with that predicted by the AASHTO Specifications³. The current load distribution criteria, assuming $S/4$ as the distribution factor, indicates that for the Hubby Bridge each stringer should be designed for about 14 percent of the total weight of the truck (28 percent of a wheel load, front and rear). The test results indicated a distribution value of 10 percent to each stringer for both the centered load and the eccentric load. For the Chestnut Ford Bridge however, the current load distribution criteria, assuming $S/4.5$ as the distribution factor, indicates that each stringer should be designed for 14 percent of the total weight of the truck. The test results indicate a value of 14 percent for the centered load and 19 percent for the eccentric load.

Moment cross sections for the floorbeams were found experimentally with the rear axle of the truck located over the floorbeams. The experimental results were between the theoretical values for a floorbeam

assumed fixed at the ends and assumed pinned at the ends. Floorbeams 3 and 5 from the Hubby Bridge tended to behave more closely to the pinned end assumption while floorbeams 4 and 6 tended to agree more closely with the fixed end assumption.

In the fatigue tests of the tension eyebars it was found that the eye of the eyebar tended to be more susceptible to fatigue failure than the forgings at the intersection between the eye and the bar. Twenty-one of the 23 undamaged eyebars fractured in the eye while the remaining two eyebars fractured in forgings, where large initial cracks were present. Of the nine eyebars that were damaged and repaired and then tested in fatigue, only one eyebar failed in the first repair and it was a repair that had been made in the field over 40 years ago.

In the static tests different types of eyebars were found to fail in different fashions but consistent for the particular type. All of the rectangular eyebars fractured in the forgings while all of the round eyebars fractured in the bars away from the forgings. The square eyebars fractured both in the forgings as well as in the bars. The minimum percentage of effectiveness found in the tests was 59 percent. This compares with the 40 percent effective rule usually assumed for rating of eyebars as commonly used in Iowa.

The fatigue strength of the eyebars varied over a wide range, but it was seen that for a stress range of 14 ksi, the fatigue life of the eyebars was approaching 2,000,000 cycles. On the Hubby Bridge, an H 10.7 truck, in the eccentric position with an included impact factor of 30 percent will produce a live load stress range in a hanger of 14 ksi stress range. For the Chestnut Ford Bridge an H 18.3 will

produce the same stress range. Assuming 10 loaded trucks of this type a day, every day of the year, it would take 28 years to reach 100,000 cycles.

It can be seen from this that the weight of this type of truck is substantially more than that usually carried by the bridge and, thus, it would not be expected that there would be any reduction in the fatigue life of the members. This was observed in the overall results of the fatigue study.

Conclusions

As a result of the service load tests and the supplementary tests, the following conclusions were reached:

1. Fatigue fractures tend to be governed by the characteristics of the eye while the static fractures tend to be governed by the quality of the forgings.
2. The fatigue life of the eyebars after being damaged and repaired was not appreciably different from that of an undamaged eyobar.
3. The experimentally determined forces of the truss members for both the Hubby Bridge and Chestnut Ford Bridge agree closely with the forces found from the theoretical analysis assuming pinned connections, this indicates that the assumption of pinned end members is valid for these particular trusses.
4. Since the truck used for the experimental loading was approximately an H 15 truck and all ratings for the critical bridge components provided by the cooperating agencies² were less than an H 15 (ranged from H 2 - H 13) the results show that the determinate assumption used is valid for analyzing the bridge for the loads in the range of rating levels.

5. The current practice of assuming the "lap", or forging, in an eyebar to be only 40 percent effective is conservative. The minimum found during testing was 59 percent. The average effectiveness of all the eyebars which fractured in the forgings was 89 percent. The average effectiveness of all the eyebars tested was 94 percent.
6. The current AASHTO Load Distribution criteria for the Hubby Bridge of S/4 is more than adequate (S/4.5 could be used if it is considered to be a multiple layer bridge deck).
7. The current AASHTO Load Distribution criteria for the Chestnut Ford Bridge deck of S/4.5 (strip type deck) agrees very closely to the centrally loaded truck but does not agree with the truck when in the eccentric position. This may be misleading in that the maximum deflection measured in each case was essentially the same (i.e., the same maximum moment).

REFERENCES

1. Sanders, W. W., Jr. and H. A. Elleby. "Feasibility Study of Dynamic Overload and Ultimate Load Tests of Full-Scale Highway Bridges." Final report to Iowa State Highway Commission, Engineering Research Institute, Iowa State University, Ames, January 1973.
2. Sanders, W. W., Jr., F. W. Klaiber, H. A. Elleby and L. W. Timm. "Ultimate Load Behavior of Full-Scale Highway Truss Bridges: Phase I - Ultimate Load Tests of the Hubby Bridge - Boone County." Interim Report to Iowa State Highway Commission, Engineering Research Institute, Iowa State University, Ames, April 1975.
3. American Association of State Highway Officials. Standard Specifications for Highway Bridges - Eleventh Edition. American Association of State Highway Officials, Washington, D.C., 1973.
4. American Association of State Highway Officials. Manual for Maintenance Inspection of Bridges. American Association of State Highway Officials, Washington, D.C., 1970.
5. Hetenyi, M. I., Beams on Elastic Foundation; Theory with Applications in the Fields of Civil and Mechanical Engineering. The University of Michigan Press, Ann Arbor, 1946.

ACKNOWLEDGMENTS

This report summarizes the results of the second phase of a research program designed to study the ultimate load behavior of full-scale highway truss bridges. The program is being conducted by the Engineering Research Institute of Iowa State University and is funded by the Highway Division-Iowa Department of Transportation and the Federal Highway Administration with supplemental funding by the Engineering Research Institute. In addition to these direct sponsors, services were provided for the research by Boone County (County Engineer's Office), Dallas County (County Engineer's Office), and the U.S. Army - Corps of Engineers. The Hubby Bridge and the Chestnut Ford Bridge were provided through the cooperation of these agencies.

The staff for the University were all from the Structural Engineering Section of the Department of Civil Engineering. The principal staff included Dr. W. W. Sanders, Jr. (Project Investigator), Dr. H. A. Elleby (Co-Investigator), and Dr. F. W. Klaiber. Assisting in the research were faculty members (Dr. M. L. Porter, Dr. L. F. Greimann and Professor D. D. Girton), graduate students (L. W. Timm, M. D. Reeves, J. P. Sorenson, L. P. Selberg, and K. A. McDowell), and undergraduate students (T. C. Wilson and J. W. Coleman).

An Advisory Committee was formed to assist and guide the research program. The committee consisted of representatives of the affected agencies and included:

- W. W. Sanders, Jr., Iowa State University (Chairman)
- H. A. Elleby, Iowa State University
- S. E. Roberts, Iowa Department of Transportation
- J. P. Harkin, Iowa Department of Transportation
- E. J. O'Connor, Iowa Department of Transportation

W. D. Ashton, U.S. Army - Corps of Engineers
S. S. Bhala, Federal Highway Administration
C. F. Schnoor, Boone County (County Engineer)
G. R. Hardy, Dallas County (County Engineer)
R. E. Van Gundy, Polk County (County Engineer)

The authors wish to express their appreciation to their University colleagues, the members of the Advisory Committee, and the representatives of all cooperating agencies for their support and efforts during this research. Appreciation is also due C. F. Galambos of the Office of Research, FHWA for his encouragement and comments. Special appreciation is expressed to C. F. Schnoor, Boone County Engineer, G. R. Hardy, Dallas County Engineer, and W. D. Ashton, Corps of Engineers, for their many efforts in making this program a success.

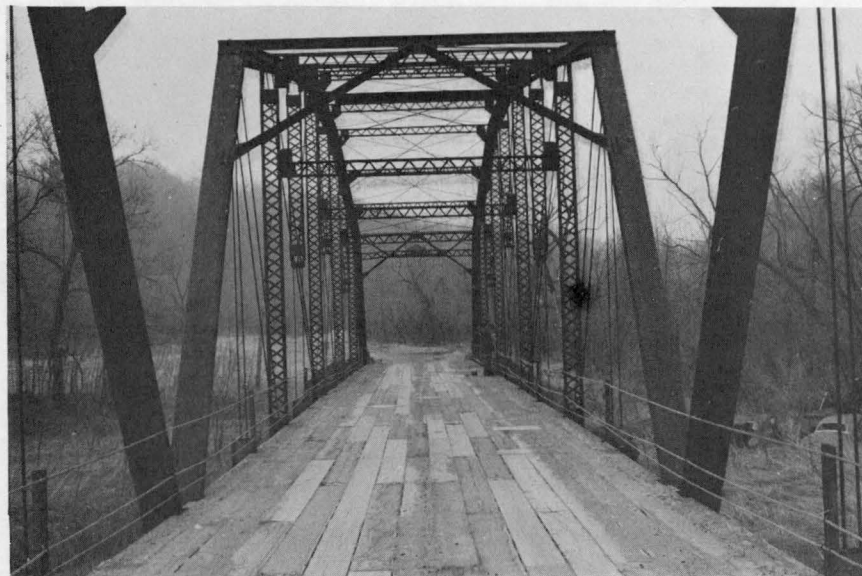
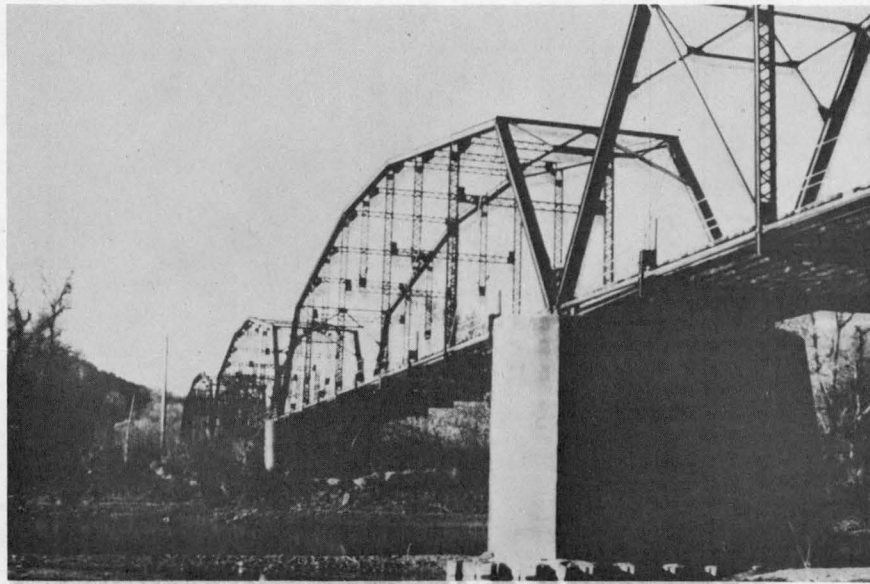
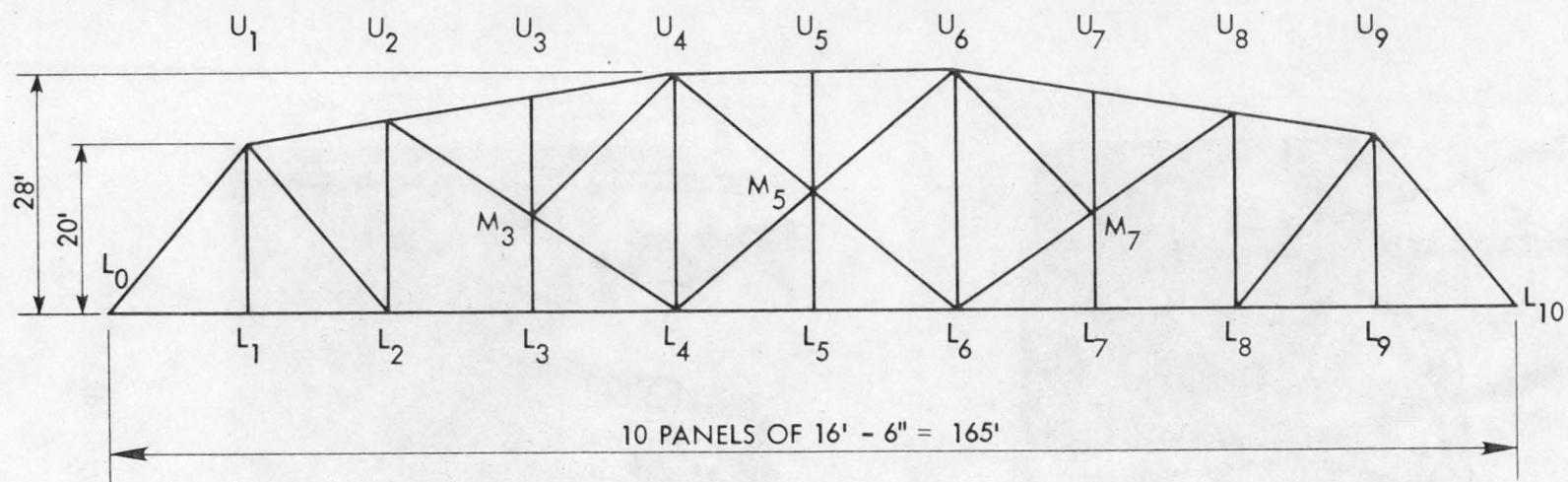
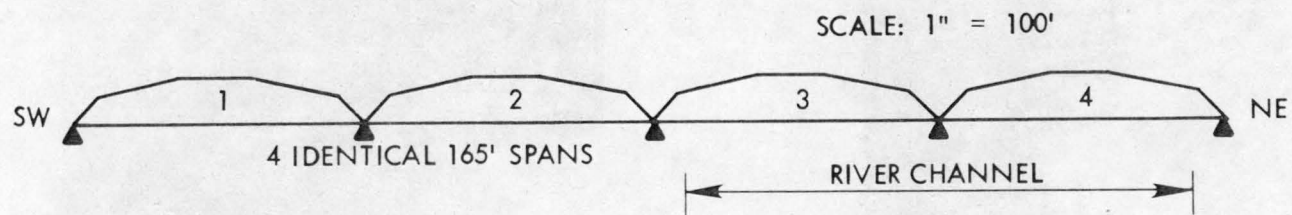


Fig. 1. Photographs of the Hubby Bridge.



a. Member Layout



b. General Layout

Fig. 2. Details of the Hubby Bridge.

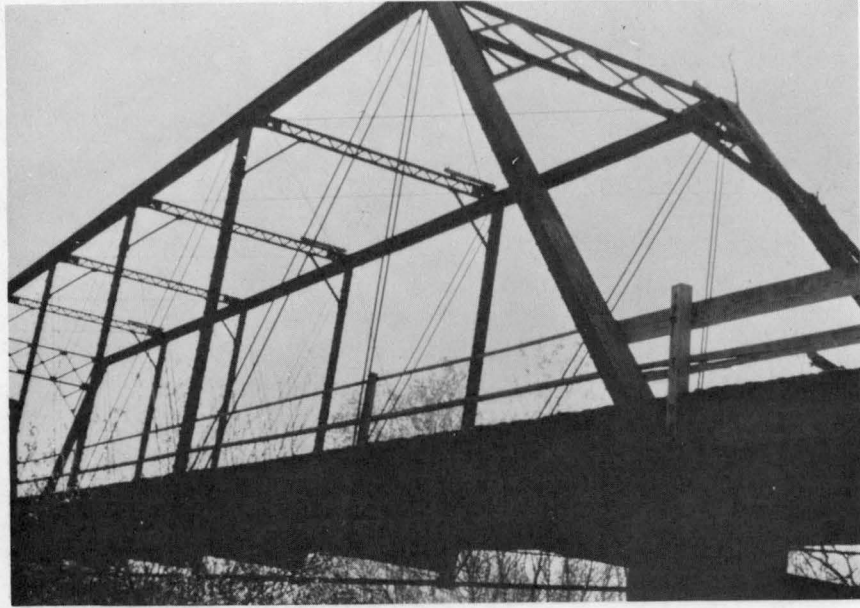
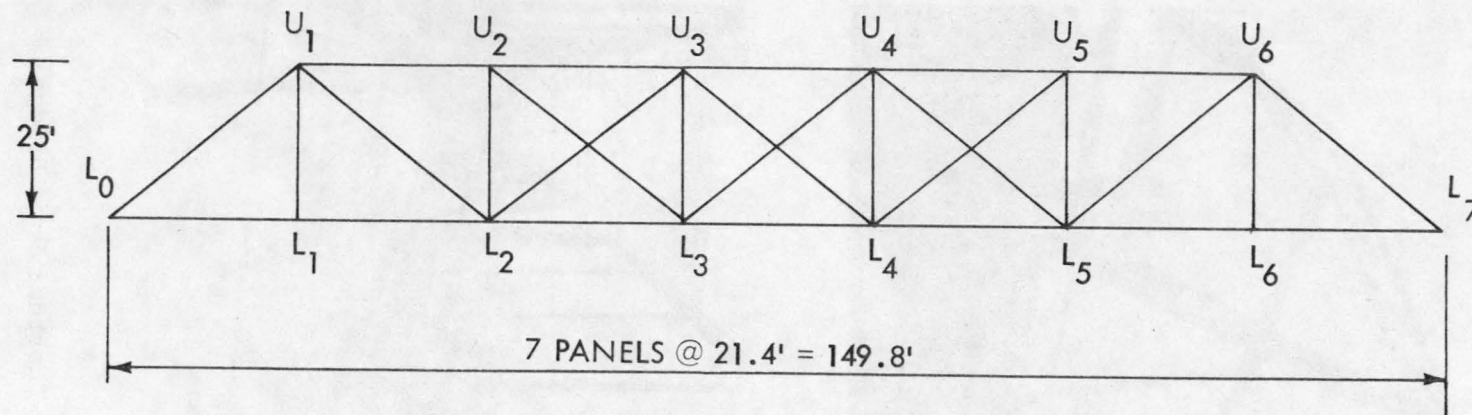
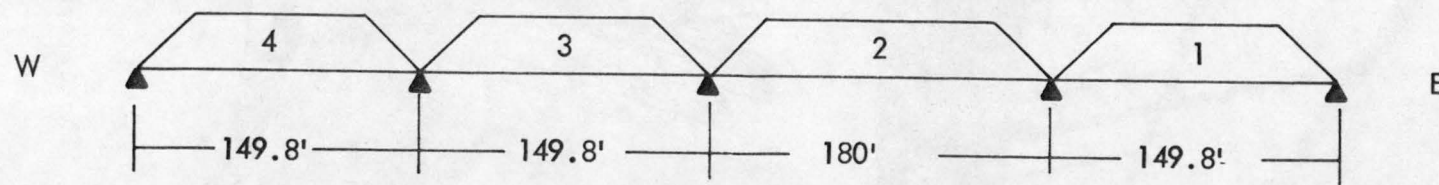


Fig. 3. Photographs of the Chestnut Ford Bridge.

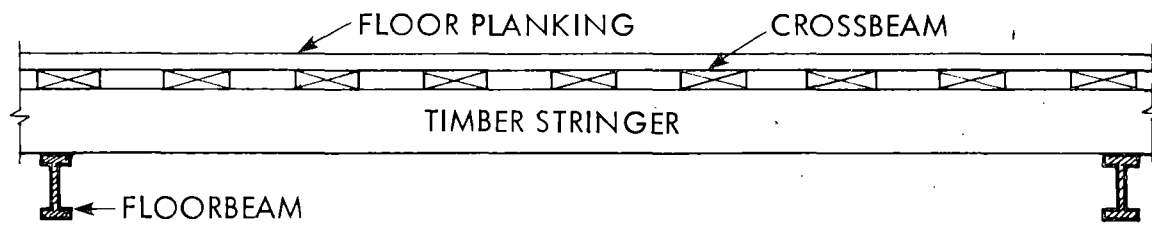


a. Member Layout (Spans 1, 3, 4)



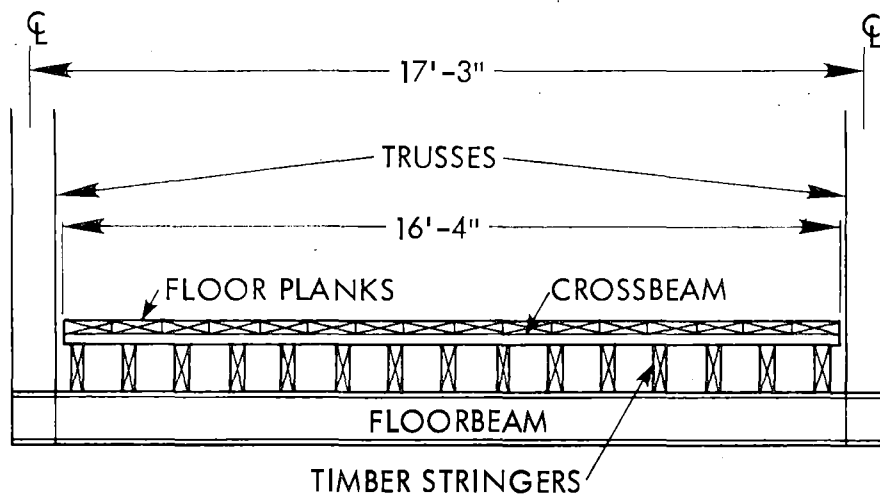
b. General Layout

Fig. 4. Details of the Chestnut Ford Bridge.



SCALE: 1" = 3'

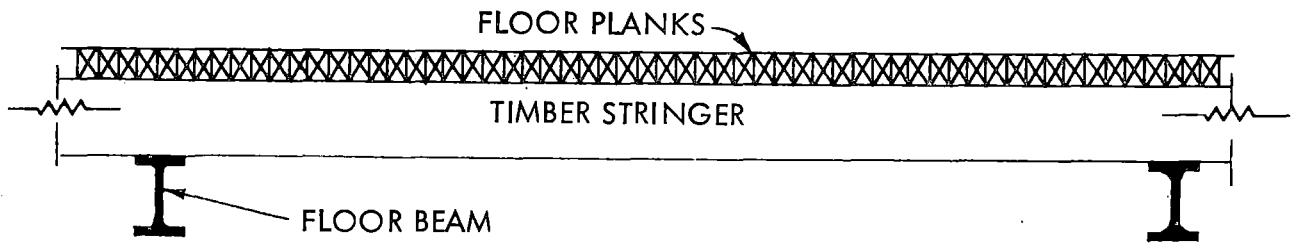
a. Elevation view.



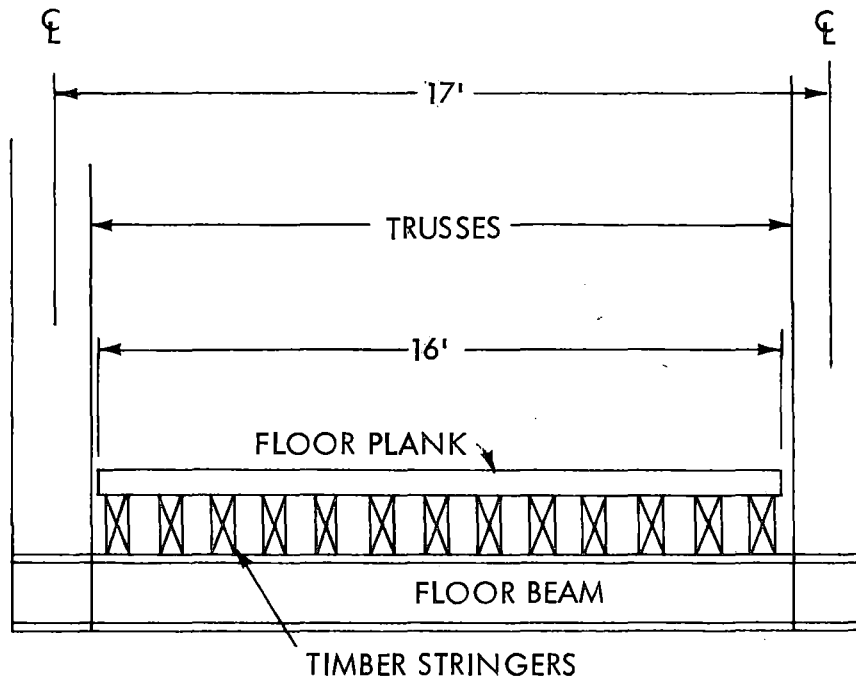
SCALE: 1" = 4'

b. End view.

Fig. 5. Timber deck layout - Hubby Bridge.



a. Elevation View



b. End View

Fig. 6. Timber deck layout - Chestnut Ford Bridge.

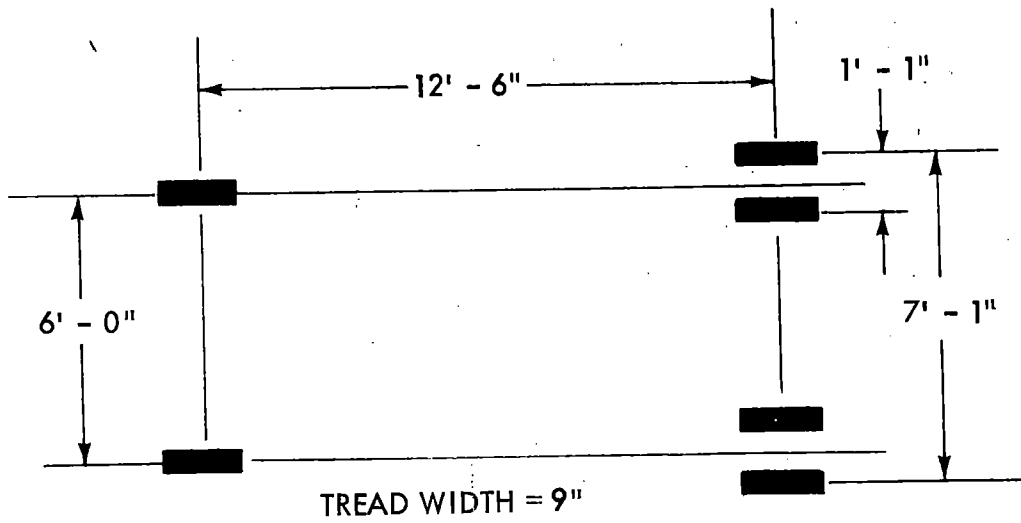


Fig. 7. Description of truck for Hubby Bridge testing (wheel locations).

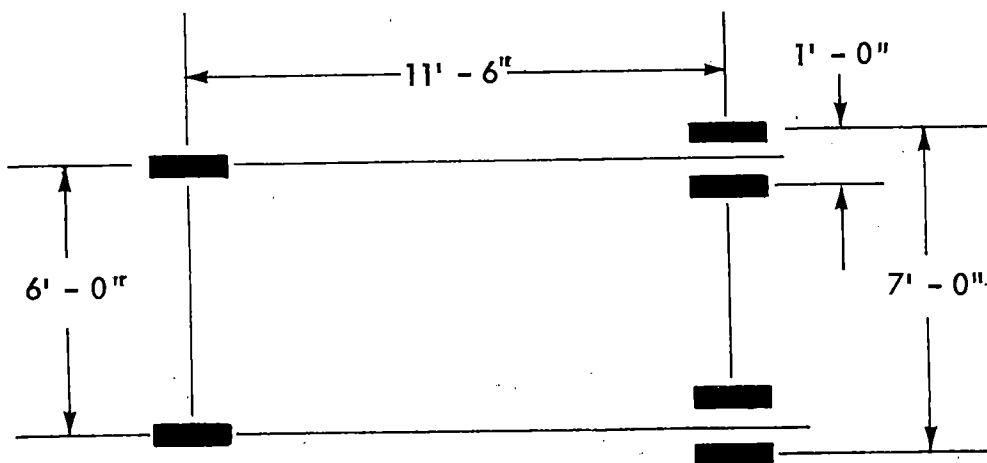


Fig. 8. Description of truck for Chestnut Ford Bridge testing (wheel locations).

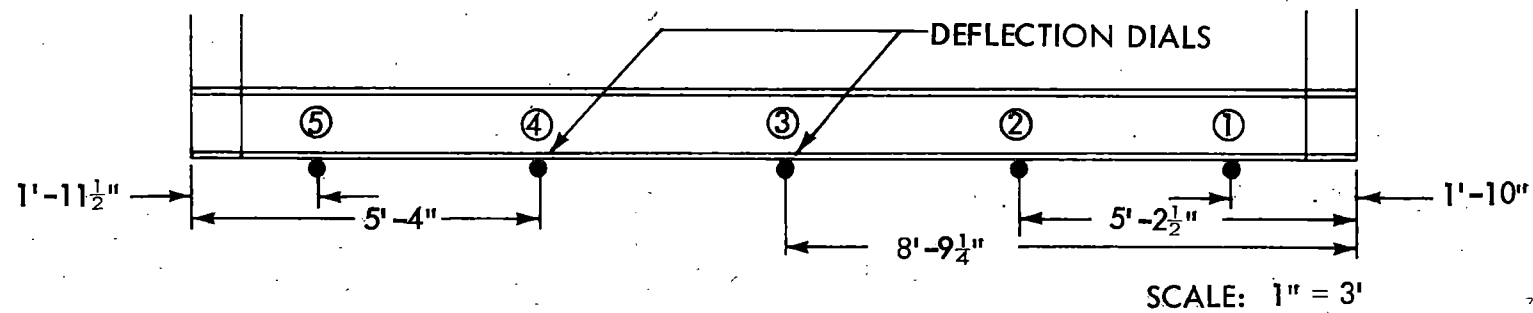


Fig. 9. Location of deflection dials for Span 1 - Hubby Bridge.

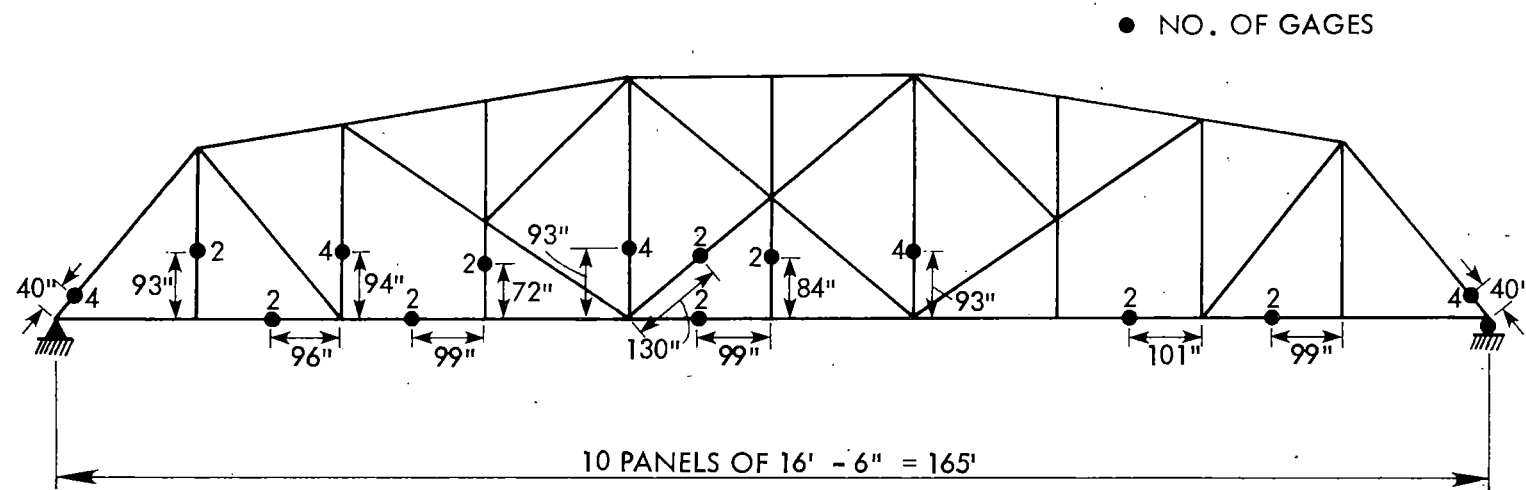


Fig. 10. Location of strain gages on Span 1 - Hubby Bridge.

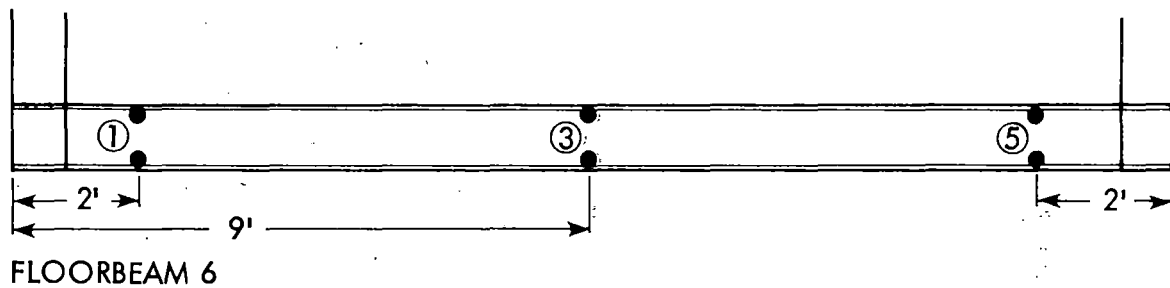
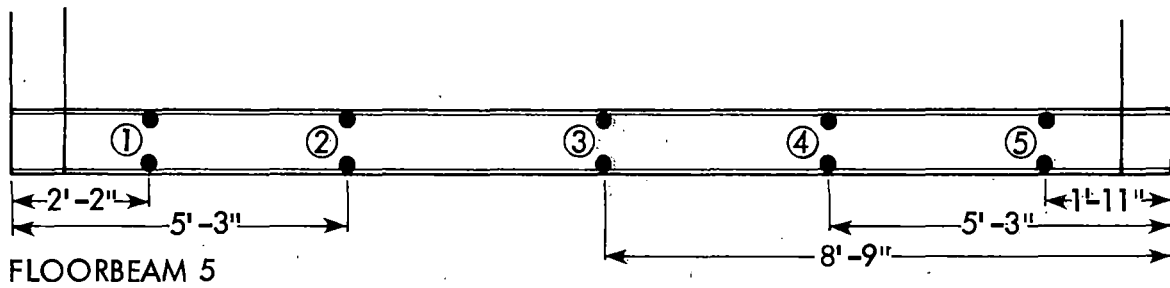
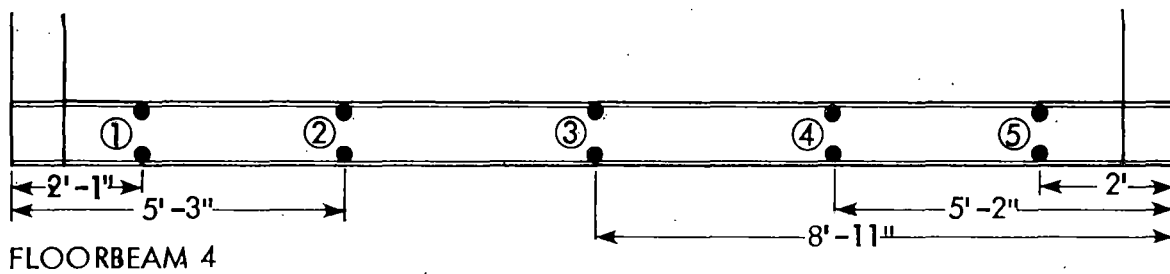
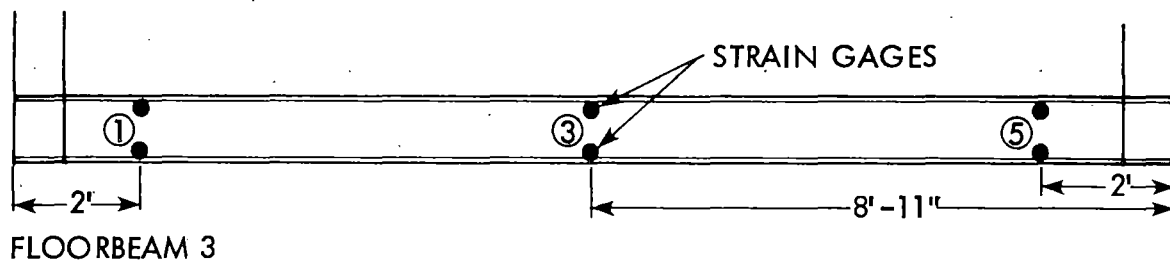


Fig. 11. Location of strain gages on floorbeams in Span 1 - Hubby Bridge.



Fig. 12. Photograph of truck being weighed.



Fig. 13. Photograph of truck on the centerline of the bridge.



Fig. 14. Photograph of truck on the edge of the bridge.

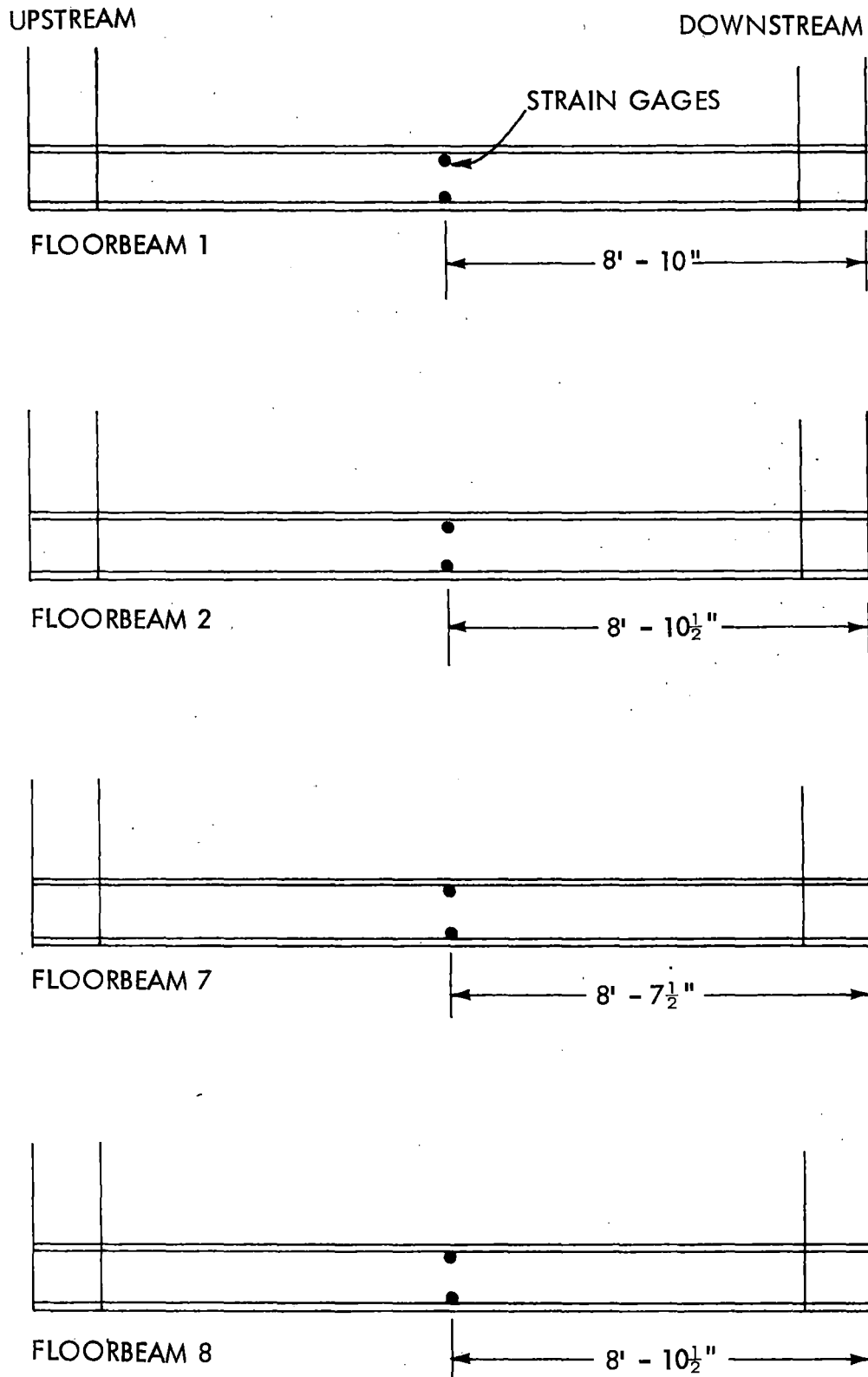


Fig. 15. Location of strain gages on floorbeams in Span 2 - Hubby Bridge.

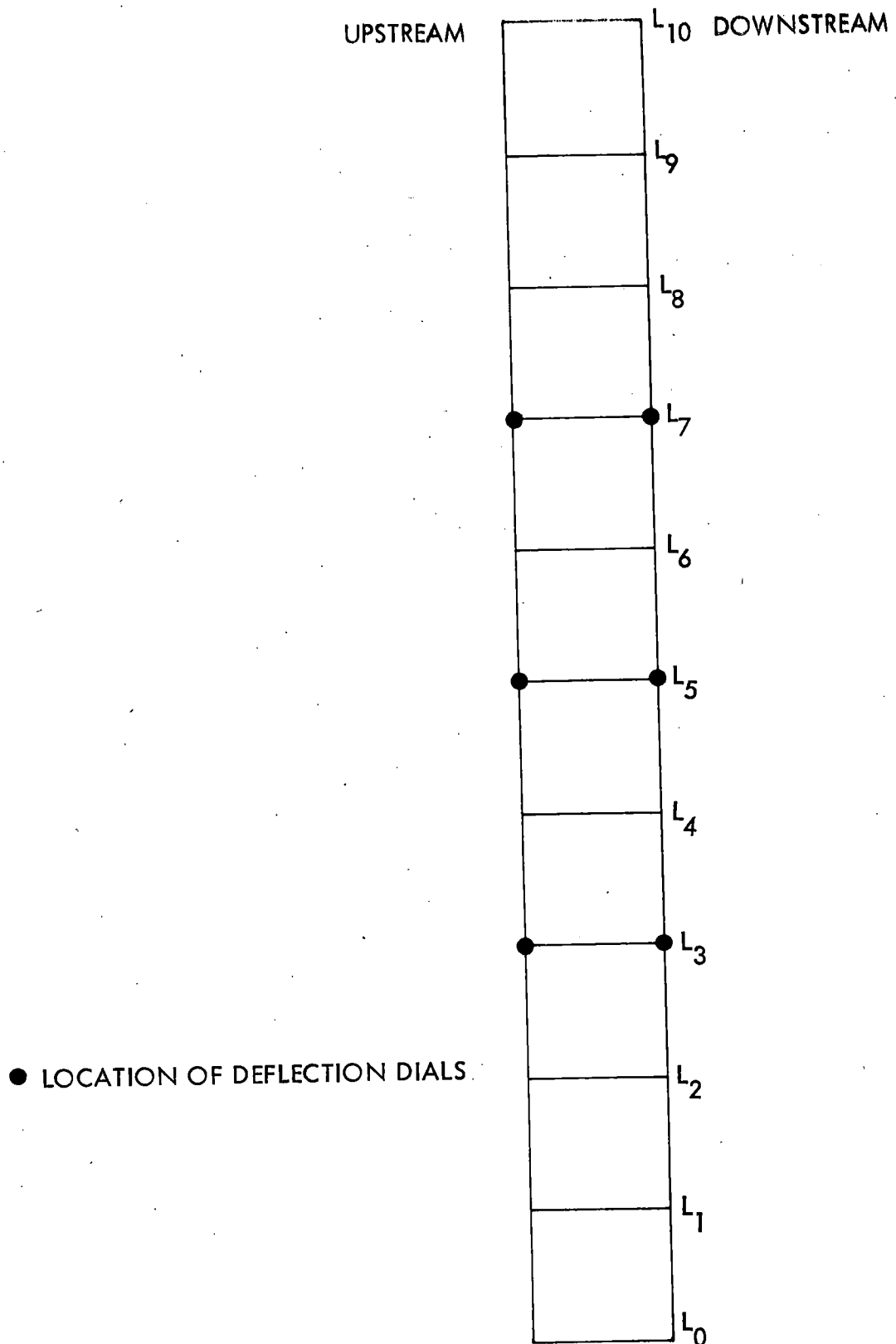


Fig. 17. Location of deflection dials for Span 2 - Hubby Bridge.

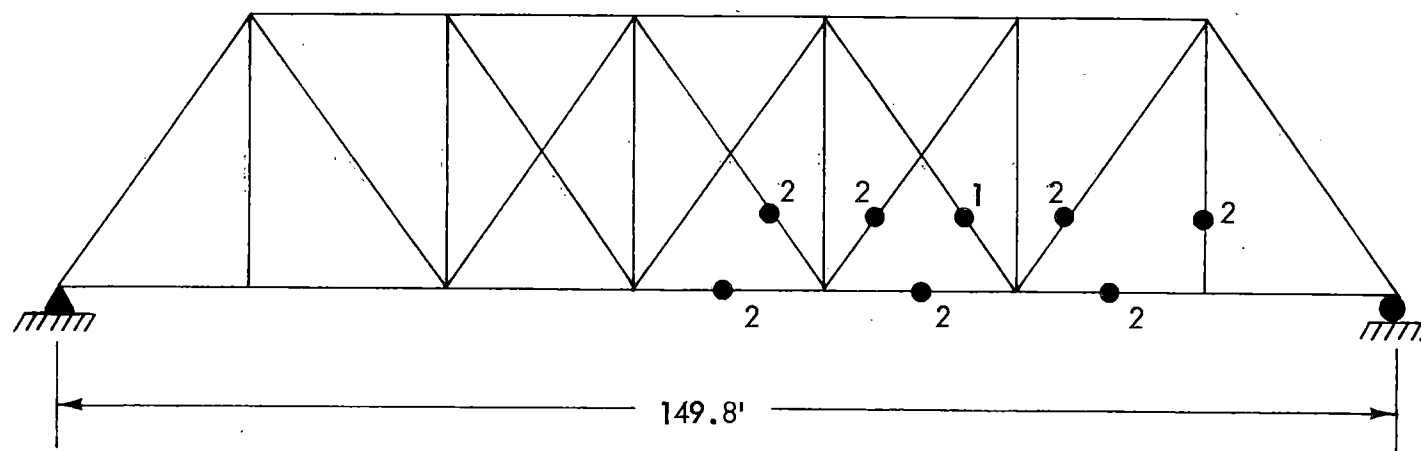


Fig. 18. Location of strain gages on Chestnut Ford Bridge.

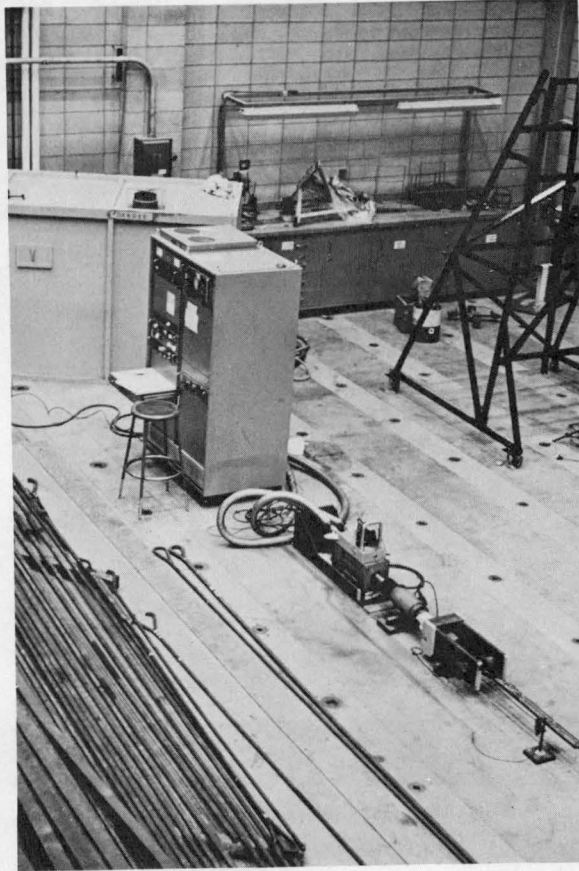


Fig. 19. Photograph of fatigue apparatus.

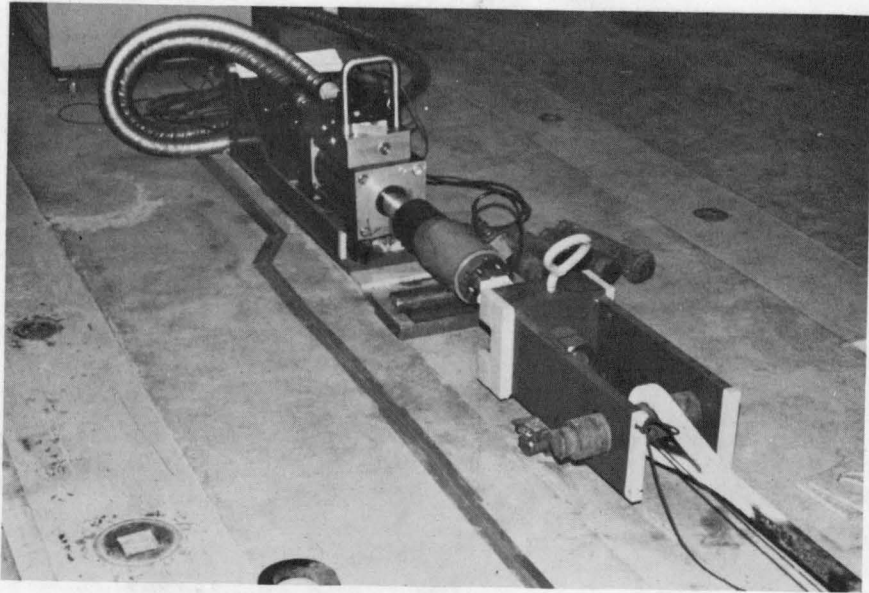


Fig. 20. Photograph of pin in fatigue test apparatus.

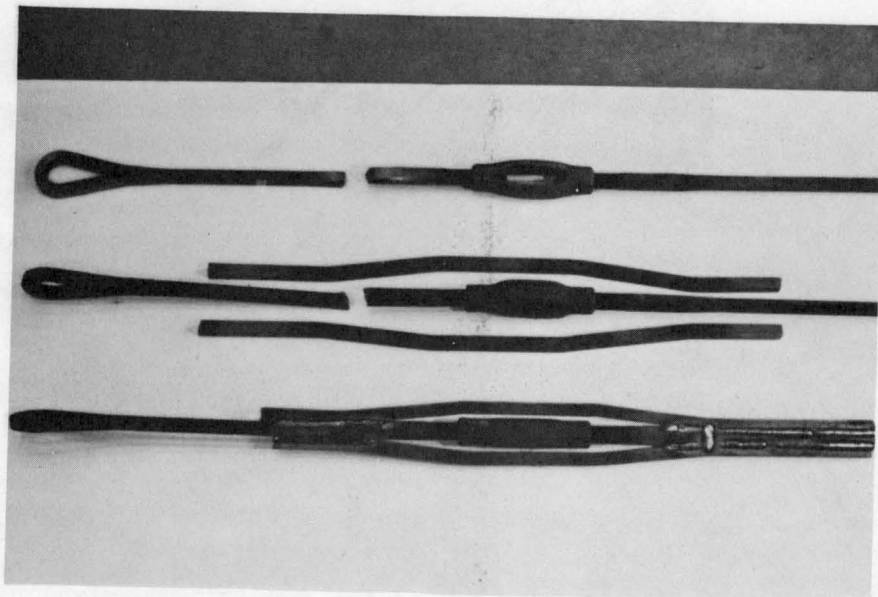


Fig. 21. Photograph showing the repair for a fracture in the forging at a turnbuckle.

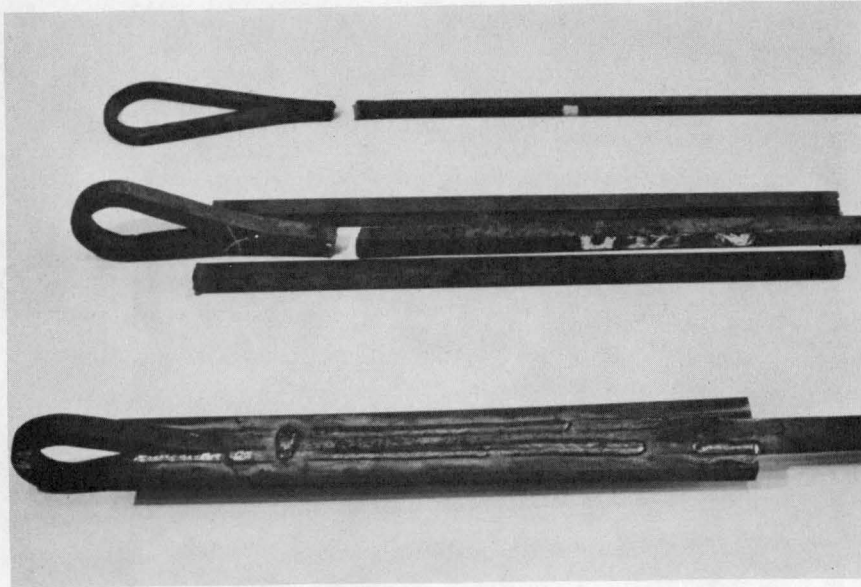


Fig. 22. Photograph showing the repair for a fracture in the forging at the neck of an eye.

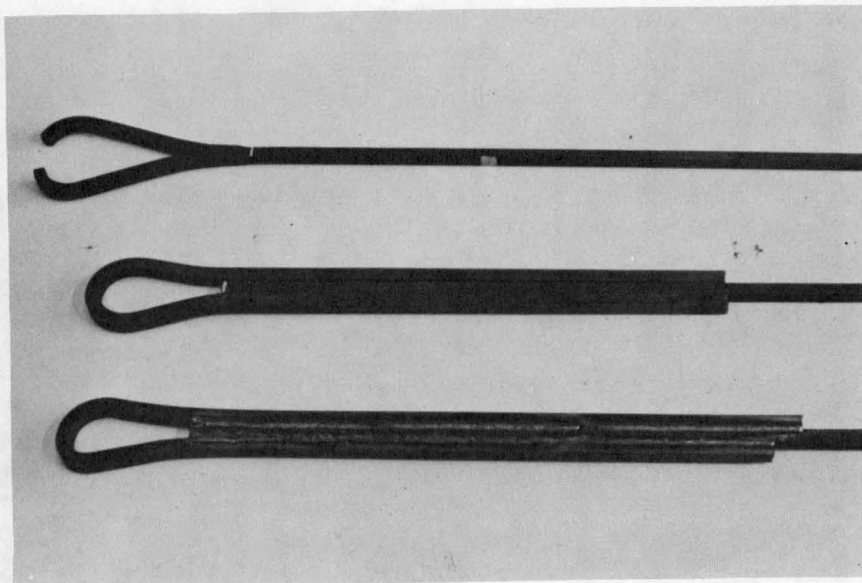


Fig. 23. Photograph showing the repair for a fracture in the eye of an eyebar.

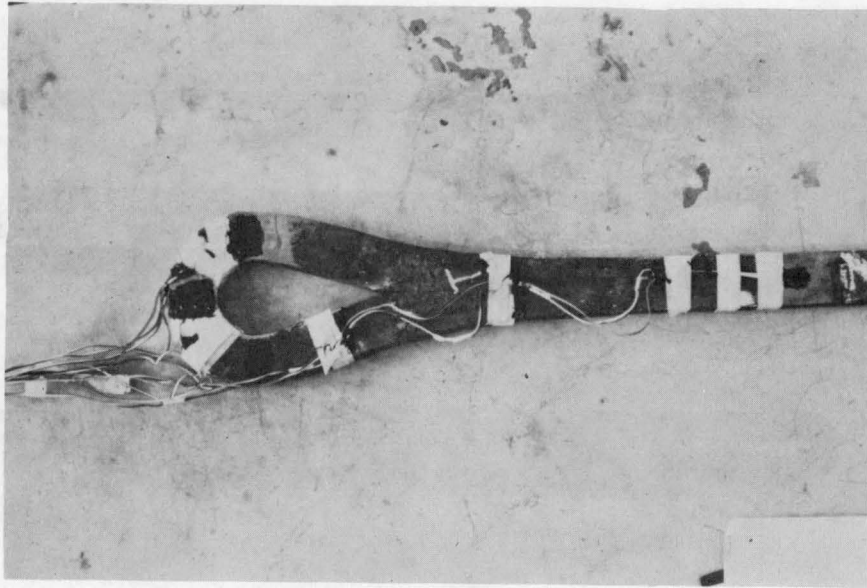


Fig. 24. Photograph showing typical static test specimen with strain gages.

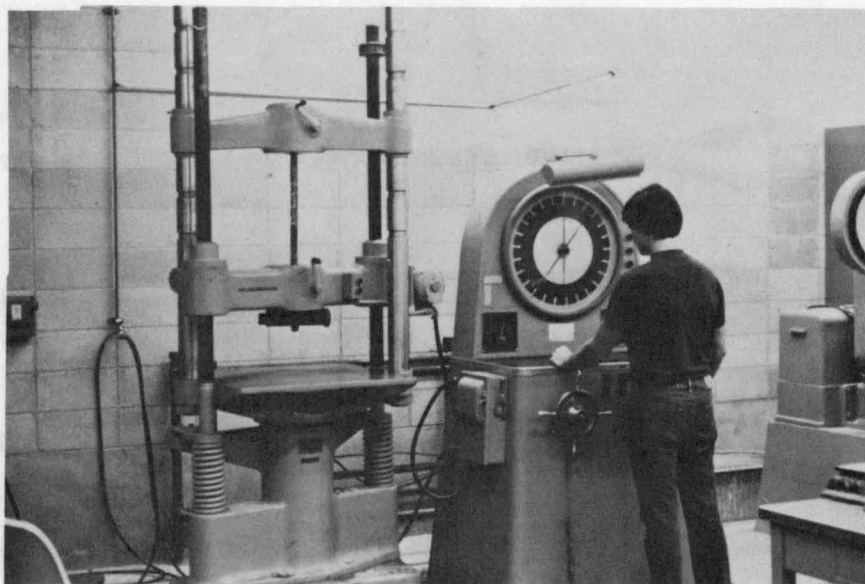


Fig. 25. Photograph showing static test apparatus.

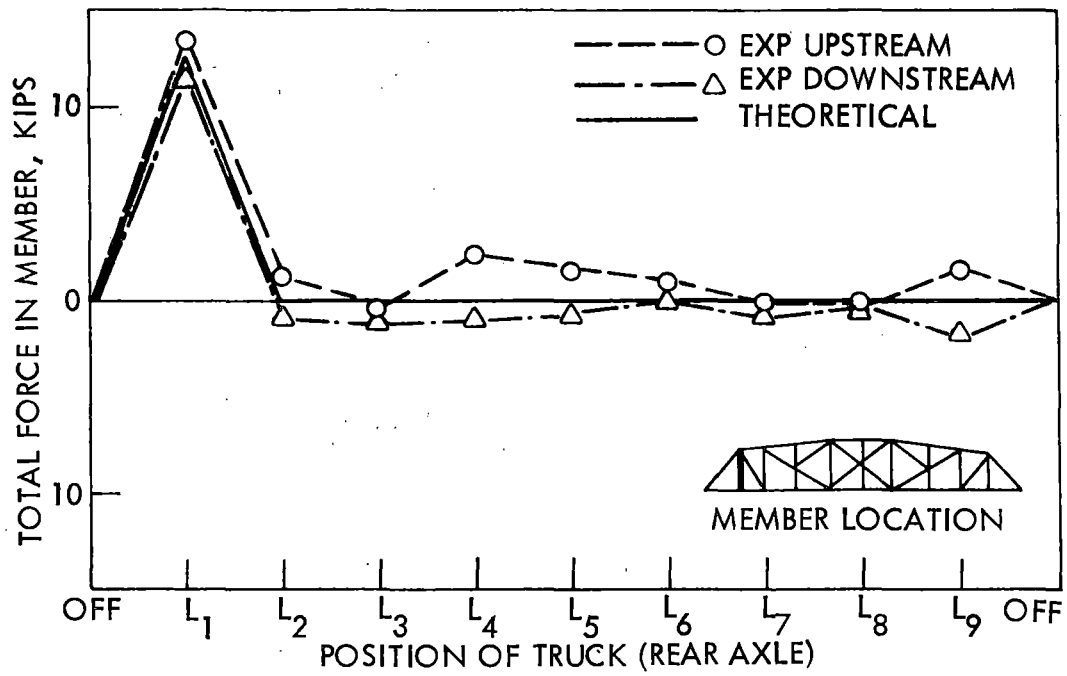
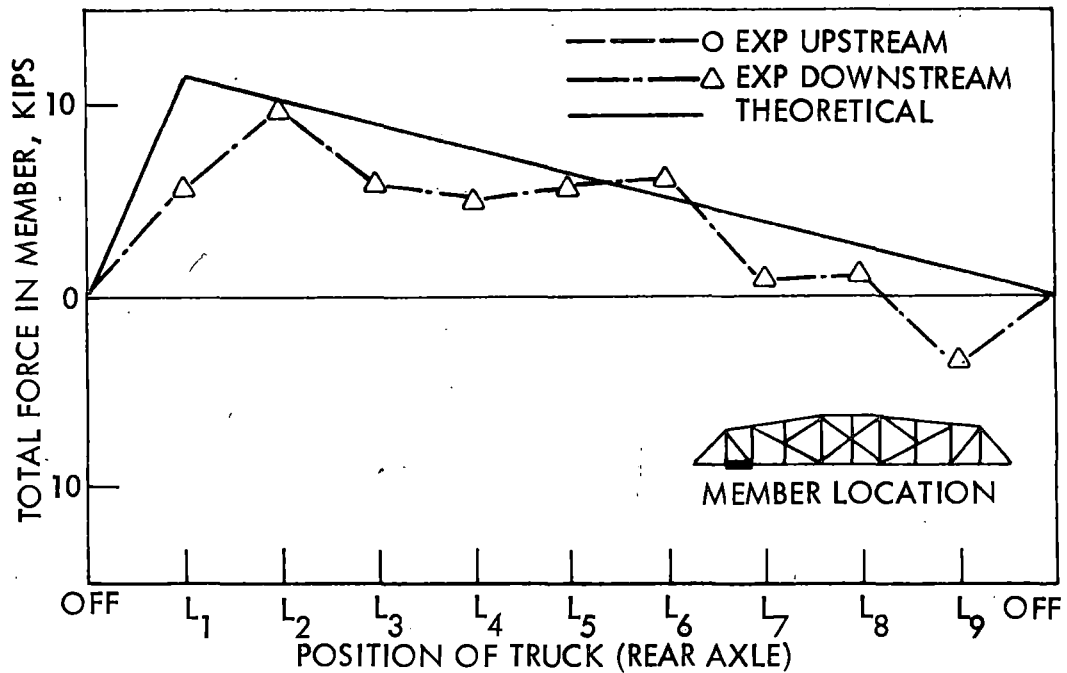
a. Member L_1U_1 b. Member L_1L_2

Fig. 26. Influence lines for Span 1 - Hubby Bridge.

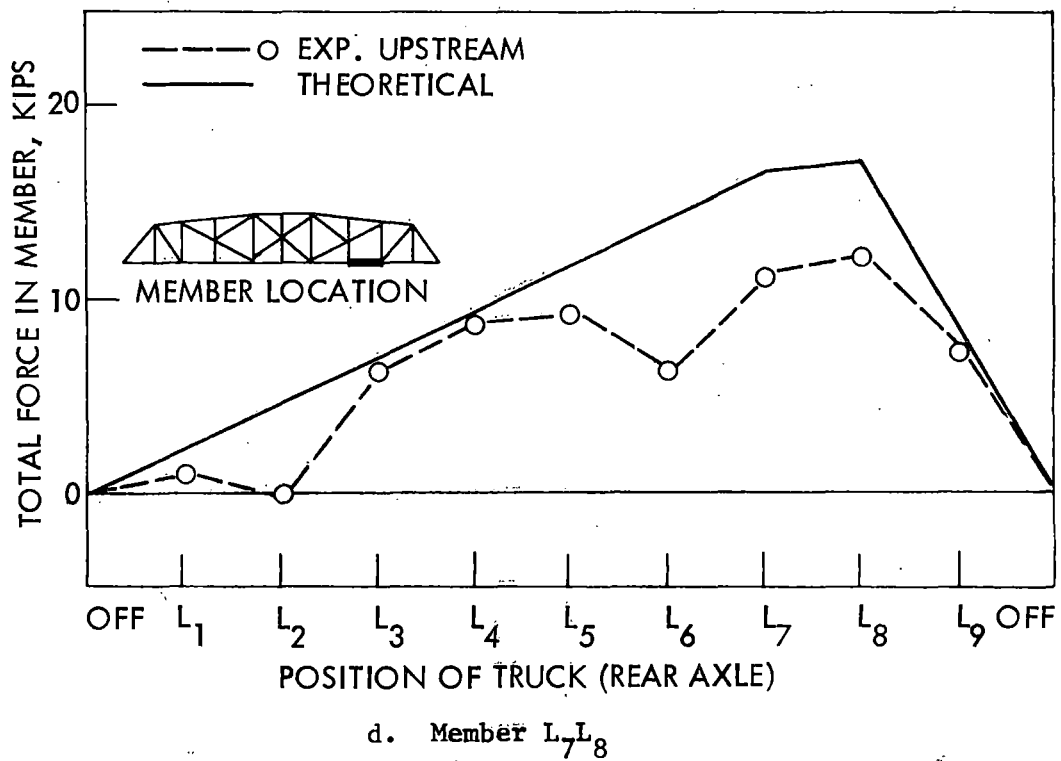
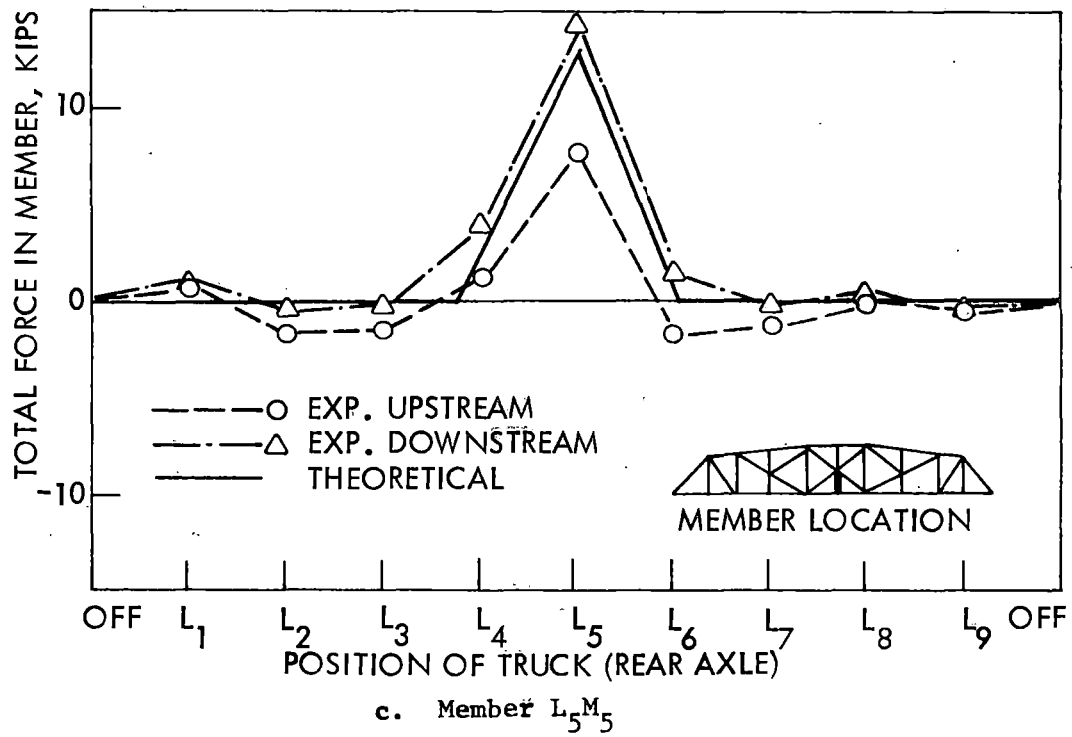


Fig. 26. Cont.

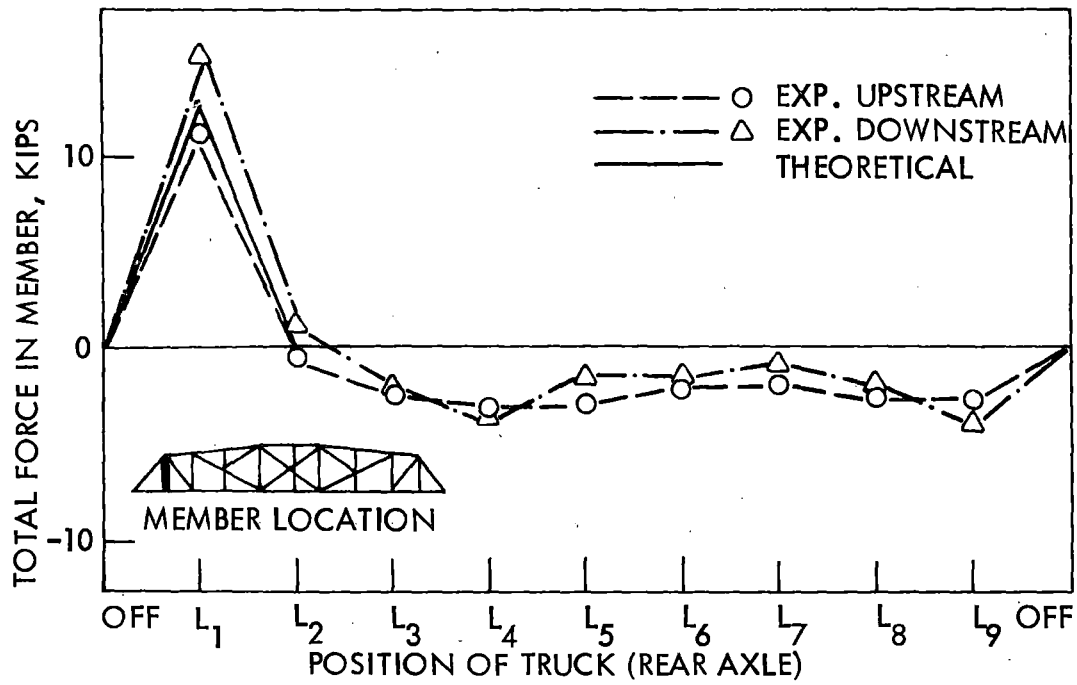
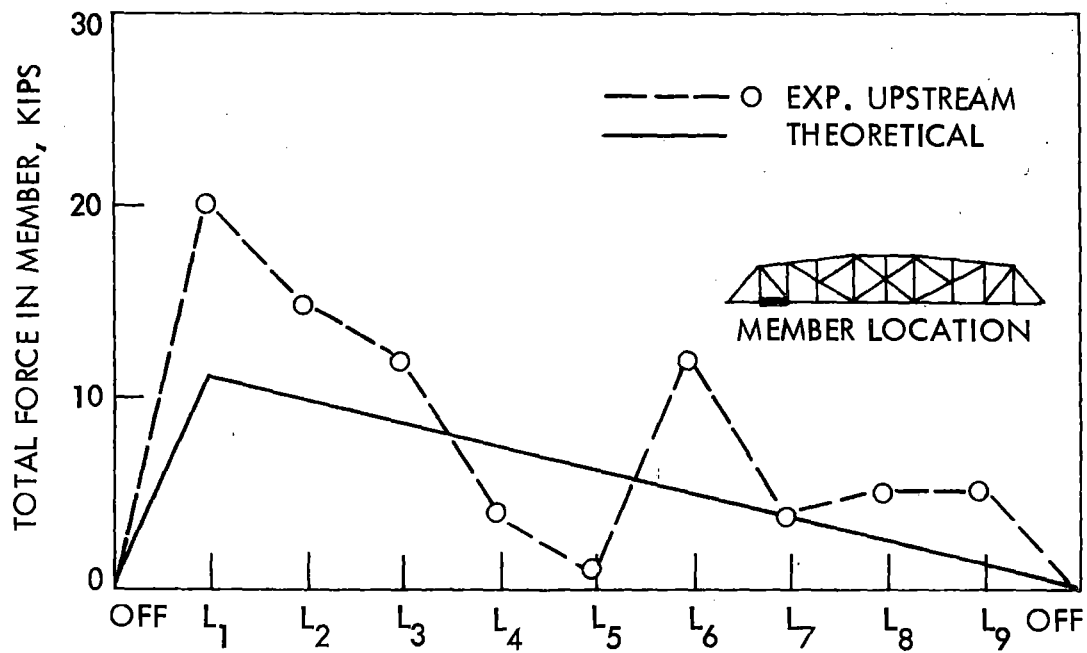
a. Member L_1U_1 b. Member L_1L_2

Fig. 27. Influence lines for Span 2 - Hubby Bridge.

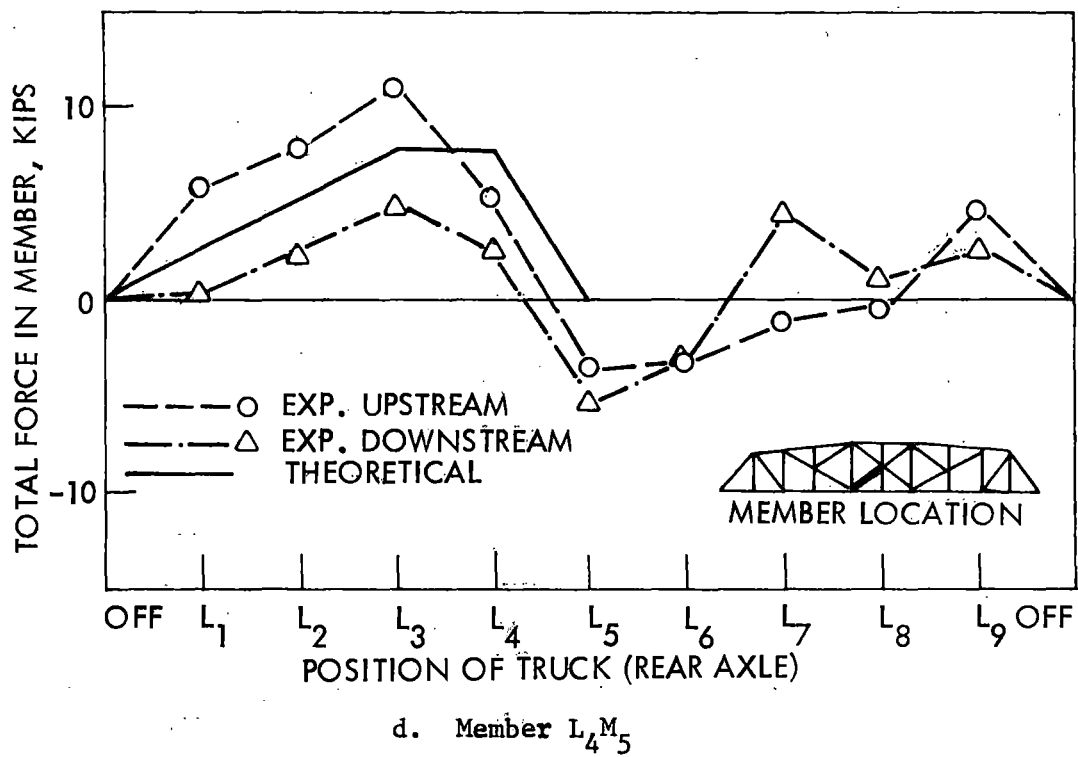
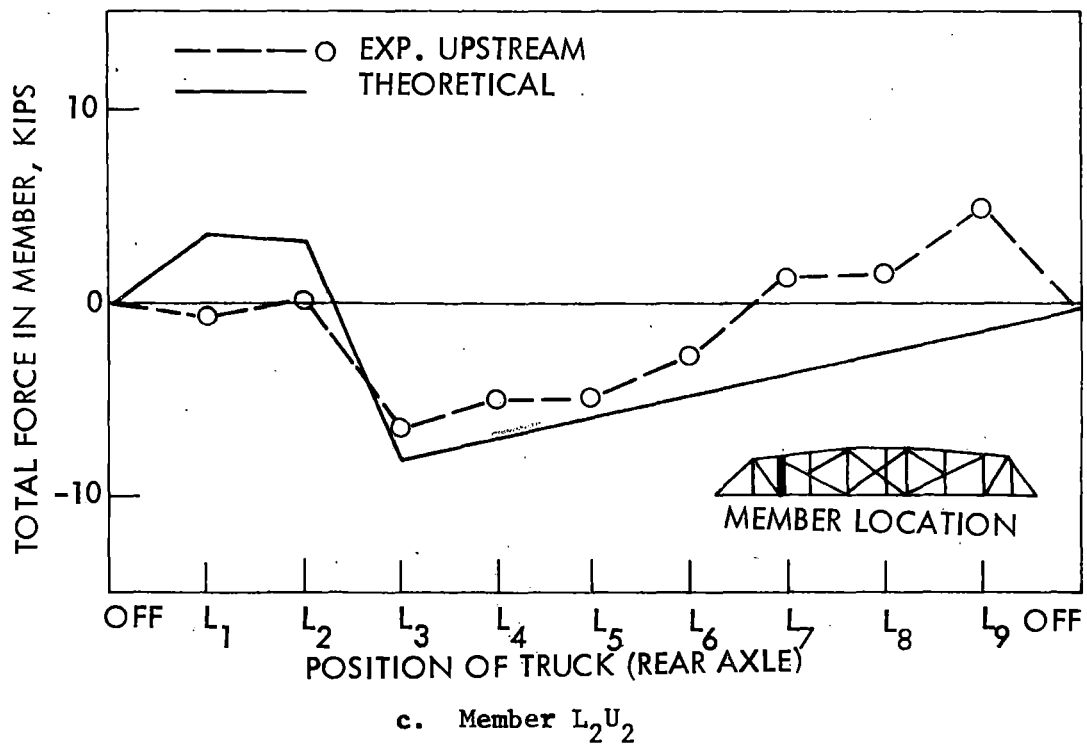


Fig. 27. Cont.

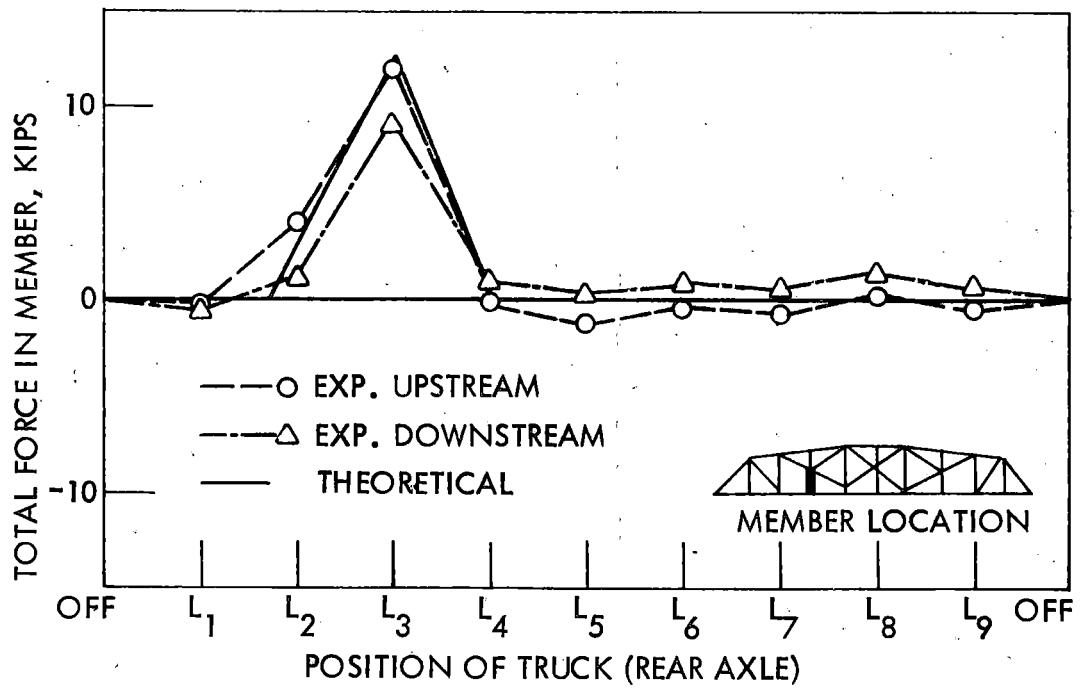
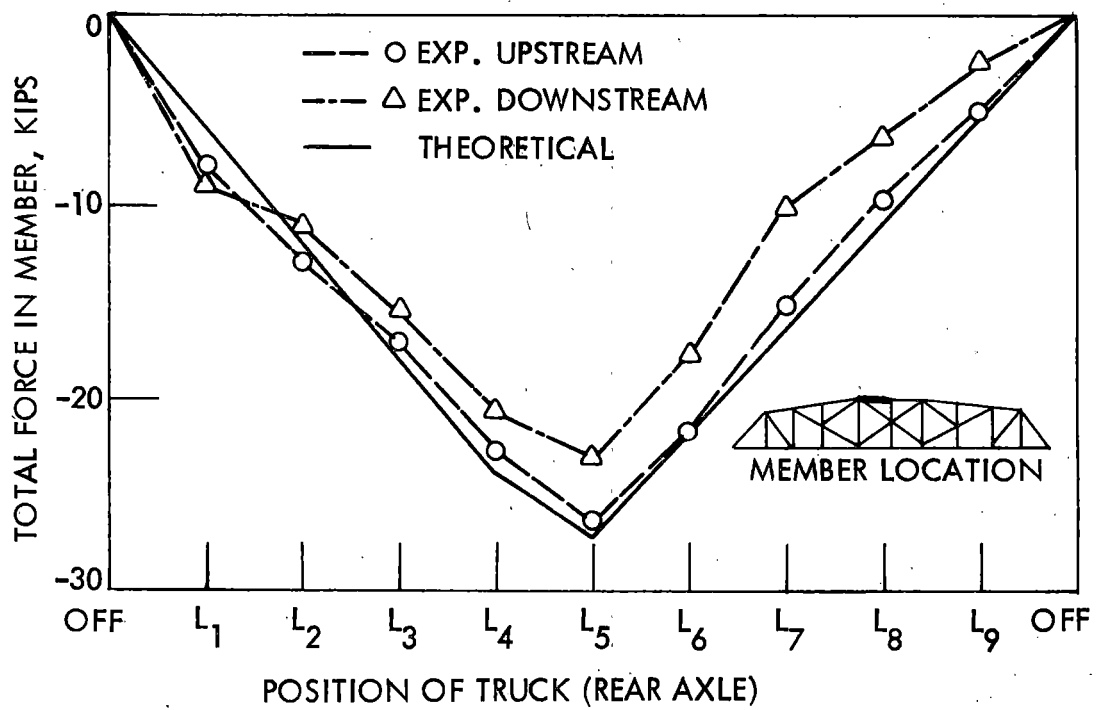
e. Member L_3M_3 f. Member U_4U_5

Fig. 27. Cont.

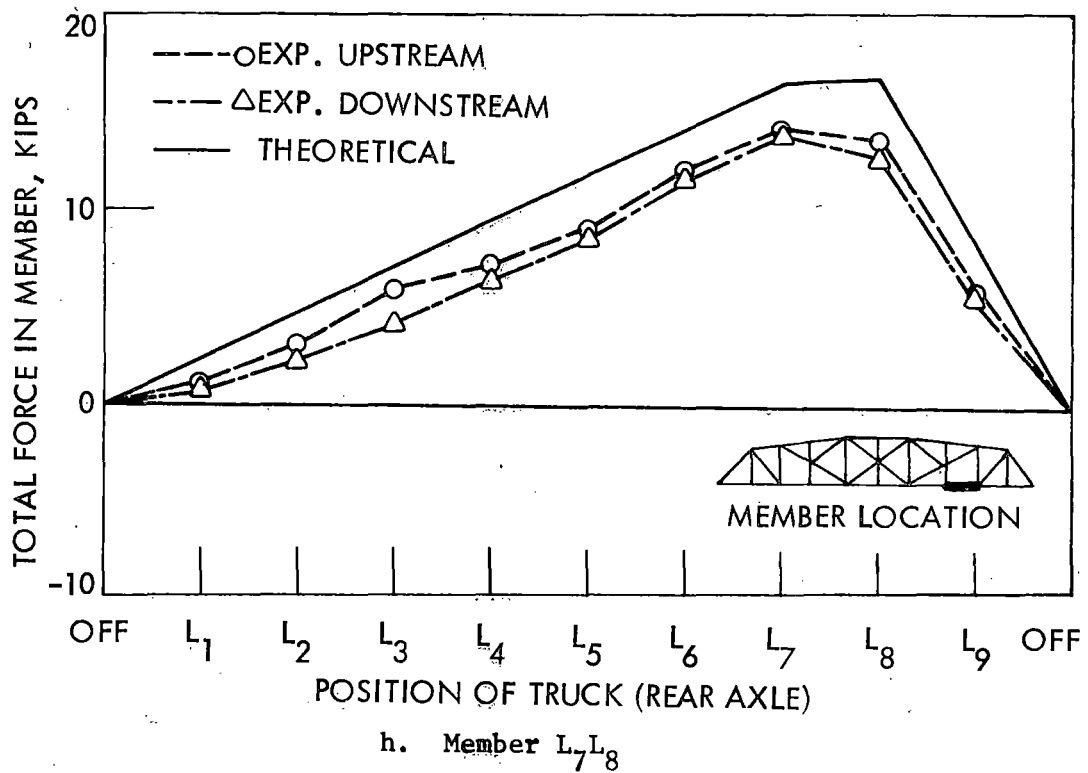
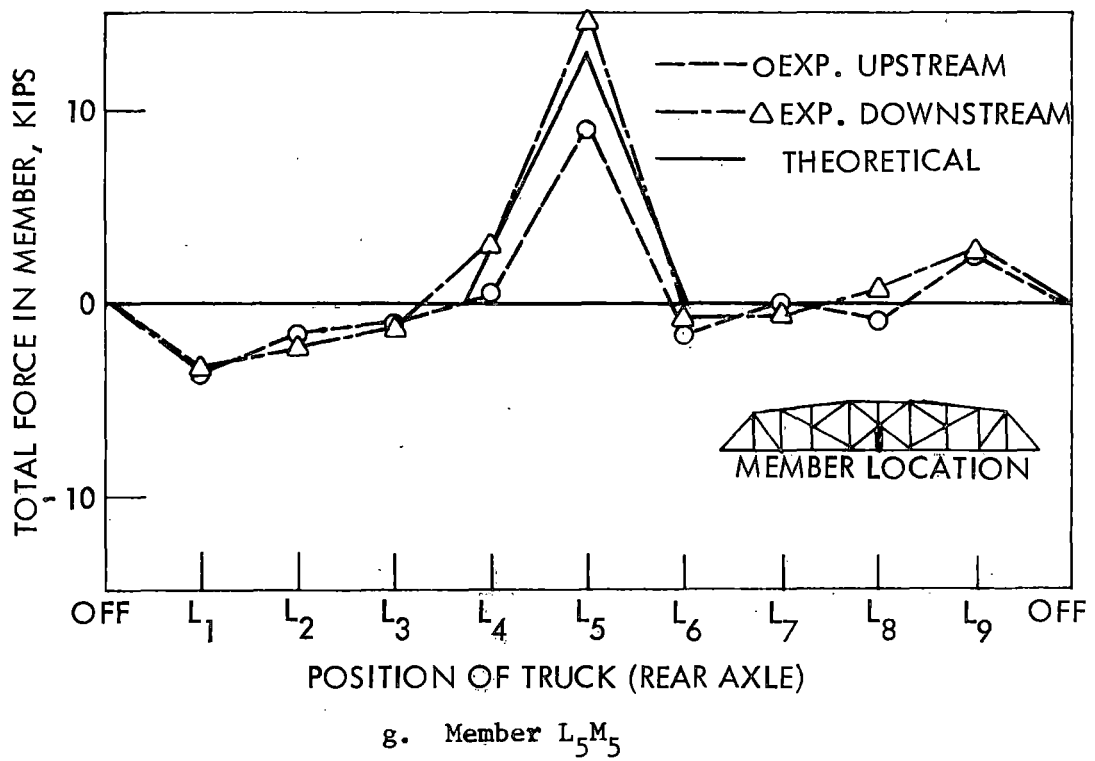


Fig. 27. Cont.

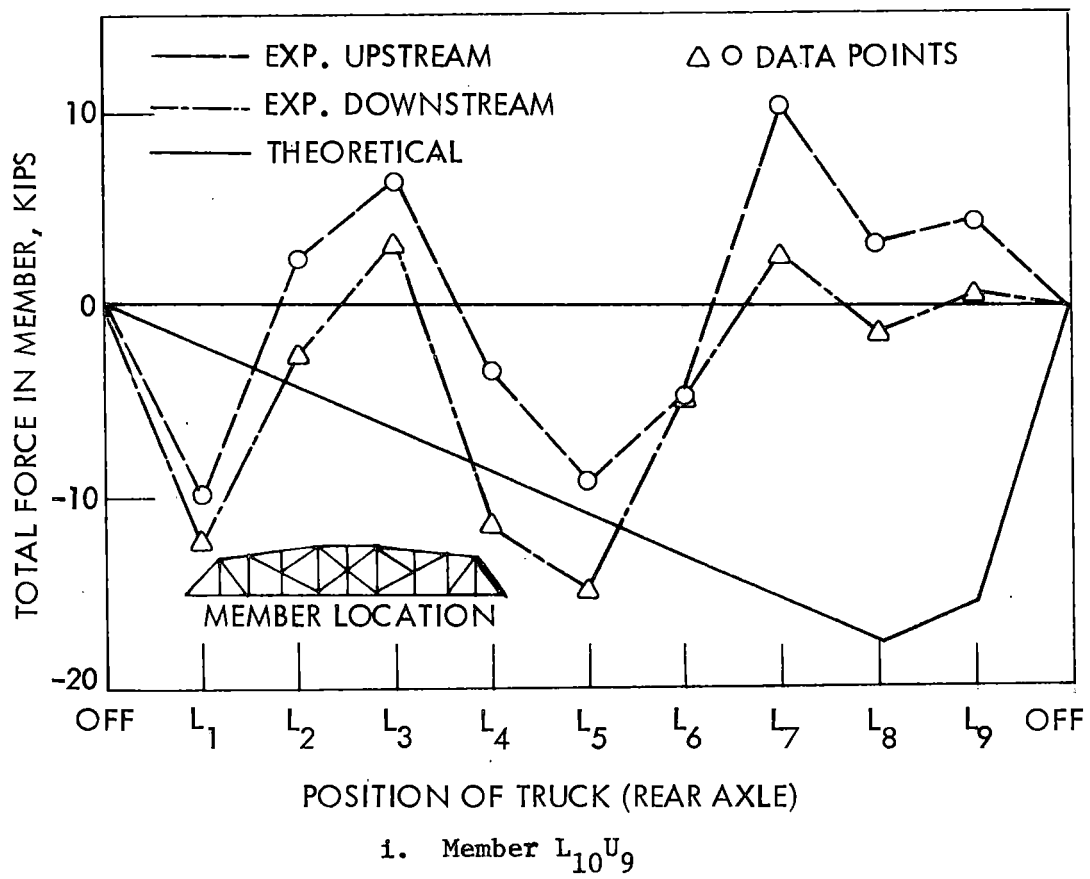


Fig. 27. Cont.

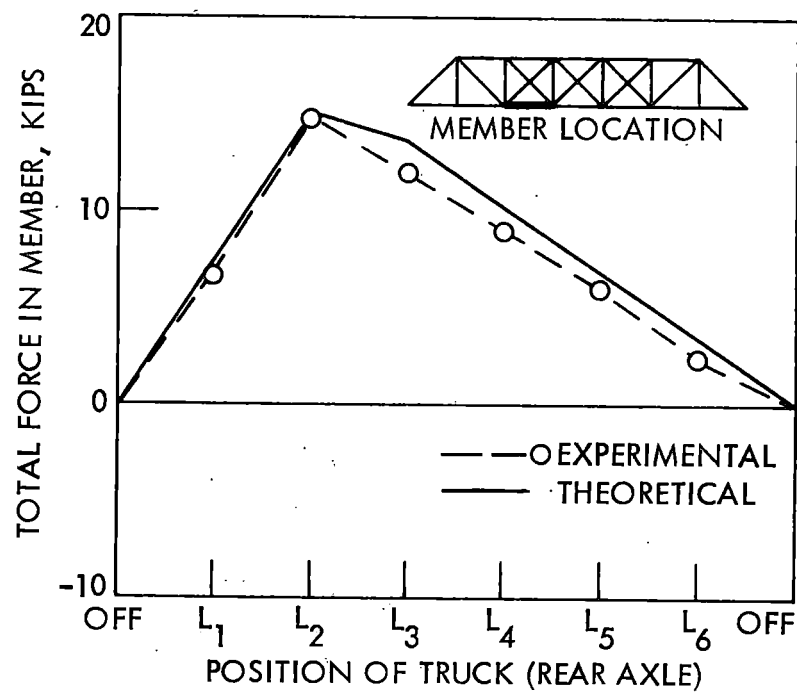
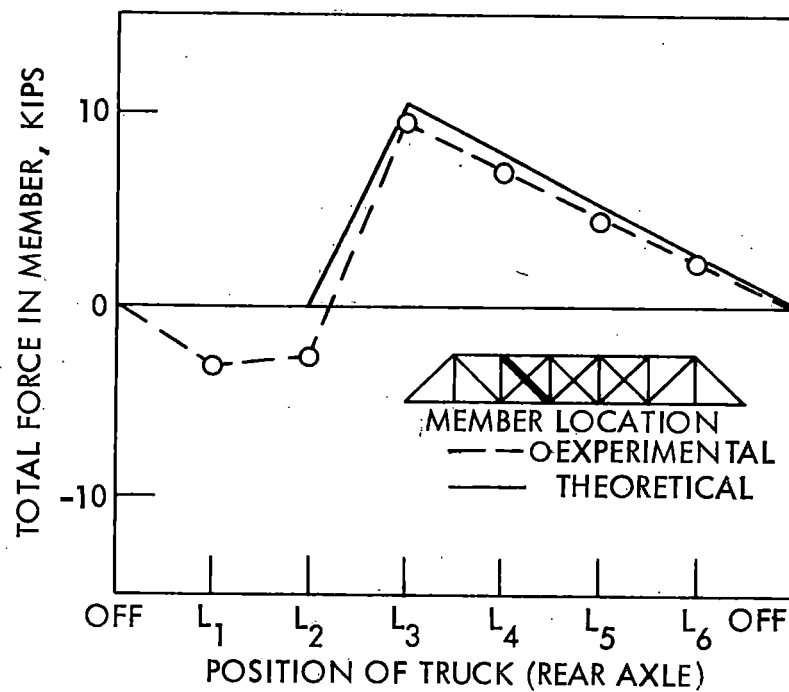
a. Member L_2L_3 b. Member L_3U_2

Fig. 28. Influence lines - Chestnut Ford Bridge: truck on centerline.

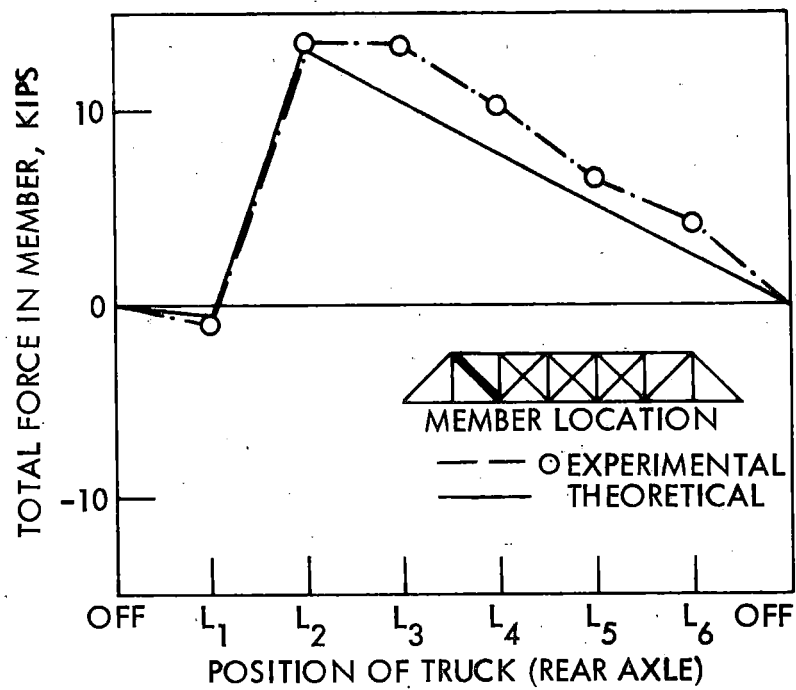
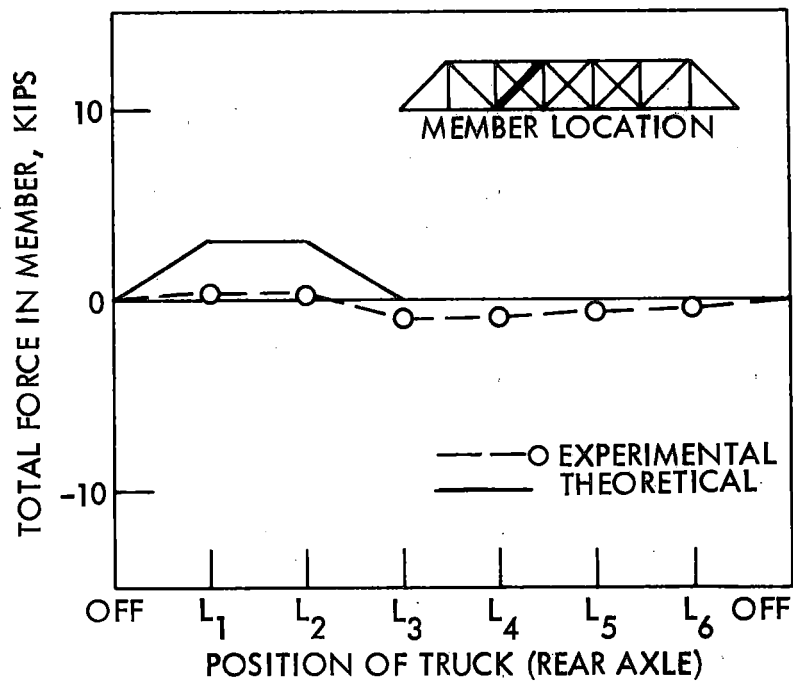
c. Member L_2U_1 d. Member L_2U_3

Fig. 28. Cont.

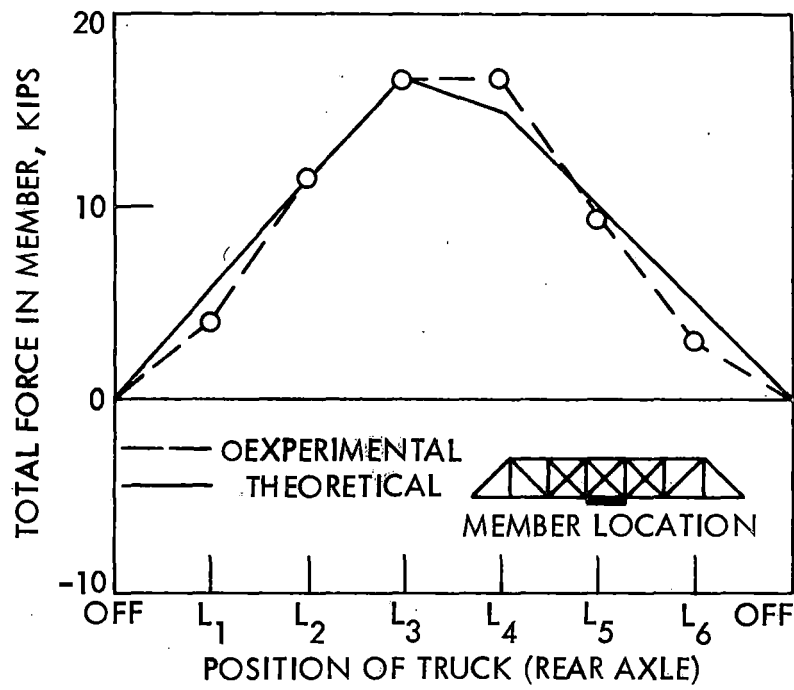
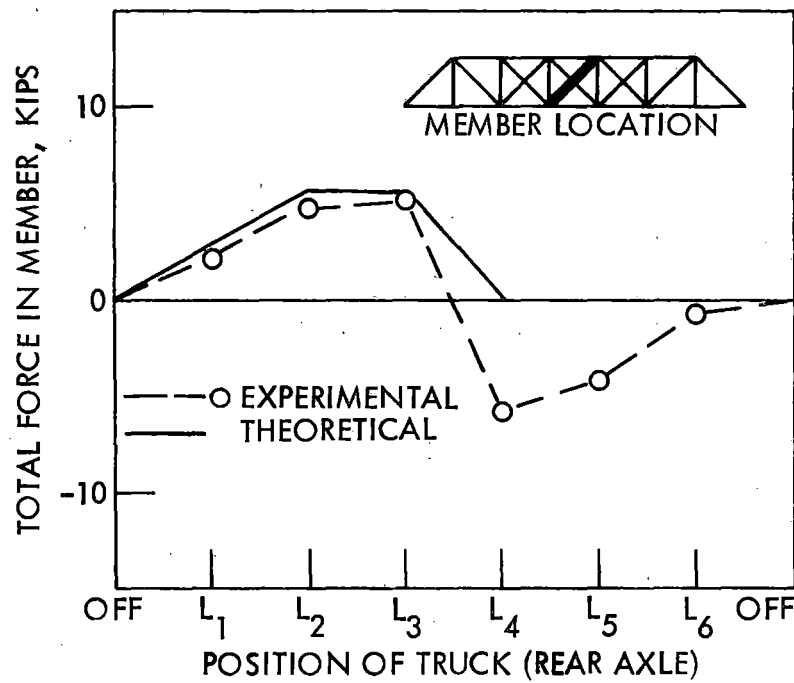
e. Member L_3L_4 f. Member L_3U_4

Fig. 28. Cont.

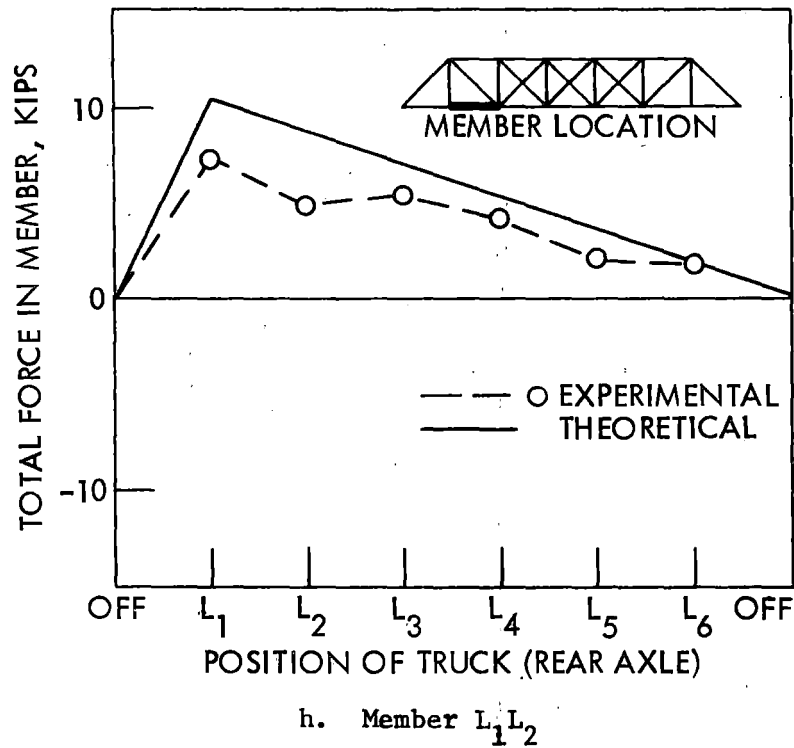
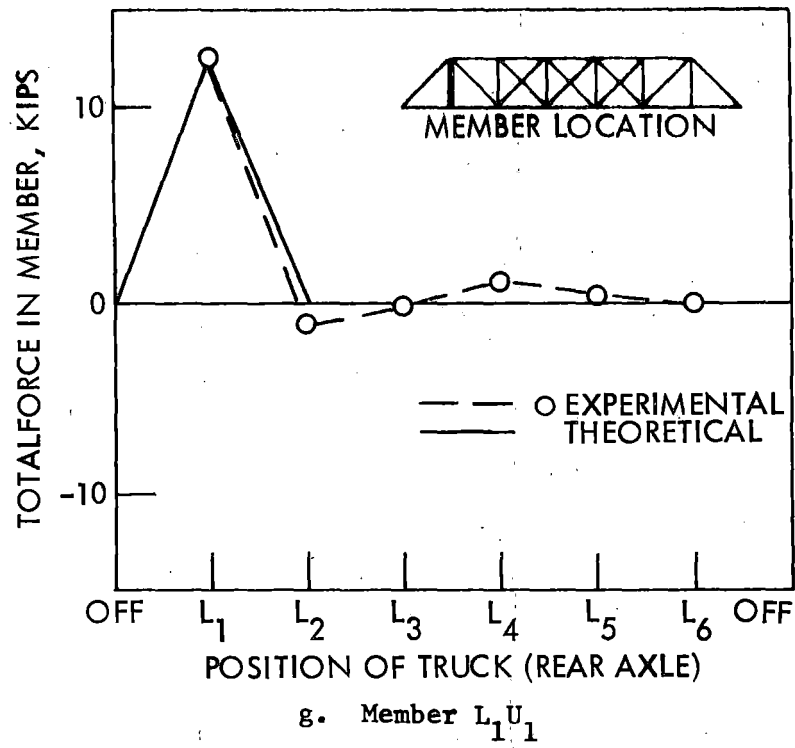


Fig. 28. Cont.

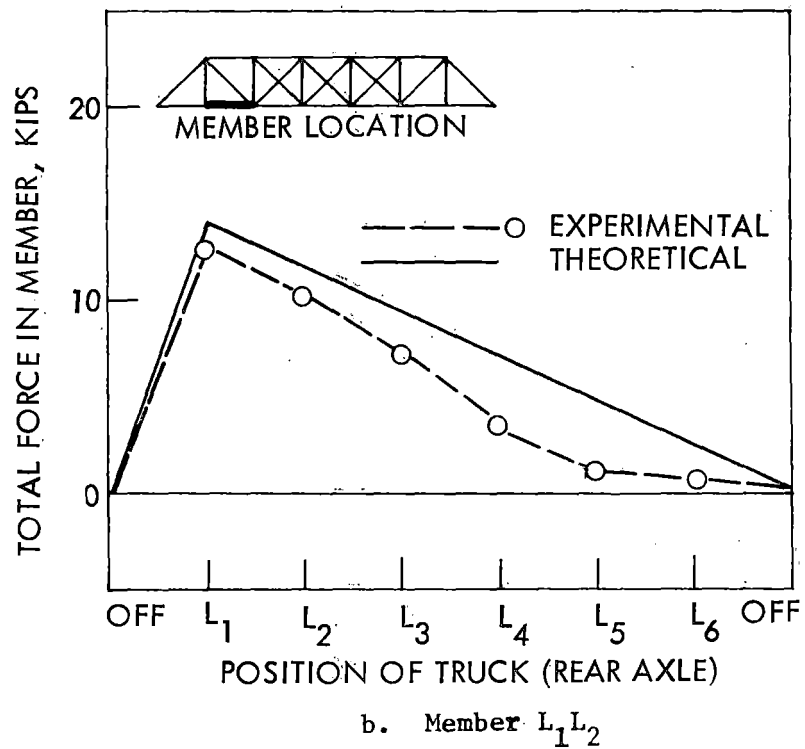
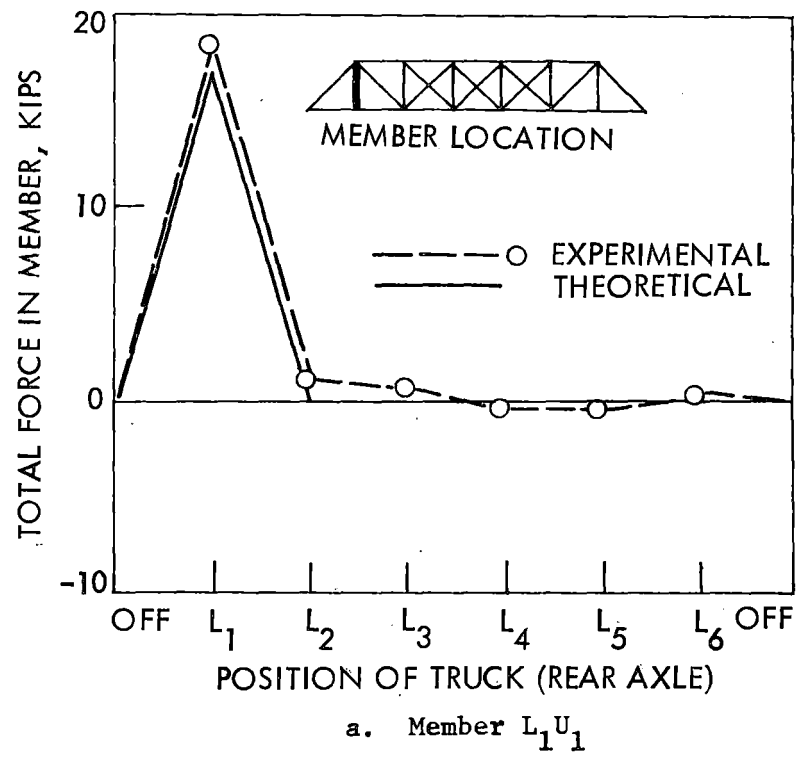


Fig. 29. Influence lines - Chestnut Ford Bridge: truck 2' from left edge.

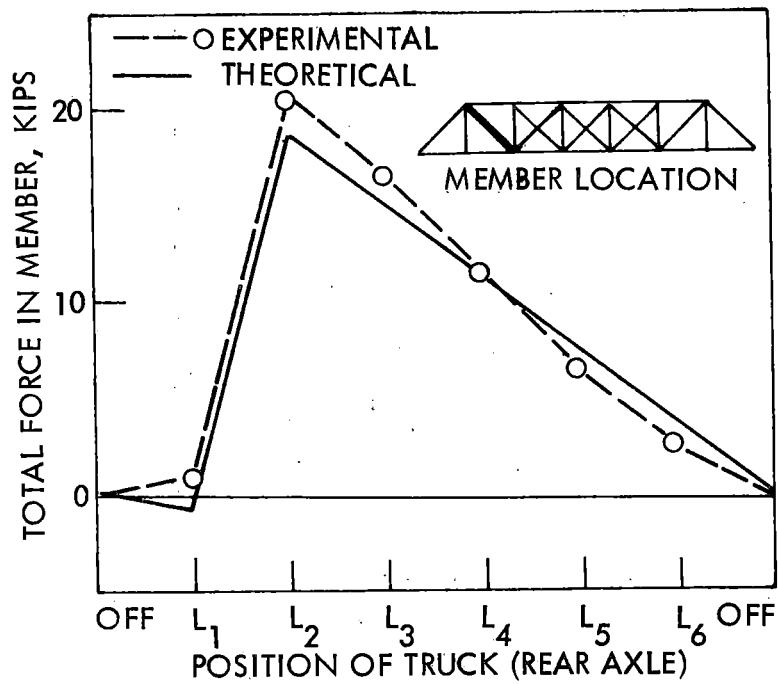
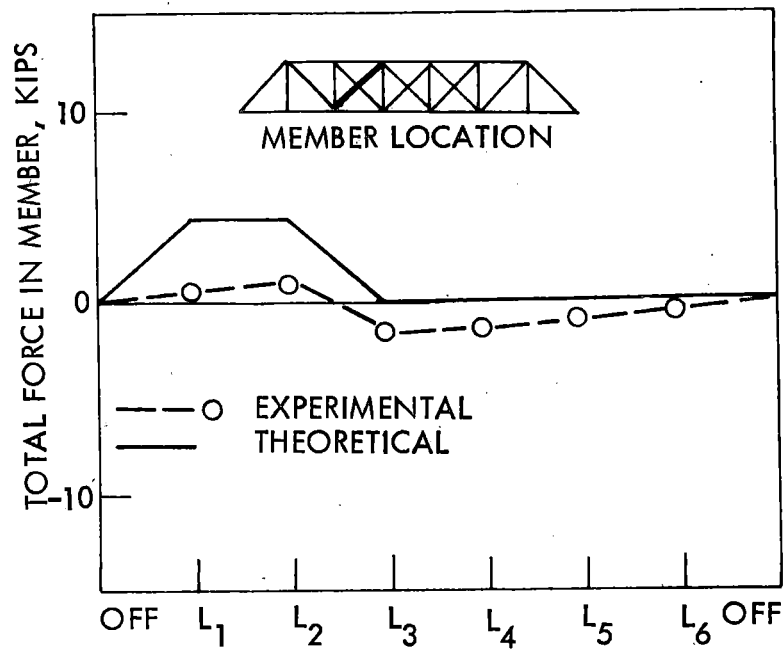
c. Member L_2U_1 d. Member L_2U_3

Fig. 29. Cont.

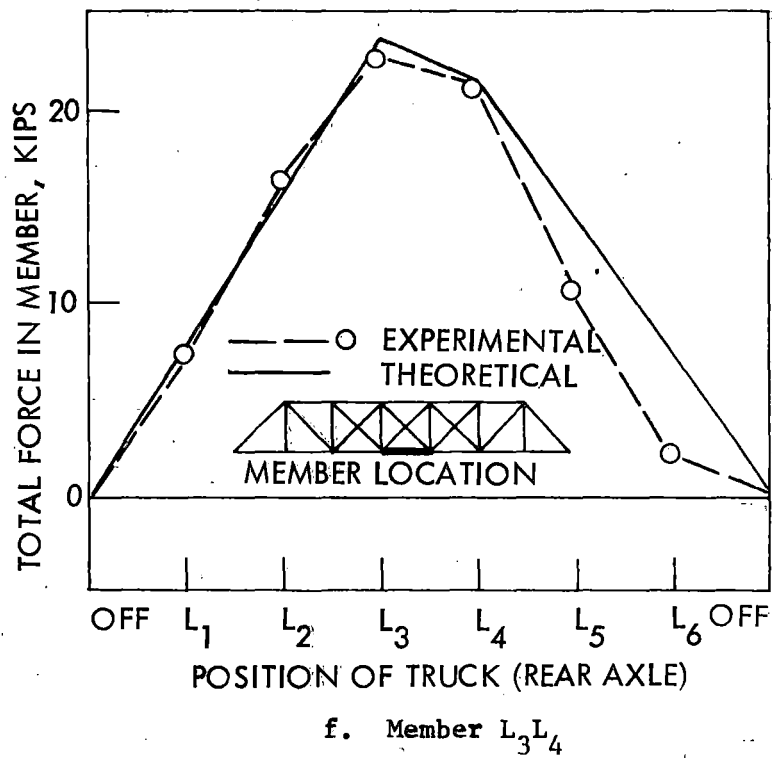
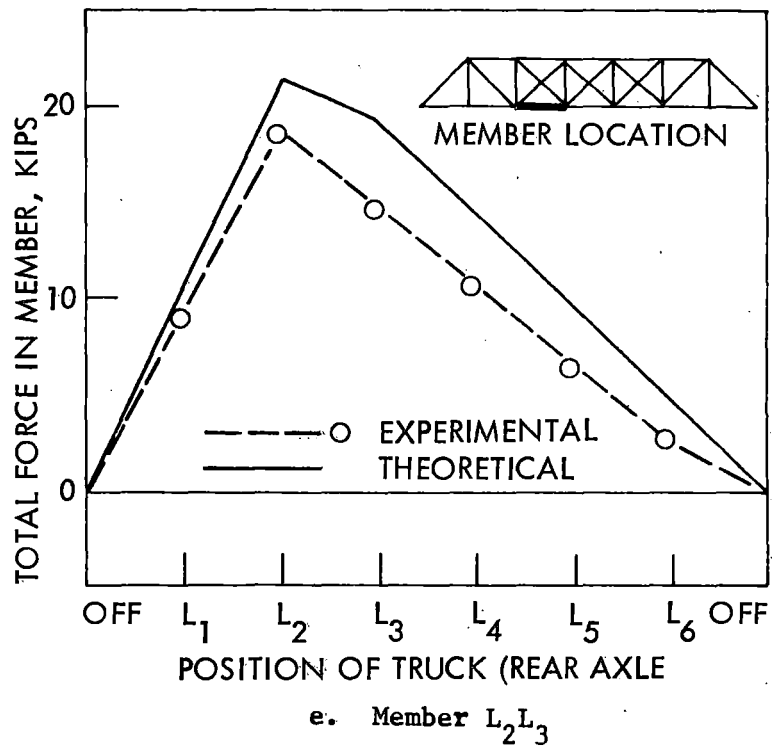


Fig. 29. Cont.

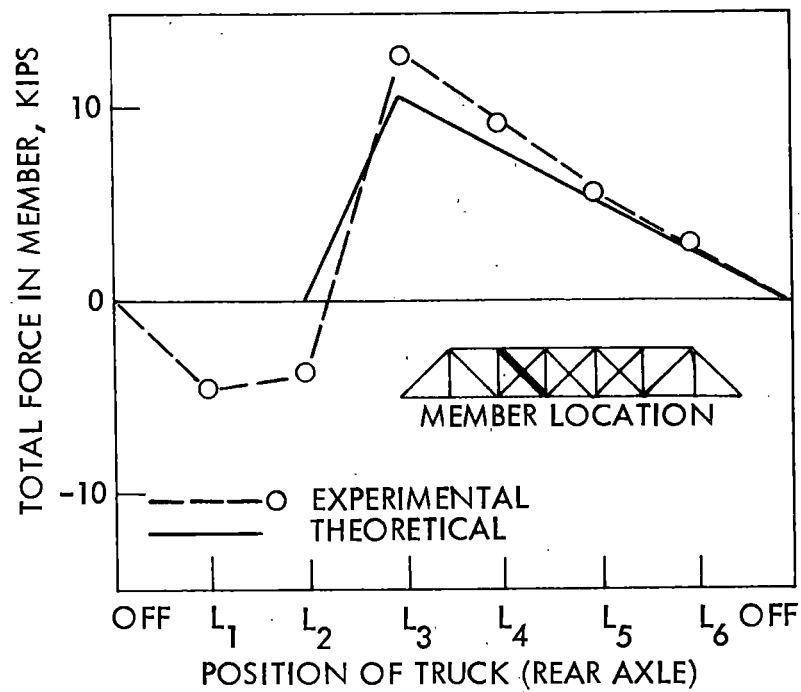
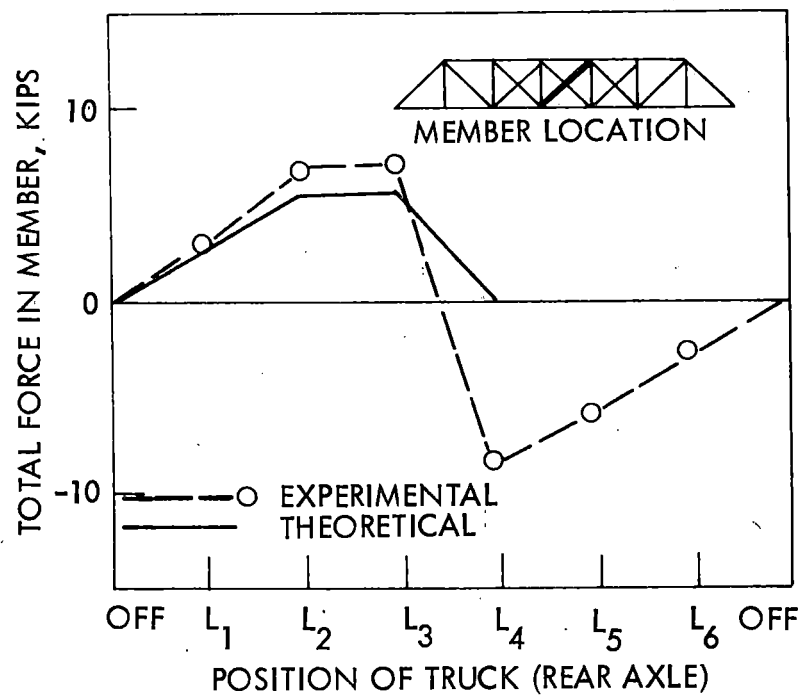
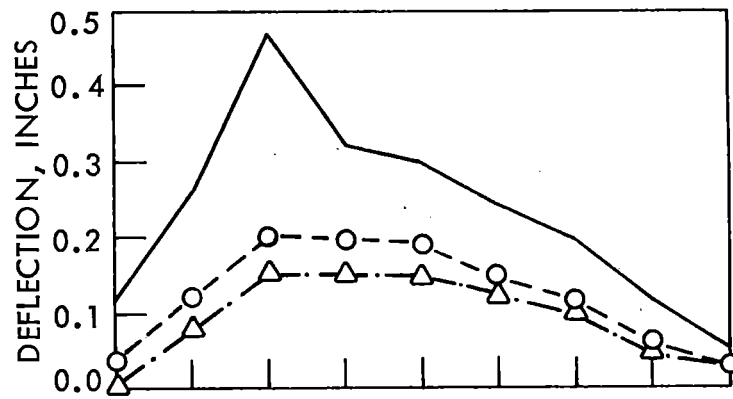
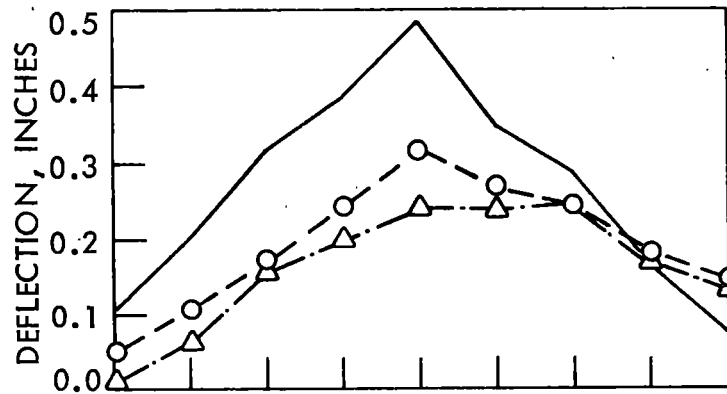
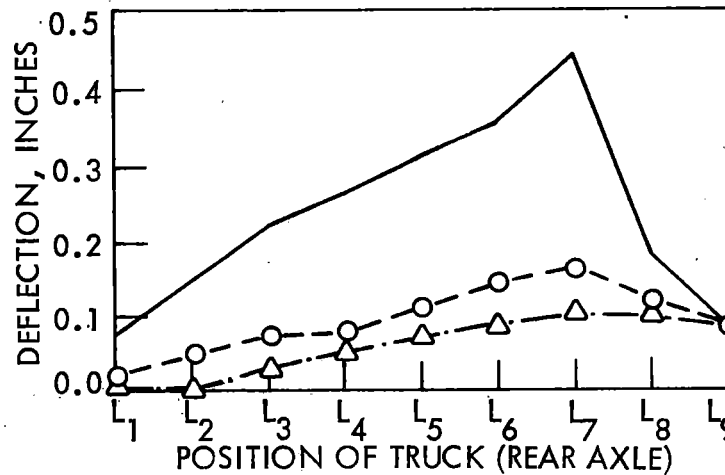
g. Member L_3U_2 h. Member L_3U_4

Fig. 29. Cont.

a. Deflection at L_3 .b. Deflection at L_5 .c. Deflection at L_7 .

— — — ○ EXP. UPSTREAM
 — · — · — △ EXP. DOWNSTREAM
 — — — — — THEORETICAL

Fig. 30. Influence lines for truss deflection: Span 2 - Hubby Bridge.

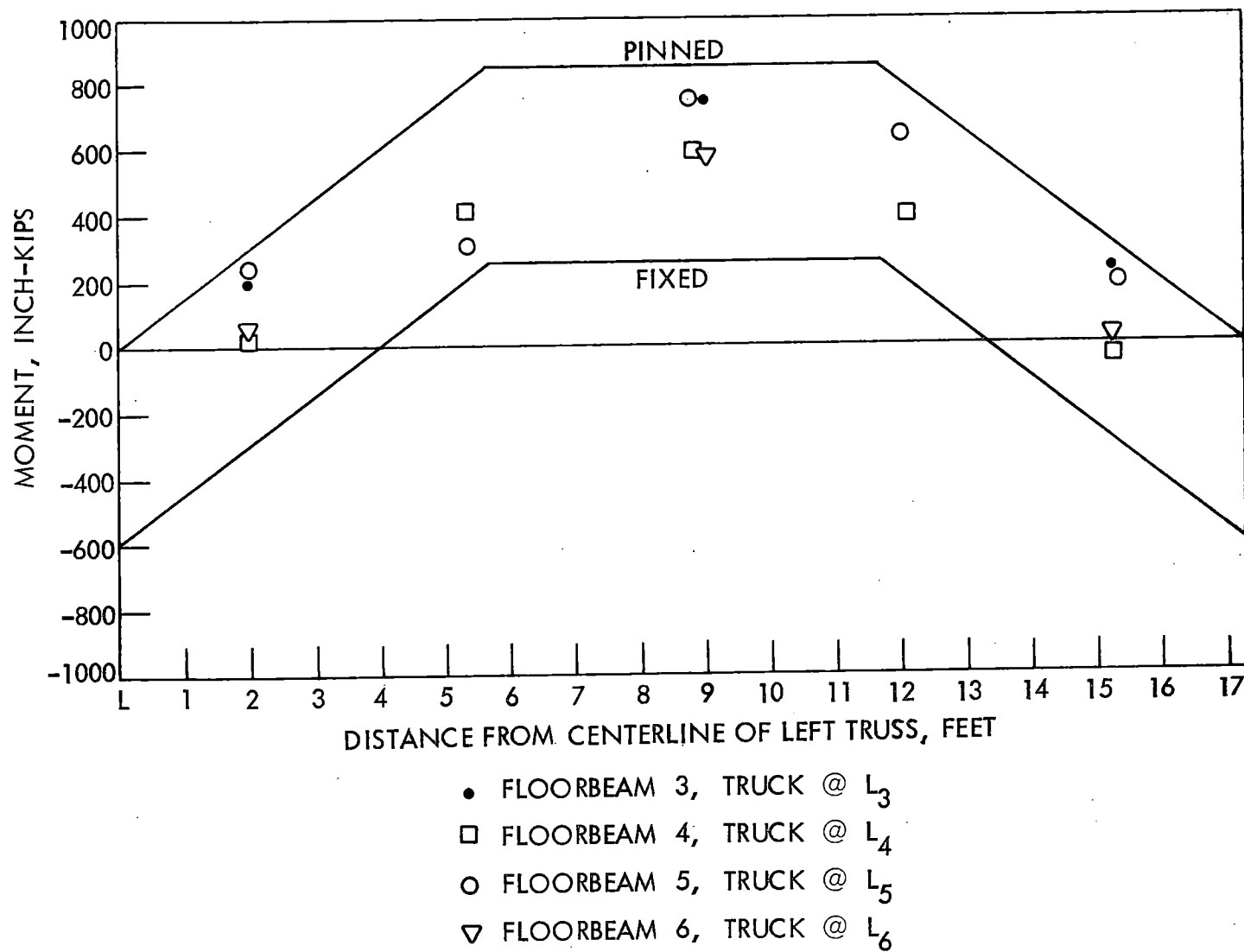
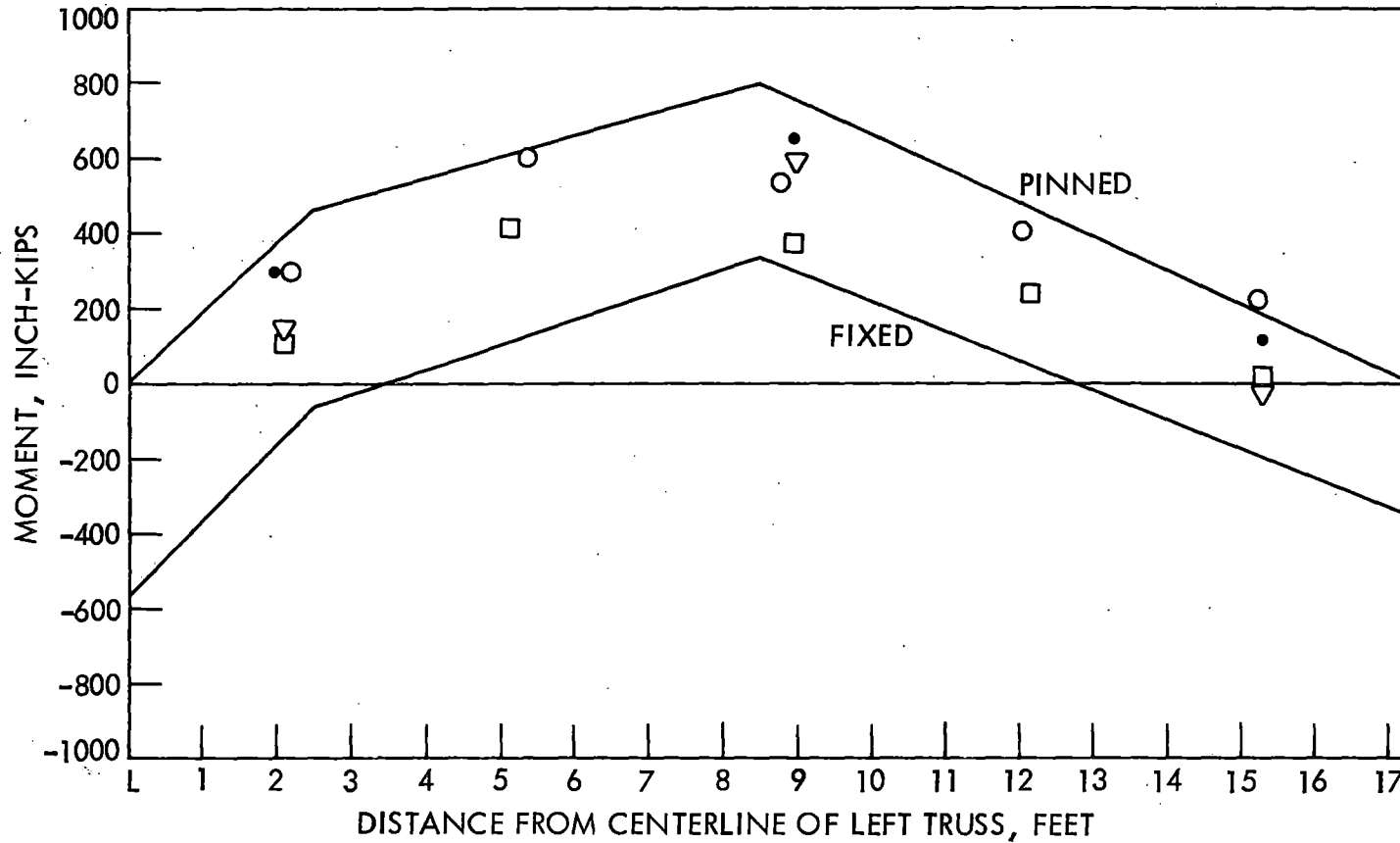


Fig. 31a. Moment for floorbeams at L_3 , L_4 , L_5 , L_6 : truck on L .



- FLOORBEAM 3, TRUCK @ L_3
- FLOORBEAM 4, TRUCK @ L_4
- FLOORBEAM 5, TRUCK @ L_5
- ▽ FLOORBEAM 6, TRUCK @ L_6

Fig. 31b. Moment for floorbeams at L_3 , L_4 , L_5 , L_6 : truck on left edge.

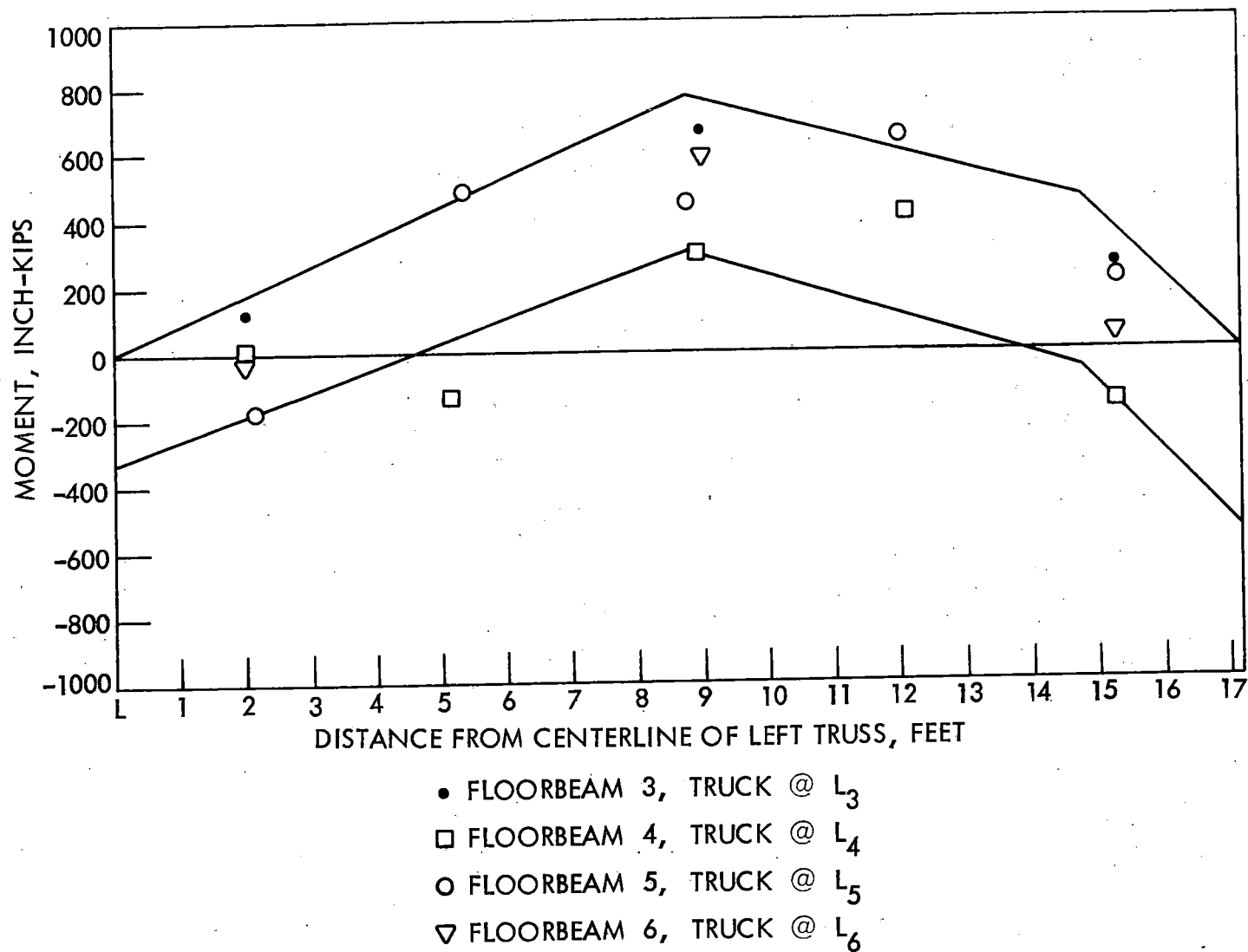


Fig. 31c. Moment for floorbeams at L_3 , L_4 , L_5 , L_6 : truck on right edge.

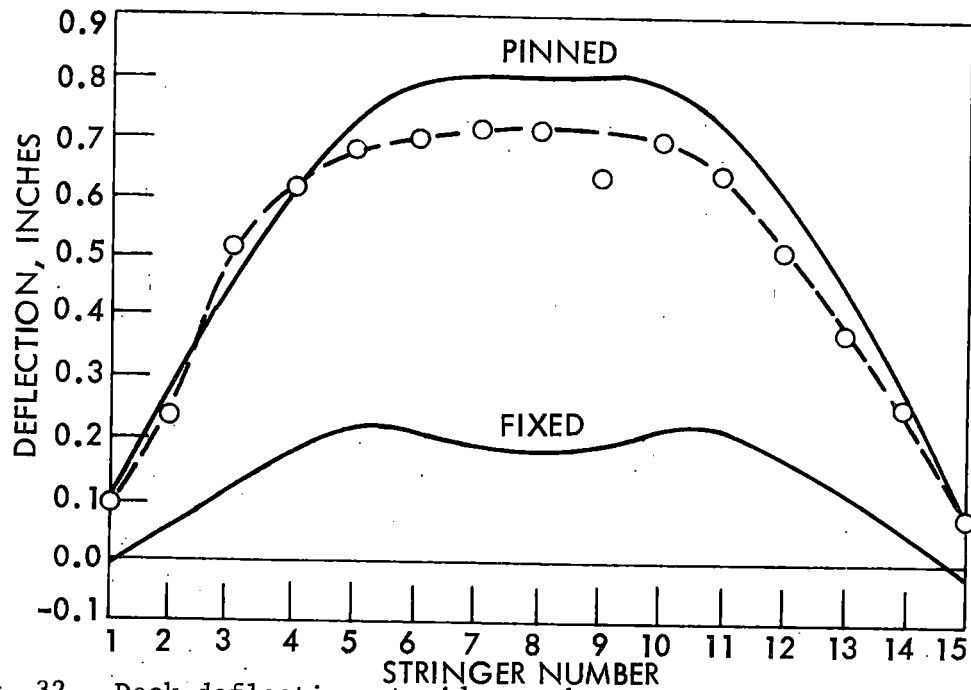


Fig. 32. Deck deflection at mid-span between L_2 and L_3 , Span 2 - Hubby Bridge, truck on centerline of deck.

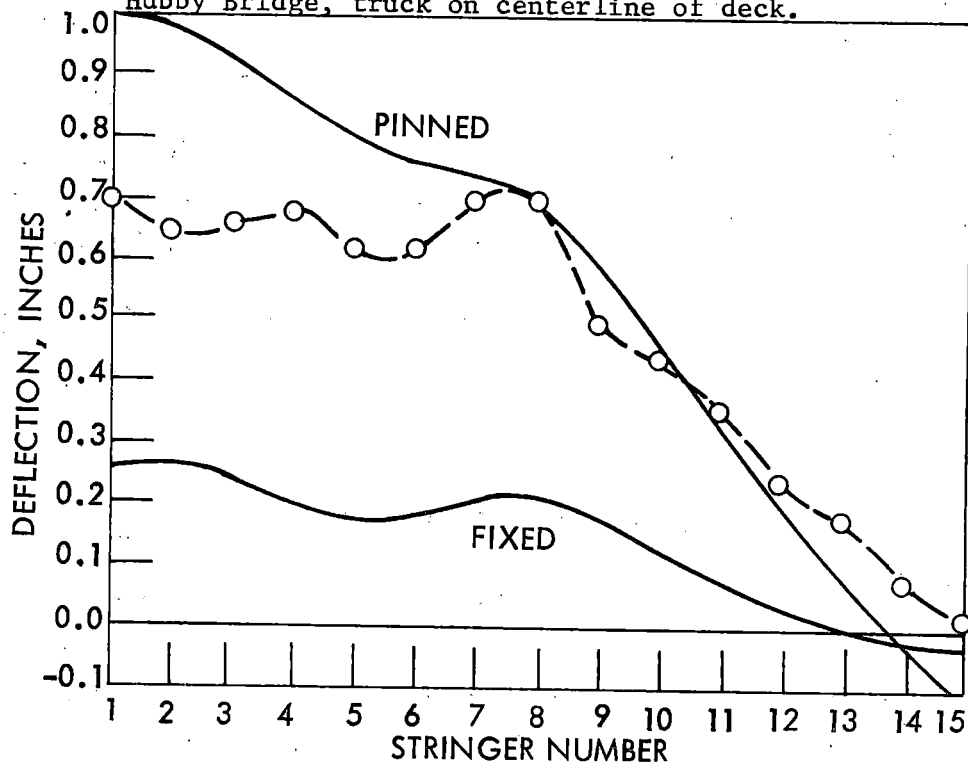


Fig. 33. Deck deflection at mid-span between L_2 and L_3 , Span 2 - Hubby Bridge, truck 2' from left edge of deck.

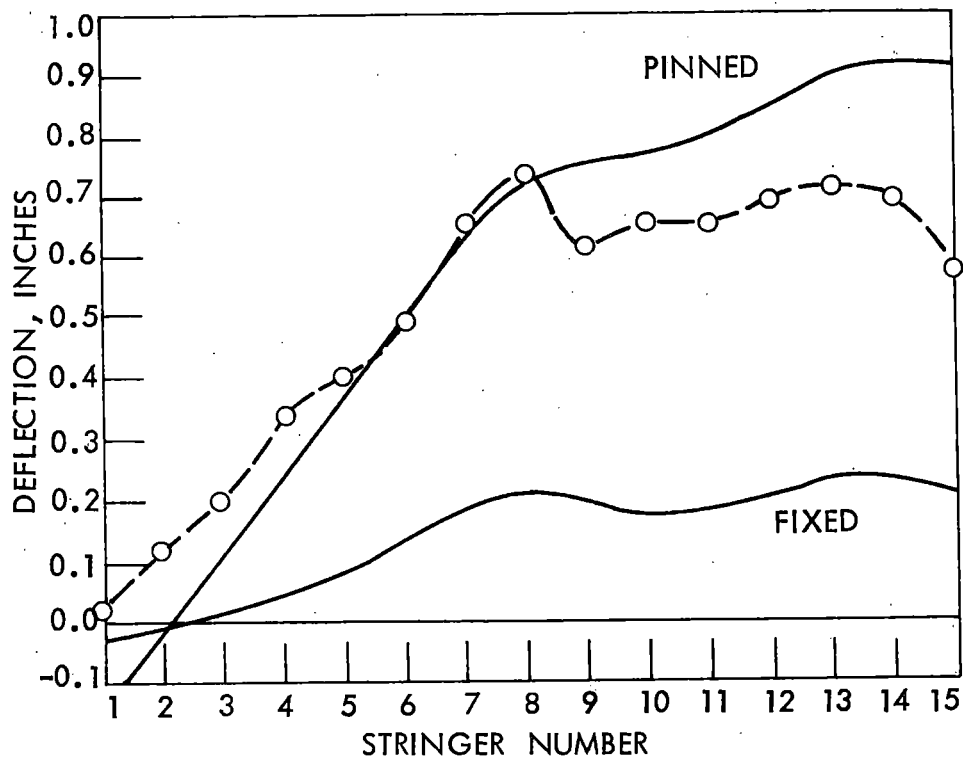


Fig. 34. Deck deflection at mid-span between L_2 and L_3 , Span 2 - Hubby Bridge, truck 2' from right edge of deck.

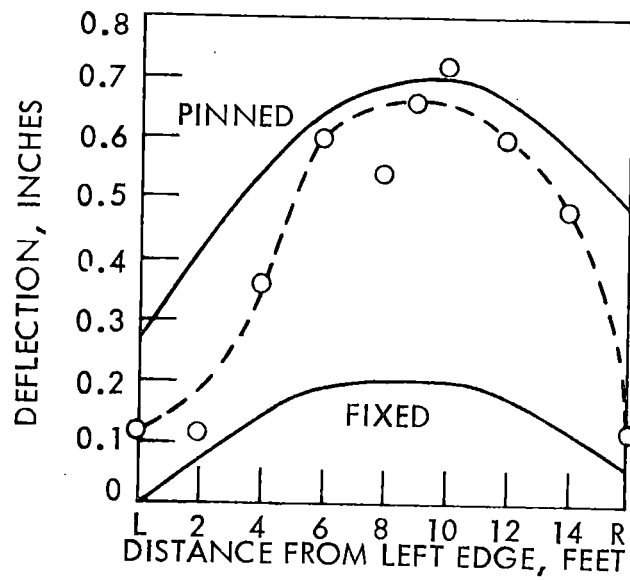


Fig. 35. Deck deflection at mid-span of panel, Chestnut Ford Bridge: truck on centerline of deck.

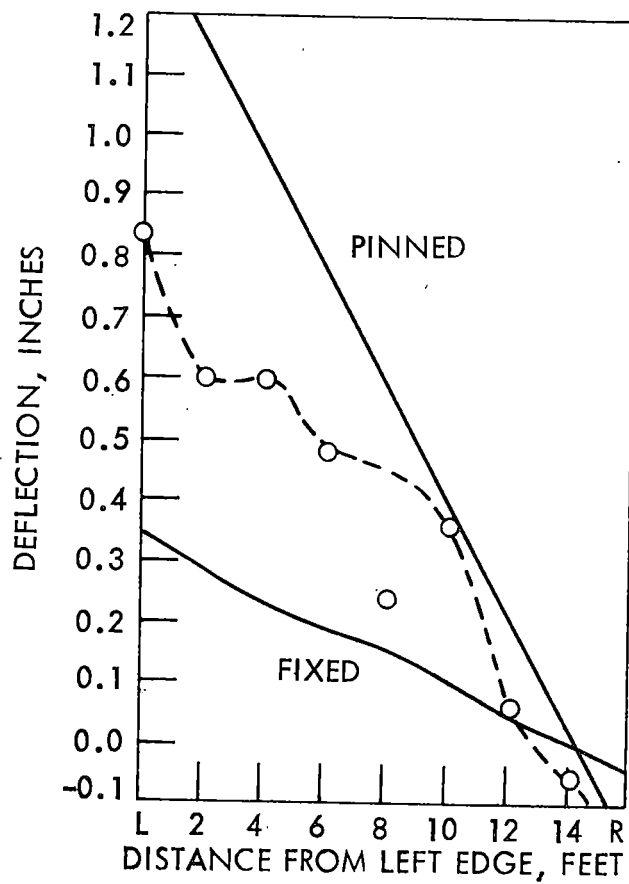


Fig. 36. Deck deflection at mid-span of panel, Chestnut Ford Bridge: truck 2' from left edge.

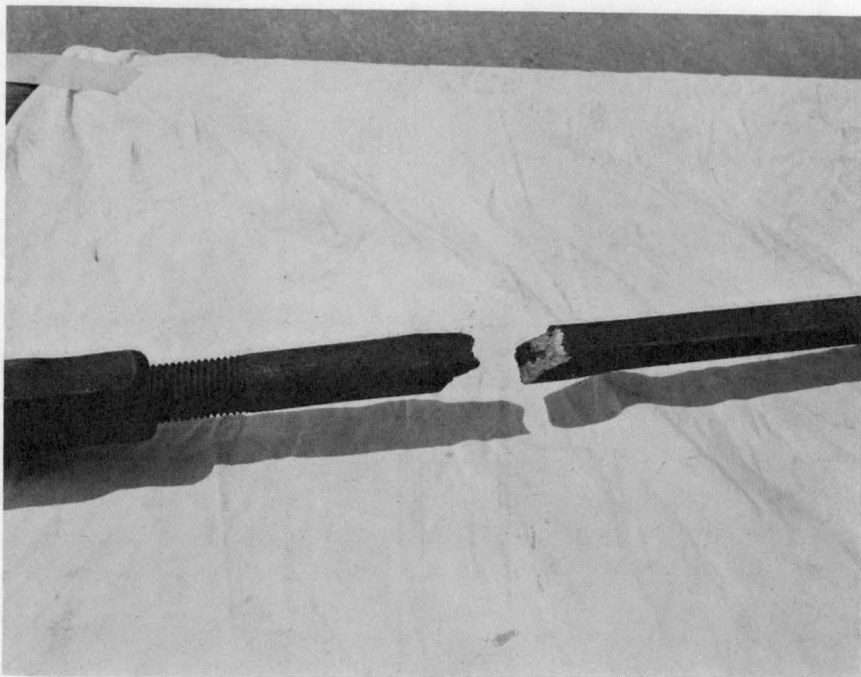


Fig. 38. Photograph showing fatigue fracture in forging near a turnbuckle.

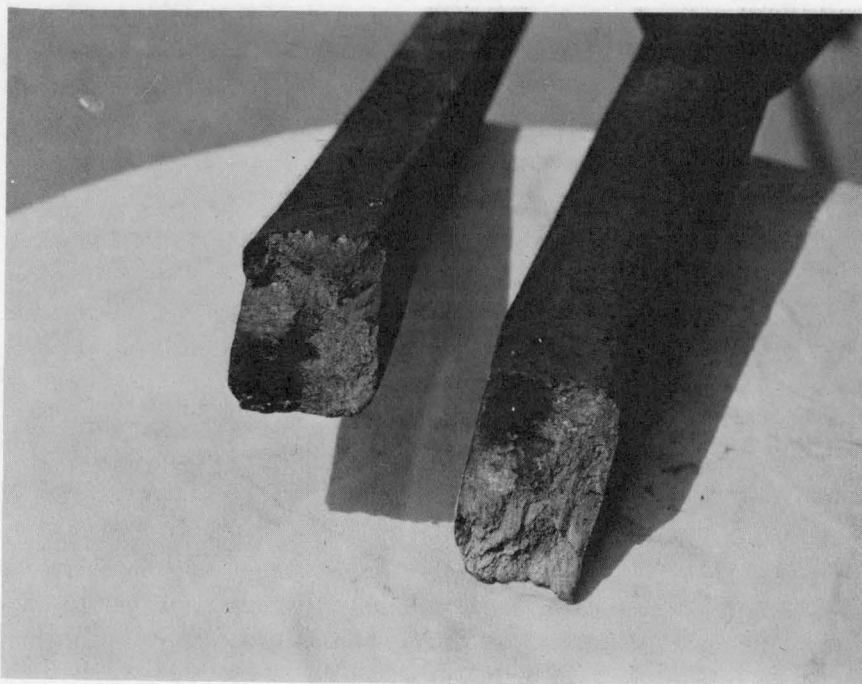


Fig. 39. Photograph showing extent of an initial crack in a forging.

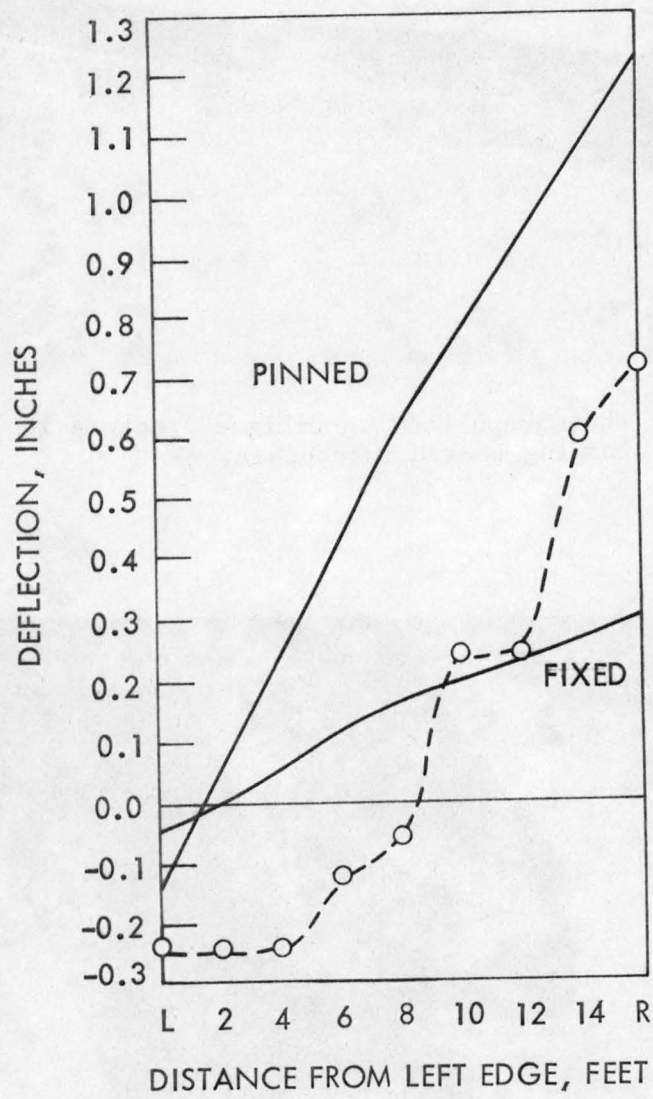


Fig. 37. Deck deflection at mid-span of panel, Chestnut Ford Bridge: truck 2' from right edge.

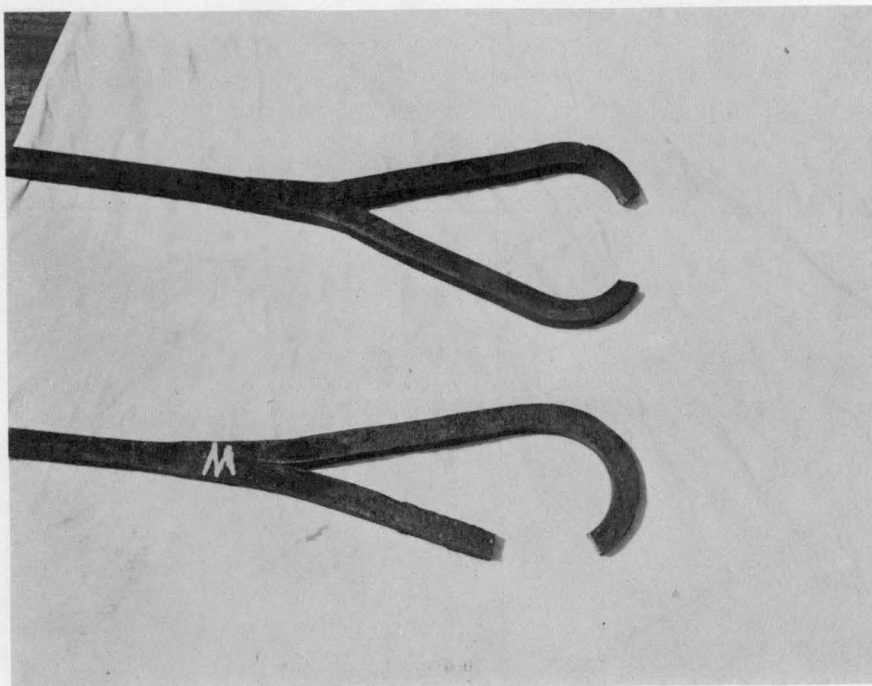


Fig. 40. Photograph showing two typical locations of fracture in an eye.

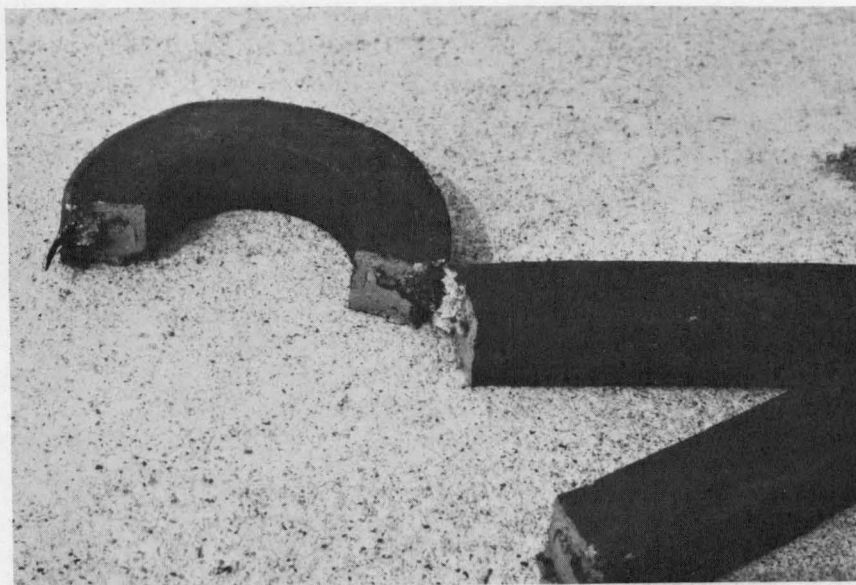


Fig. 41. Photograph showing a fracture on both sides of an eye.

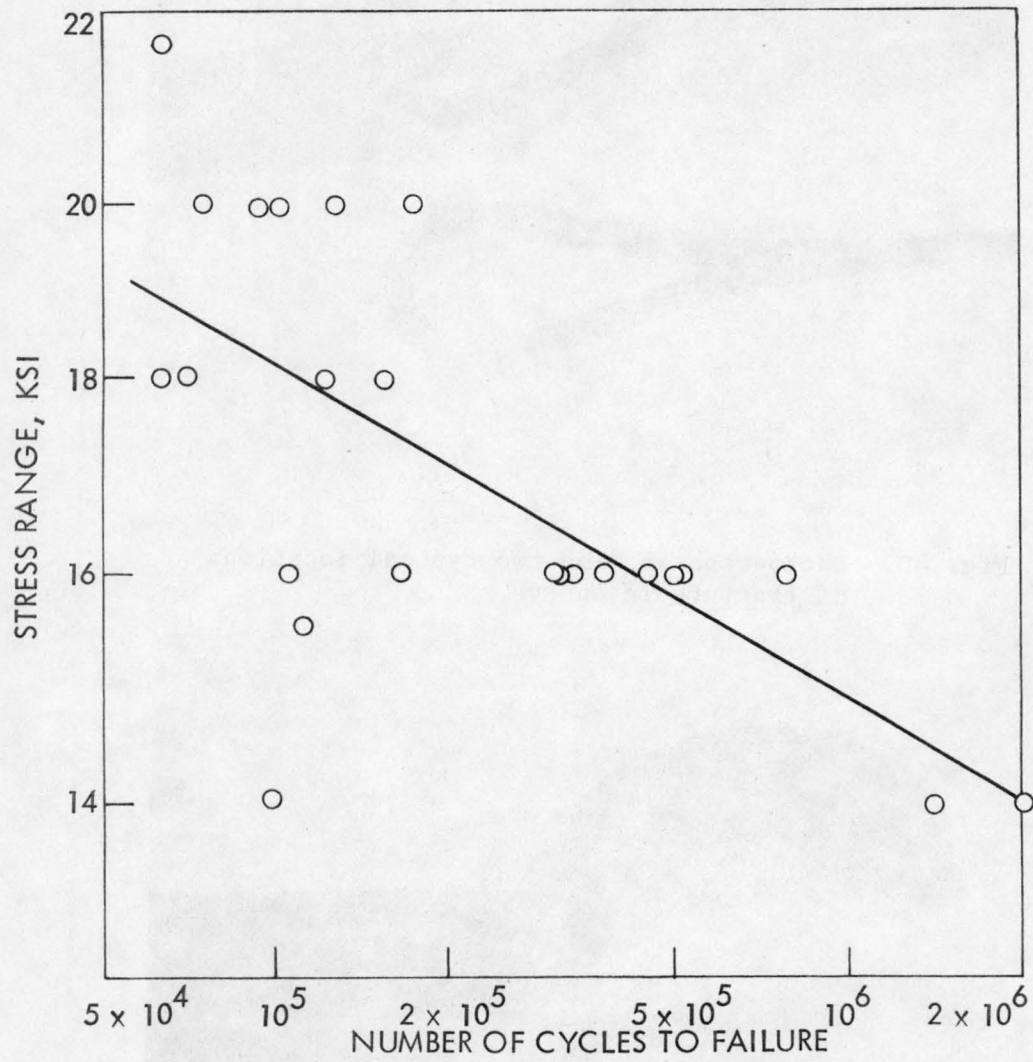


Fig. 42. S-N curve for undamaged eyebars.

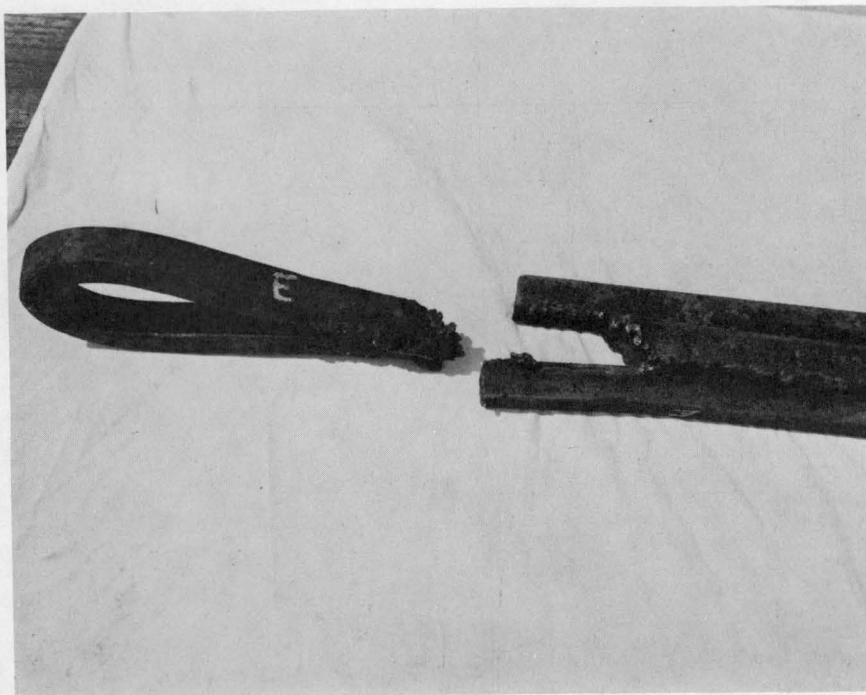


Fig. 43. Photograph showing repair and fracture of an eyebar that was repaired in the field.

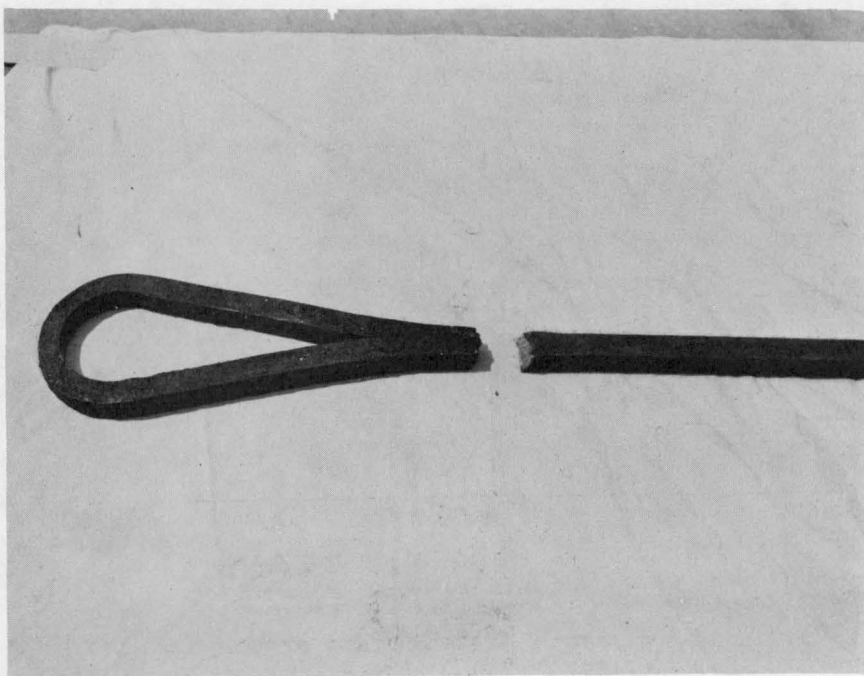


Fig. 44. Photograph showing the fatigue fracture in the forging near an eye.

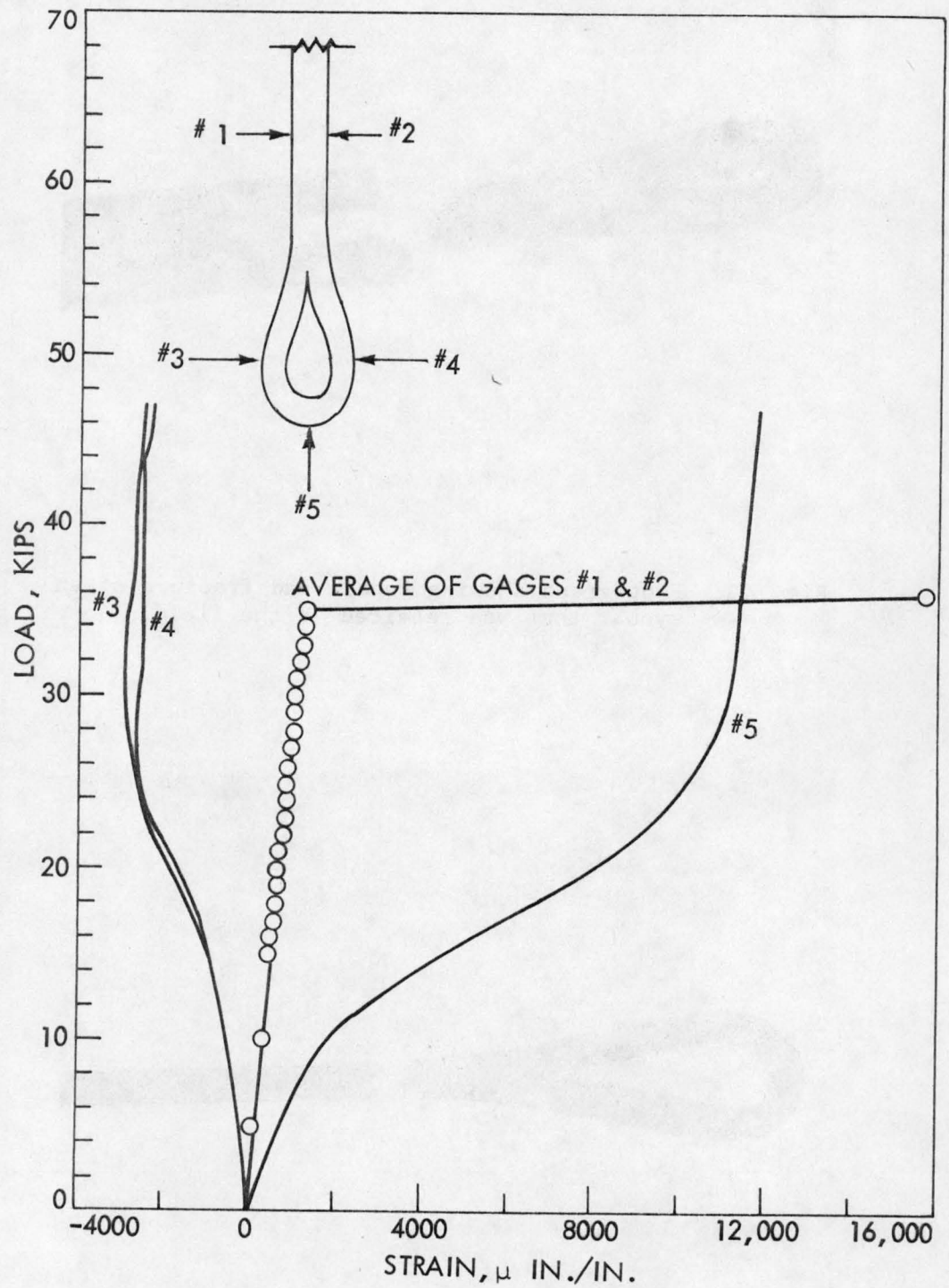


Fig. 45. Load vs strain distribution around an eye made from a square bar.

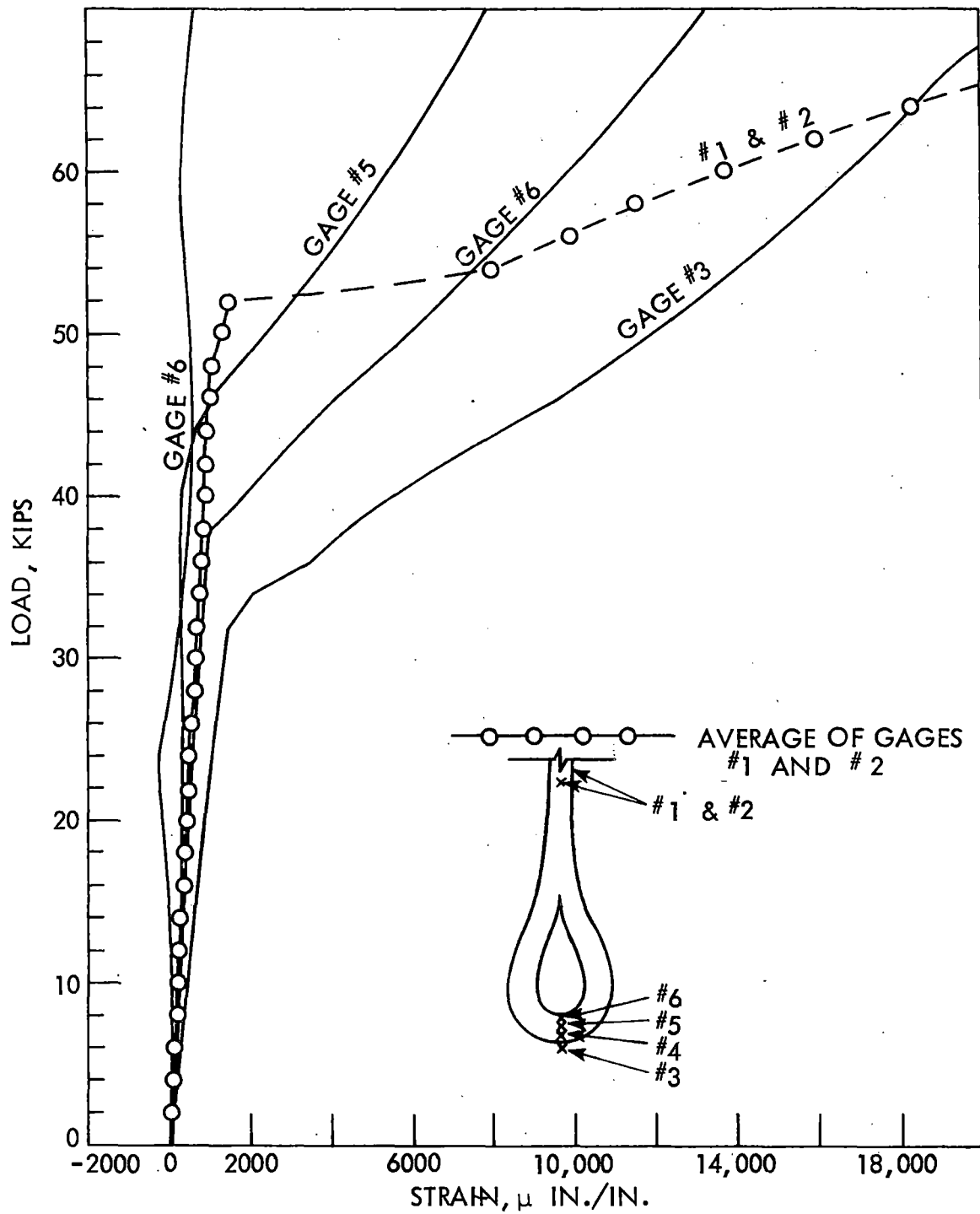


Fig. 46a. Load vs. strain distribution in tip of eye (total range).

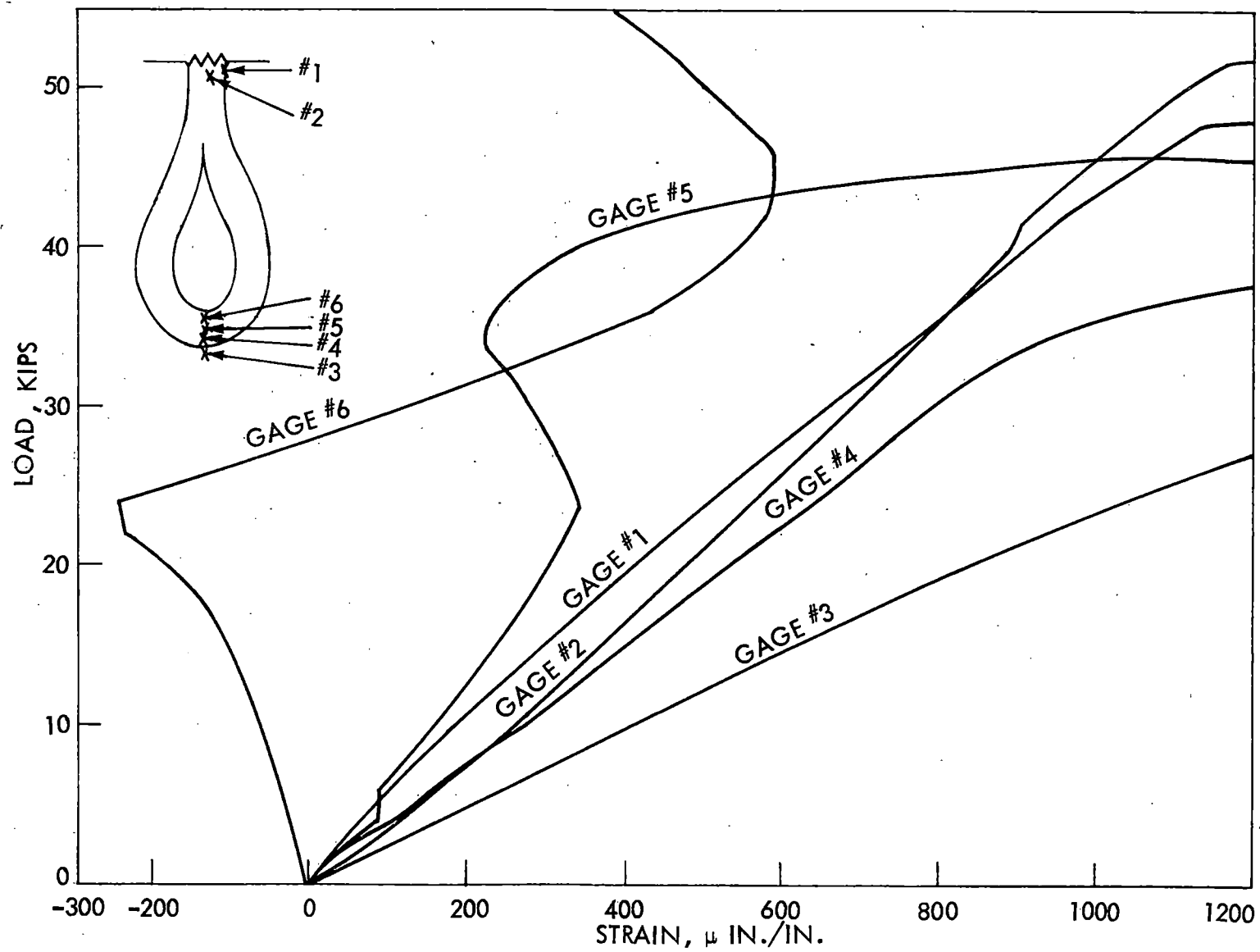


Fig. 46b. Load vs strain distribution in tip of eye (elastic range).

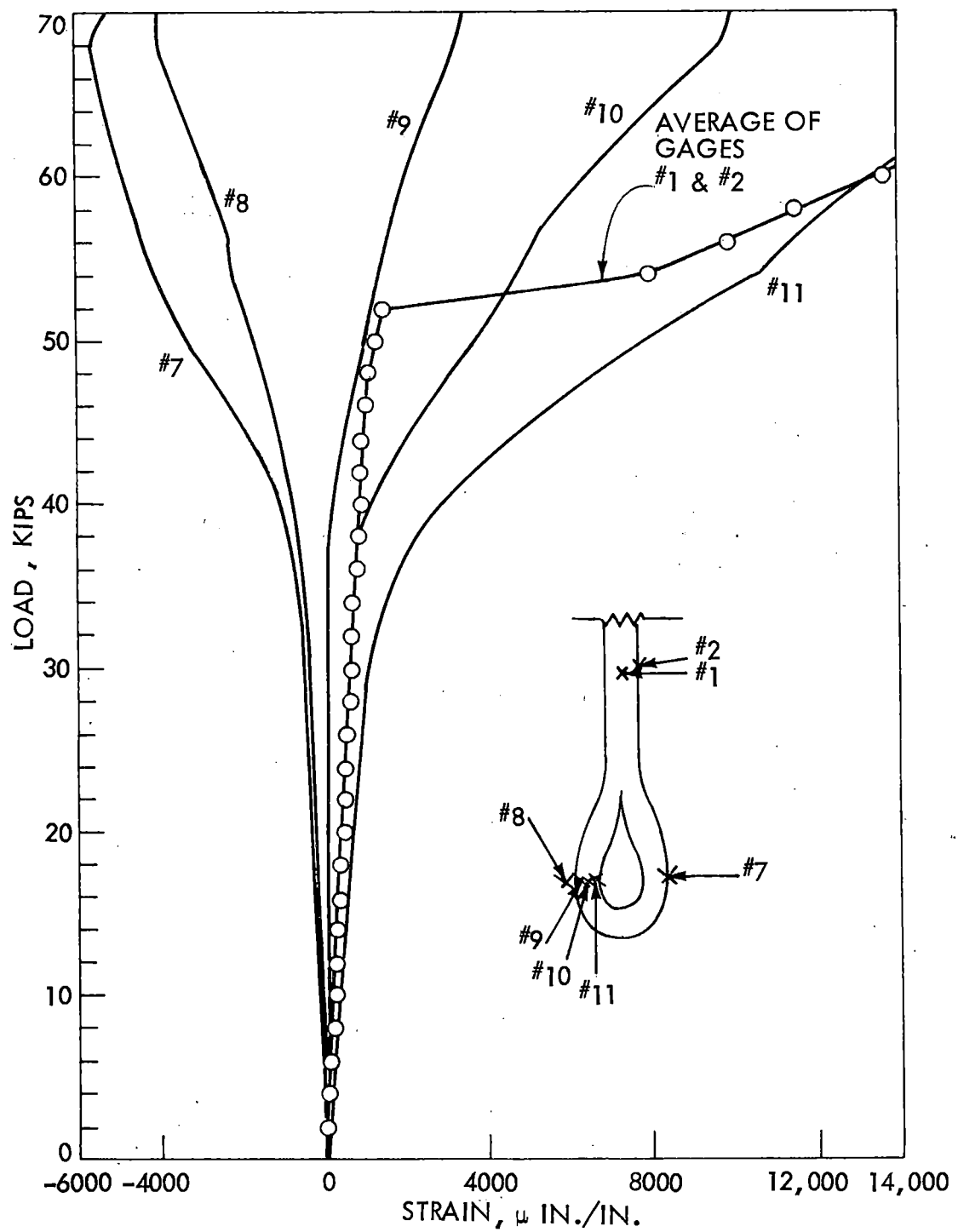


Fig. 47a. Load vs strain distribution in side of eye (total range).

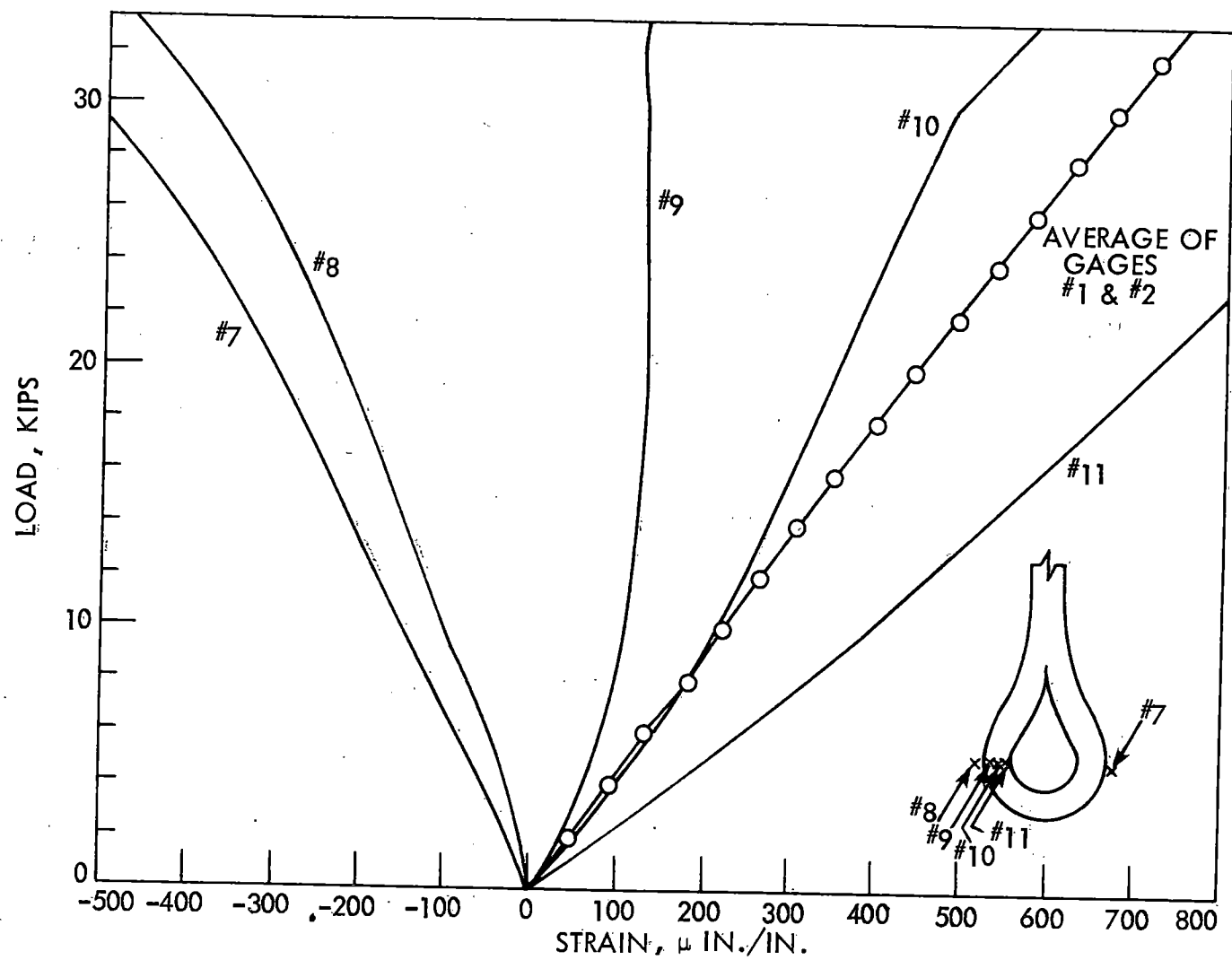


Fig. 47b. Load vs strain distribution in side of eye (elastic range).